RUHR-UNIVERSITÄT BOCHUM

Advanced Materials Processing and Microfabrication

VORLESUNG Wintersemester 2024/2025

Prof. Dr.-Ing. Alfred Ludwig

MEMS und Nanotechnologie

Miniaturisierung und Funktionsintegration

Miniaturisierung integrierter Schaltungen
(integrated circuits, ICs): von der Mikroelektronik zur Nanoelektronik

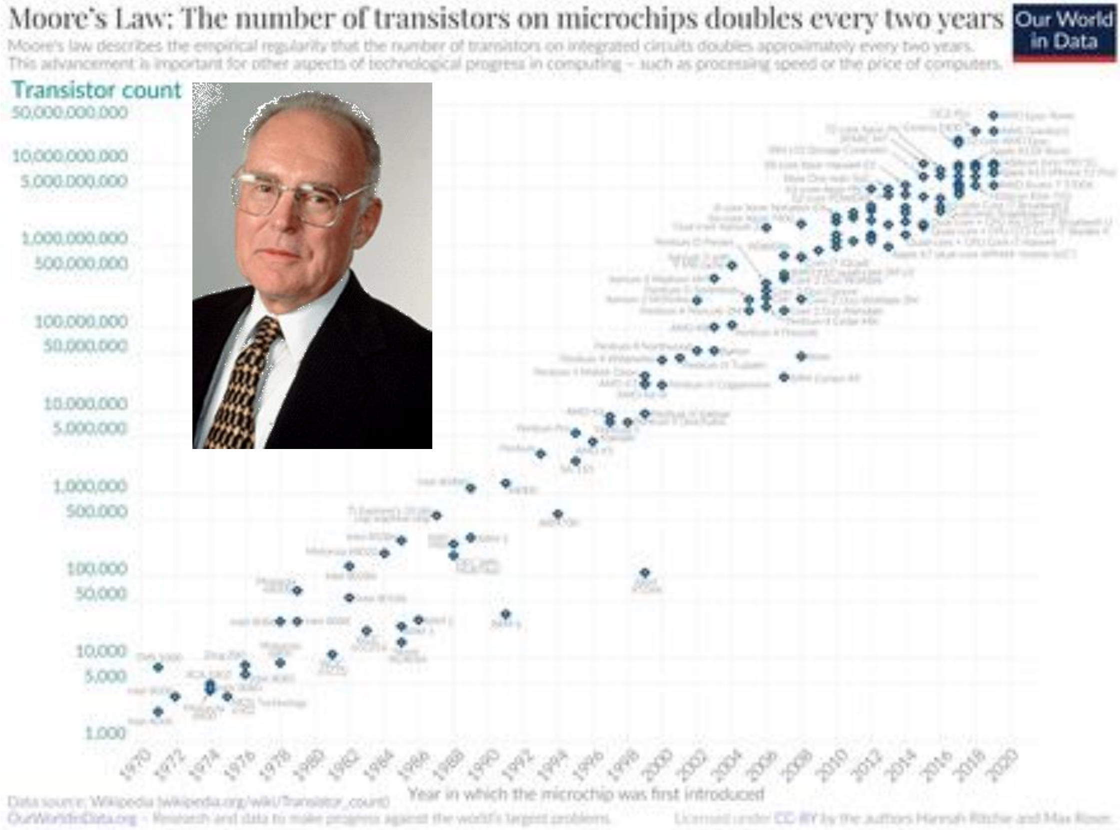

https://en.wikipedia.org/wiki/Moore%27s_law

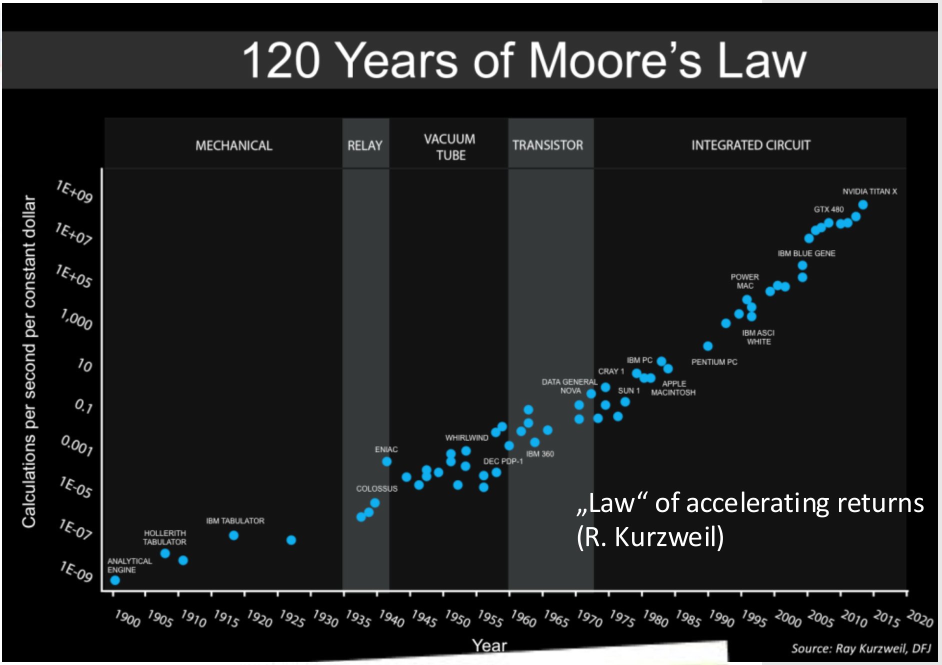

„Law" of accelerating returns
(R. Kurzweil)

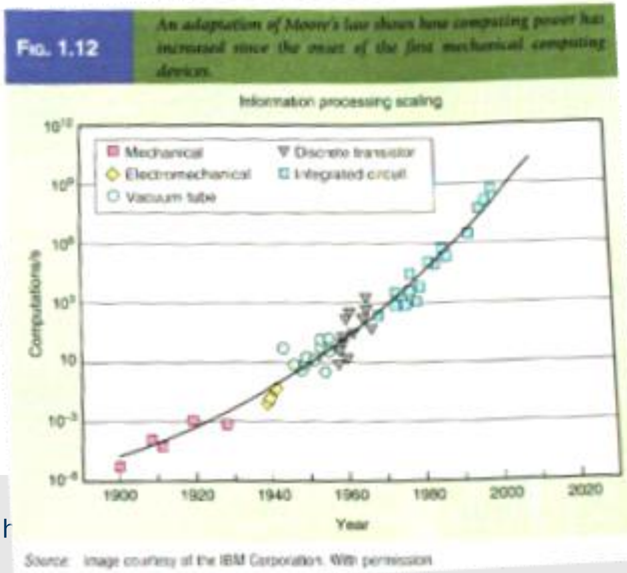

Fig. 1.12 An adaptation of Moore's law shows how computing power has increased since the onset of the first mechanical computing devices.

Source: Image courtesy of the IBM Corporation. With permission

The logic density of Si integrated circuits (ICs) has followed a curve (bits per square inch/transistors) = $2^{(t - 1962)}$ where t is the year. The amounts of information storable on a given amount of Si roughly doubled every year since the technology was invented. This relation, first mentioned in 1964 by semiconductor engineer Gordon Moore (co-founder of Intel) held until the late 1970s, at which point the doubling period slowed to 18 months. The doubling period remained at that value up to late 1999.

MEMS und Nanotechnologie

Miniaturisierung und Funktionsintegration

Miniaturisierung integrierter Schaltungen

Abmessungen für Transistoren

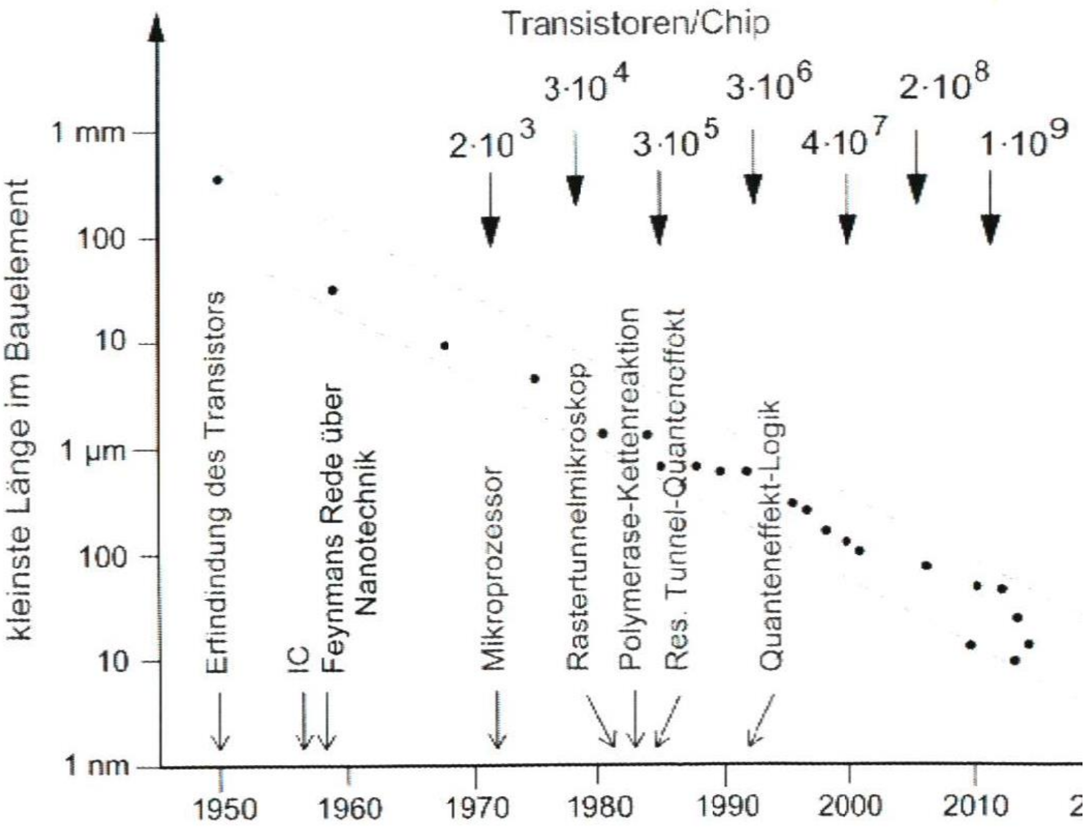

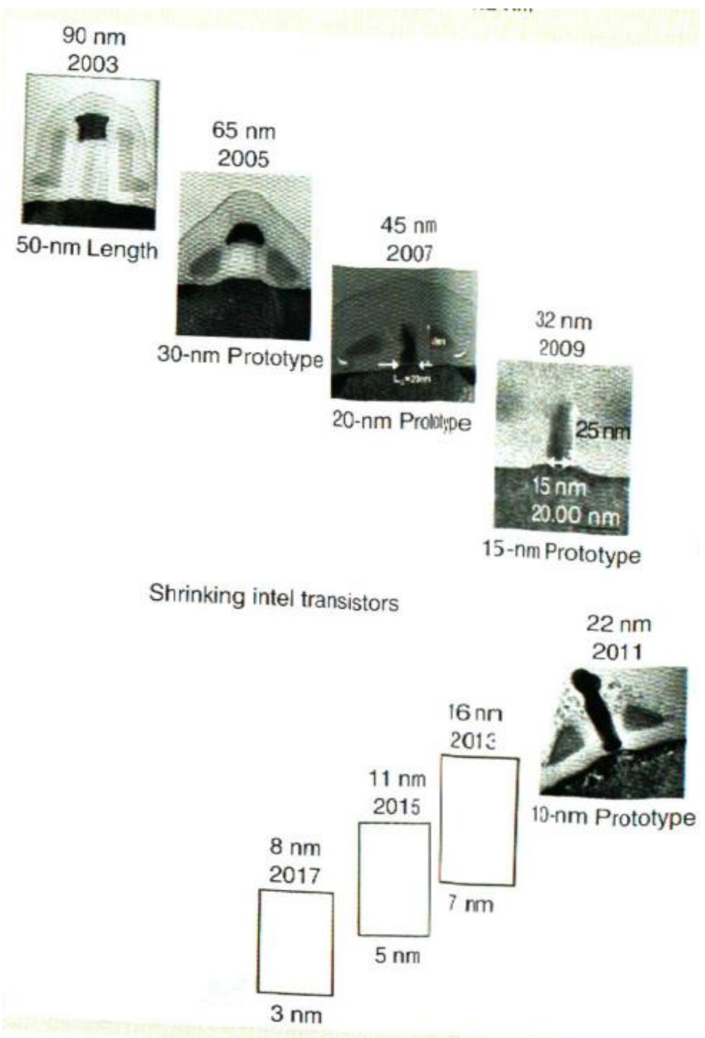

Shrinking intel transistors

d with permission of George Thompson, Intel Corporation.

Quellen: Fahrner 2003; Hornyak, Dutta, Tibbals, Rao 2008

MEMS und Nanotechnologie

Miniaturisierung und Funktionsintegration

Miniaturisierung integrierter Schaltungen

Abmessungen für Transistoren

Saturday, December 14, 2024

Intel Unveils 6 nm Gate Length Silicon RibbonFET CMOS and Breakthroughs in Semiconductor Scaling at IEDM 2024

Intel Corporation / Intel Foundry has demonstrated and extensively characterized gate-all-around Silicon RibbonFET CMOS transistors with a 6 nm gate length (LG). The study showcases nanoribbon silicon thickness (Tsi) scaling down to 3 nm, enhancing short-channel effects without compromising performance. Effective workfunction engineering mitigates threshold voltage increases caused by quantum confinement at scaled Tsi, enabling reduced threshold voltage at highly scaled gate lengths. Injection velocity of 1.13x10^7 cm/s is maintained at LG=6nm without degradation down to Tsi=3 nm, highlighting advancements crucial for continued gate length scaling and the ongoing realization of Moore's Law.

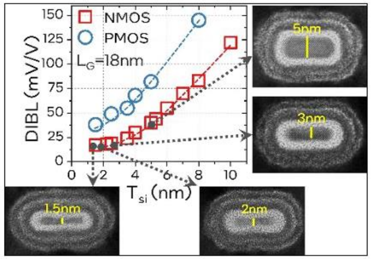

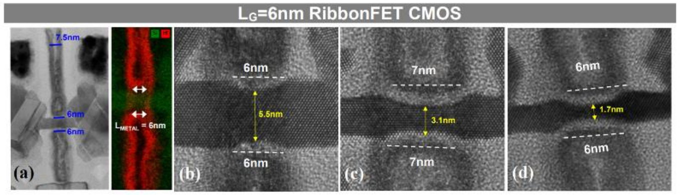

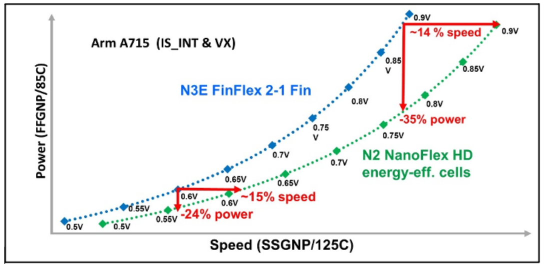

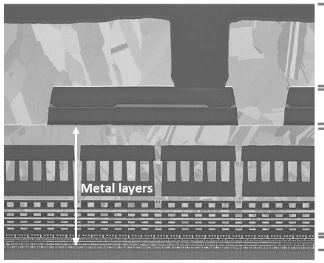

Cu RDL and passivation: Lower R, better perf., robust CPI and higher D2D IO density for seamless 3DIC integration

~> 200fF/mm² SHP-MiM with Cu RDL for robust power delivery

MoL/BEOL offering ~20% RC reduction and optimized rules for densest designs

N2 NS transistors offers excellent energy efficiency and NanoFlex innovations

TSMC's New, Industry-Leading 2nm CMOS Logic Platform: In a late-news paper, TSMC researchers will unveil the world's most advanced logic technology. It is the company's forthcoming 2nm CMOS (i.e., N2), platform, designed for energy-efficient computing in AI, mobile, and HPC applications. It offers a 15% speed gain (or 30% power reduction) at >1.15x chip density versus the most advanced logic technology currently in production, TSMC's own 3nm CMOS (N3) platform, introduced in late 2022.

The new N2 platform features GAA nanosheet transistors; middle-/back-end-of-line interconnects with the densest SRAM macro ever reported (~38Mb/mm²); and a holistic, system-technology co-optimized (STCO) architecture offering great design flexibility. That architecture includes a scalable copper-based redistribution layer and a flat passivation layer (for better performance, robust CPI, and seamless 3D integration); and through-silicon vias, or TSVs (for power/signal with F2F/F2B stacking). The researchers say the N2 platform is currently in risk production and scheduled for mass production in 2H' 25. N2P (5% speed enhanced version of N2) targets to complete qualification in 2025 and mass production in 2026.

At left above is a graph showing that the new N2 high-density cells gain 14~15% speed@power vs. N3E FinFlex 2-1 fin cells across the V_{dd} range; a 35% power savings at higher voltage; and a 24% power savings at lower voltage.

At right above, the cross-sectional image shows that the N2 platform's Cu redistribution layer (RDL) and passivation provide seamless integration with 3D technologies.

(Paper #2.1, "*2nm Platform Technology Featuring Energy-Efficient Nanosheet Transistors and Interconnects Co-Optimized with 3DIC for AI, HPC and Mobile SoC Applications*," G. Yeap et al, TSMC)

Extremely Scaled Transistors from Intel: Intel researchers will show that silicon can continue to support the extreme gate length scaling which future technology nodes require. They will describe how they built RibbonFET CMOS transistors (Intel's version of nanosheets) with 6nm gate lengths at 45nm contacted poly pitch (CPP, the spacing between adjacent transistor gates), with no degradation of electron mobility (how fast electrons can move through a material). The researchers will show that electron mobility doesn't degrade until 3nm T_{si} (silicon thickness below which electron scattering due to surface roughness becomes an issue. They will describe how they achieved good short channel control (≤100mV/V at <4nm T_{si}), with extremely low threshold voltage at these gate lengths through clever workfunction engineering. The work shows that 3nm is a practical scaling limit for RibbonFETs.

The top image illustrates the behavior of drain-induced barrier lowering (DIBL) vs. silicon thickness (T_{si}) at L_G=18nm. It shows a reduction as T_{si} is scaled from 10nm to 1.5nm; however, DIBL reduction saturates at T_{si} <4nm, below which very little gain is obtained. PMOS DIBL is elevated vs. NMOS DIBL at the same T_{si}. Also shown are TEM micrographs of a 1NR transistor with various T_{si} values down to 1.5nm.

The bottom series of images are (a) TEM micrograph and EDX scan of a completed 6nm RibbonFET device on a 1NR vehicle, showing a disconnected subfin; (b - d) are high-resolution cross-section TEMs for T_{si}=5.5nm, 3.1nm and 1.7nm respectively, at 6nm gate length on a 1NR vehicle

(Paper #2.2, "*Silicon RibbonFET CMOS at 6nm Gate Length*," A. Agrawal et al, Intel)

https://www.blog.baldengineering.com/search/label/CMOS%20Scaling

MEMS und Nanotechnologie

Miniaturisierung in der Datenspeicherung

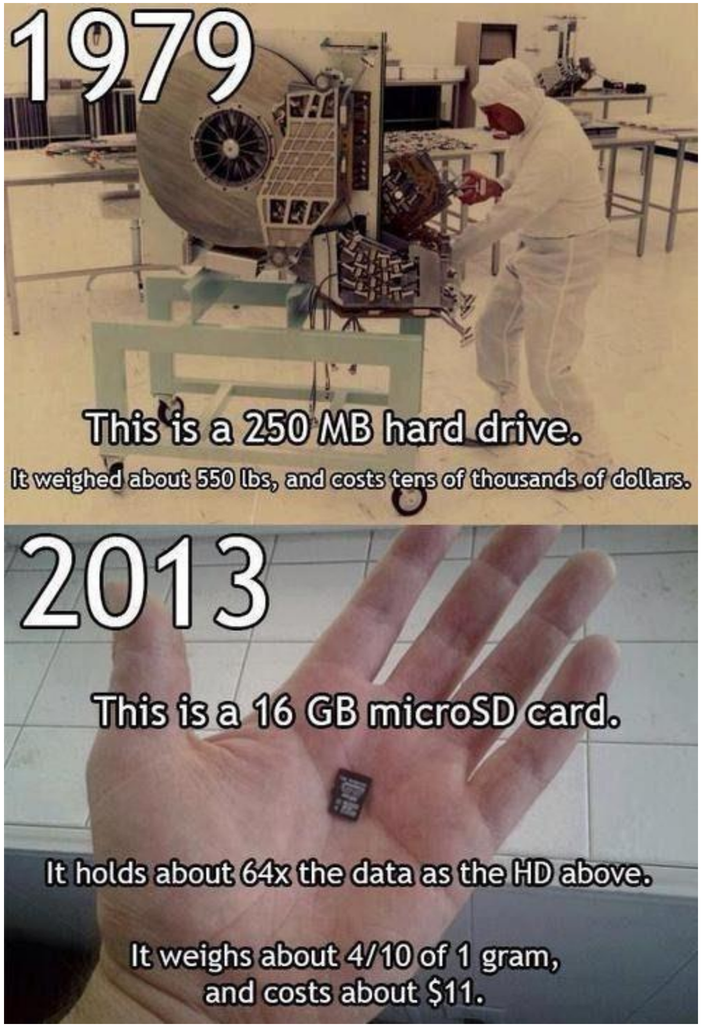

This is a 250 MB hard drive.

It weighed about 550 lbs, and costs tens of thousands of dollars.

This is a 16 GB microSD card.

It holds about 64x the data as the HD above.

It weighs about 4/10 of 1 gram, and costs about $11.

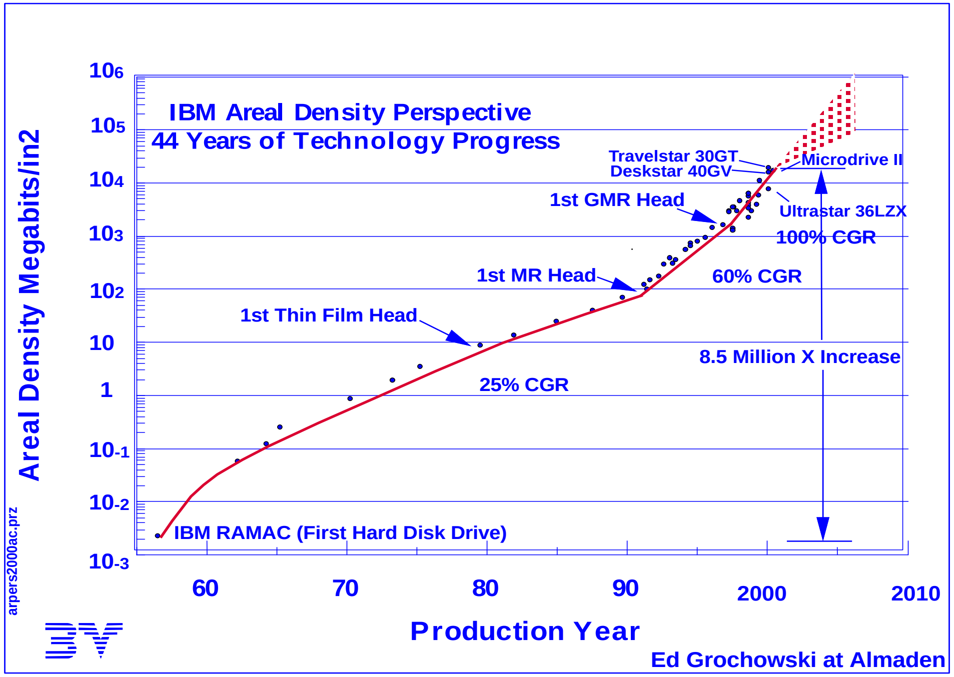

Wieviele nm^2 für ein magnetisches Bit?

Miniaturisierung in der magnetischen Datenspeicherung

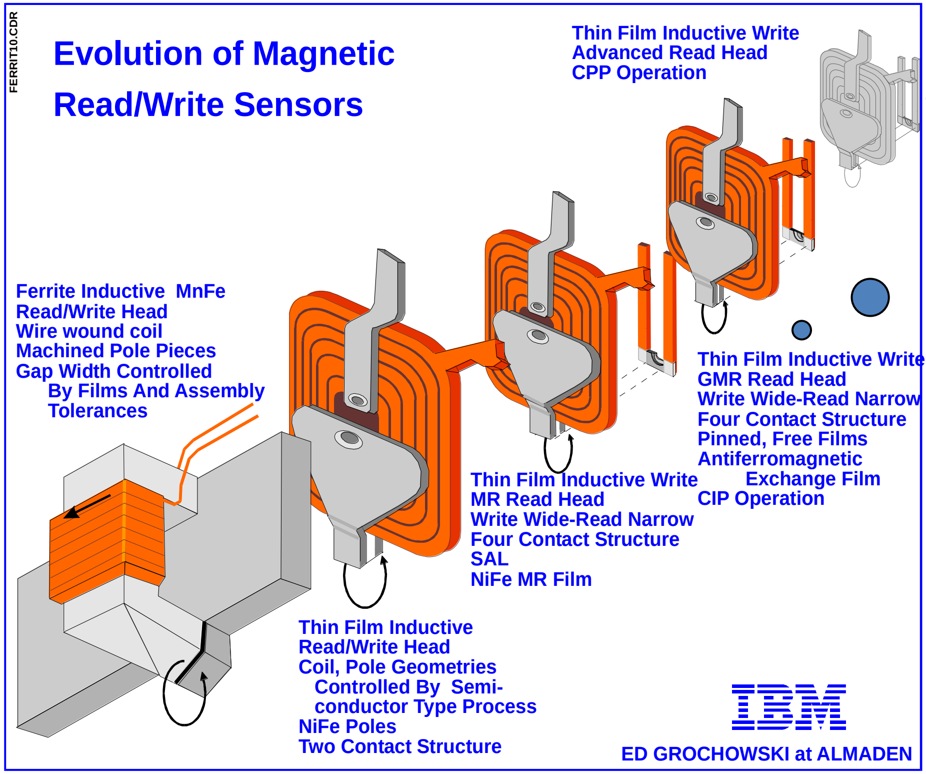

Decisive materials: Magnetic thin films

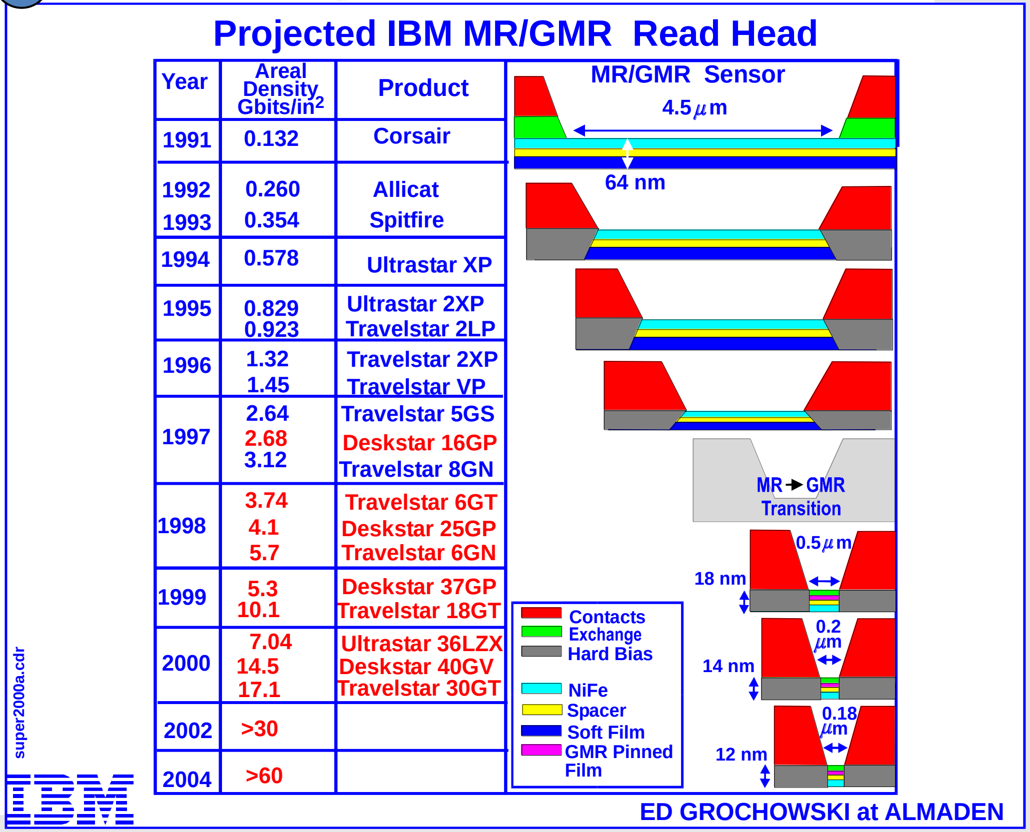

Projected IBM MR/GMR Read Head

Year	Areal Density Gbits/in²	Product
1991	0.132	Corsair
1992	0.260	Allicat
1993	0.354	Spitfire
1994	0.578	Ultrastar XP
1995	0.829 0.923	Ultrastar 2XP Travelstar 2LP
1996	1.32 1.45	Travelstar 2XP Travelstar VP
1997	2.64 2.68 3.12	Travelstar 5GS Deskstar 16GP Travelstar 8GN
1998	3.74 4.1 5.7	Travelstar 6GT Deskstar 25GP Travelstar 6GN
1999	5.3 10.1	Deskstar 37GP Travelstar 18GT
2000	7.04 14.5 17.1	Ultrastar 36LZX Deskstar 40GV Travelstar 30GT
2002	>30	
2004	>60	

Advanced Materials Processing and Microfabrication

Nanotechnolgie: Einheiten

1 Mikrometer	**1 µm**	**10^{-6} m**
1 Nanometer	**1 nm**	**10^{-9} m**
1 Angstrom	**0.1 nm**	**10^{-10} m**
1 Picometer	**1 pm**	**10^{-12} m**

Wie viele Atome passen in 1 nm^3, in 1 $µm^3$, in 1 mm^3 ?

MEMS und Nanotechnologie

Dimensionalität von Systemen

Größenordnungen, MEMS

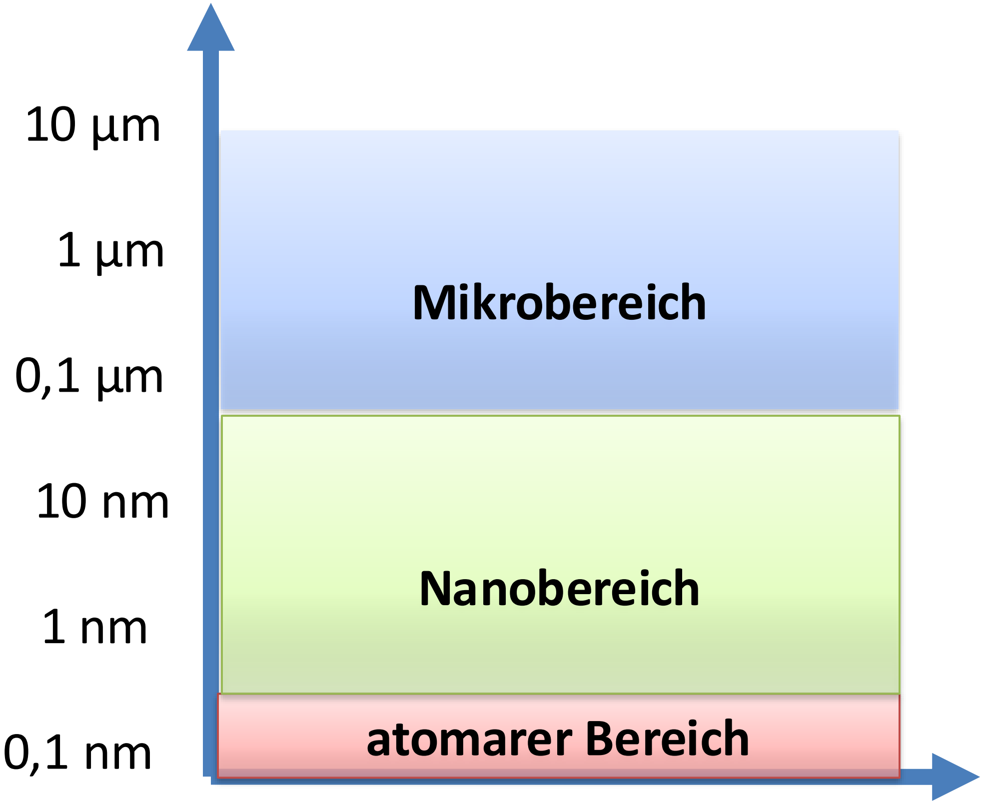

10 µm

1 µm

0,1 µm

10 nm

1 nm

0,1 nm

Mikrobereich

Nanobereich

atomarer Bereich

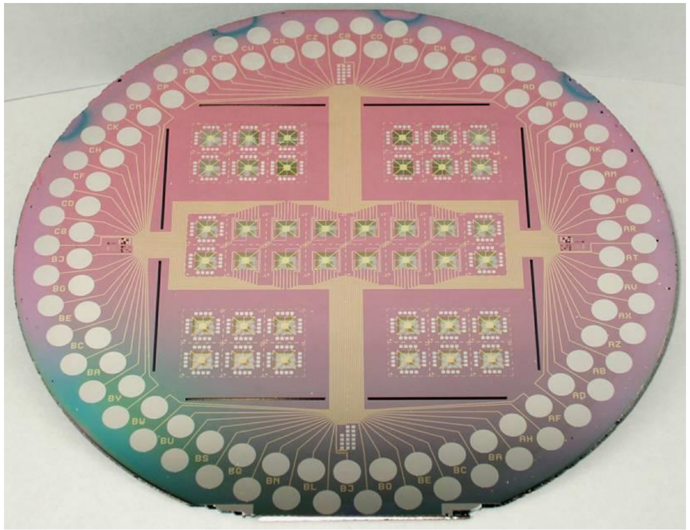

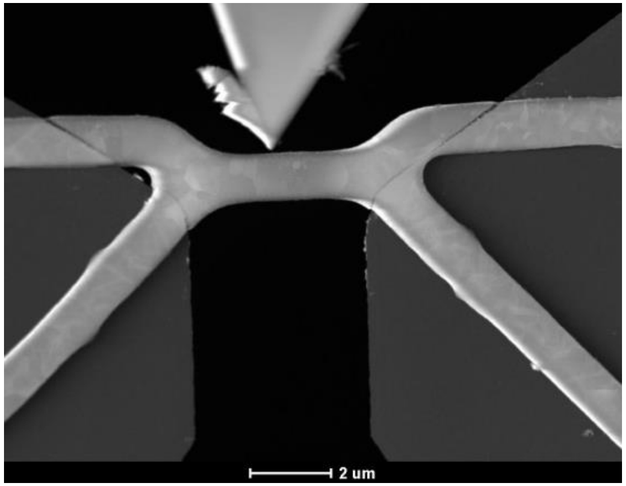

Größenordnungen bei Werkstoffen

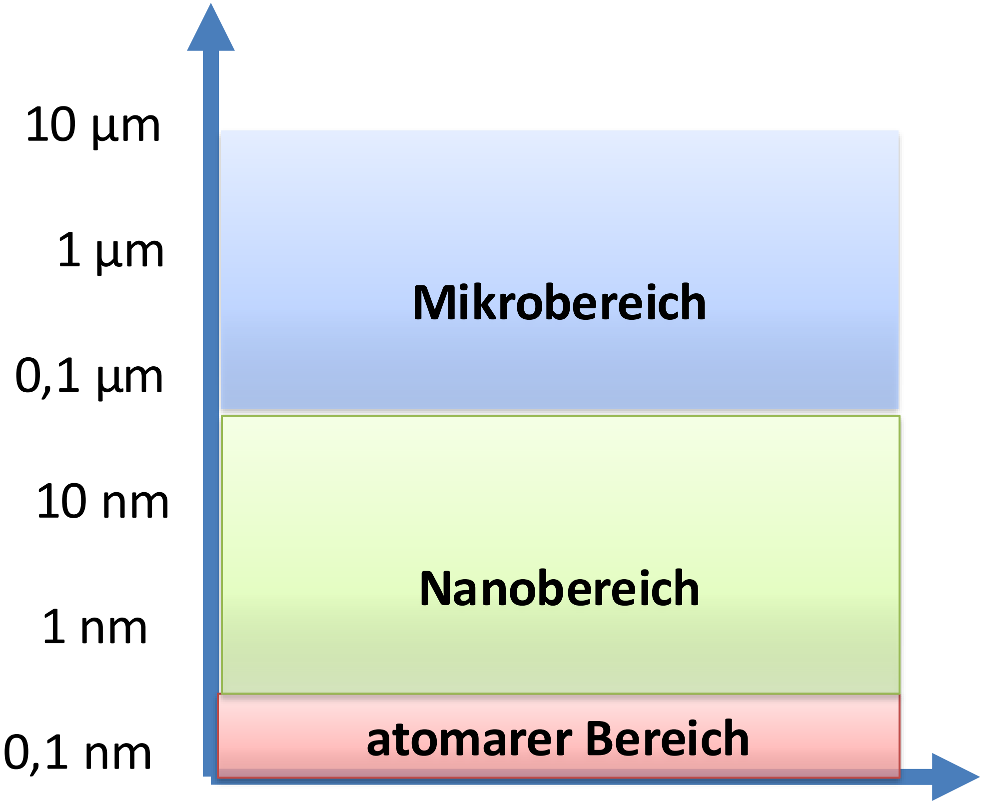

10 µm

1 µm

0,1 µm

10 nm

1 nm

0,1 nm

Mikrobereich

Nanobereich

atomarer Bereich

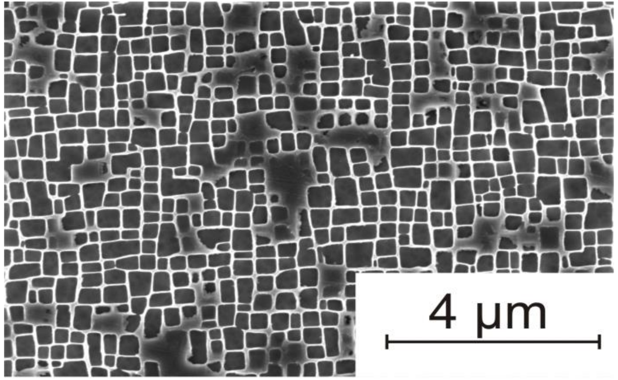

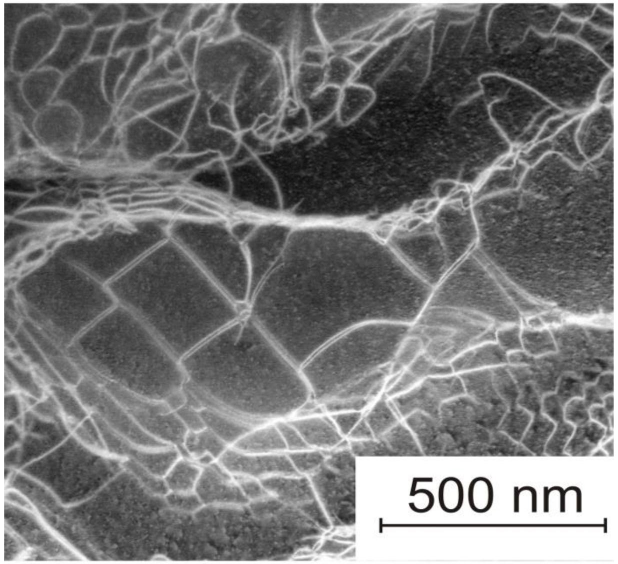

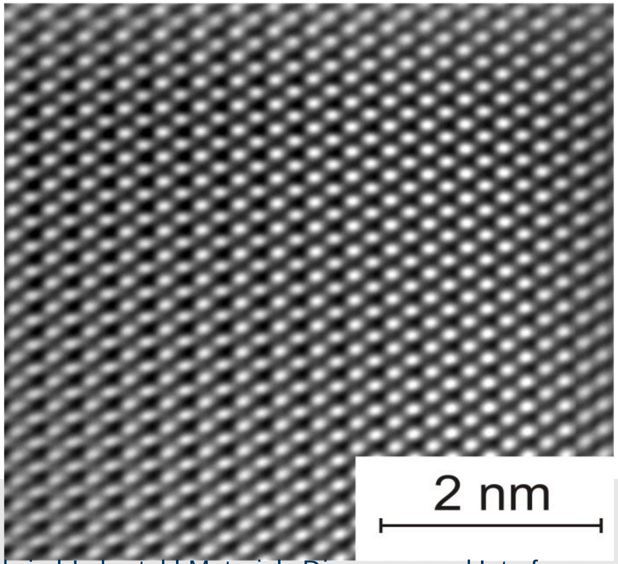

z.B. Super-legierungen

Dimensionalität von Systemen

Von 3D zu 0D und zurück

Dimensionalität	Form des Materials	Materialwissenschaft
3D	„Bulk“-Material	Ausscheidung
2D	Dünne Schicht	Korngrenze
1D	Nanodraht	Versetzung
0D	Quantenpunkt	Fremdatom

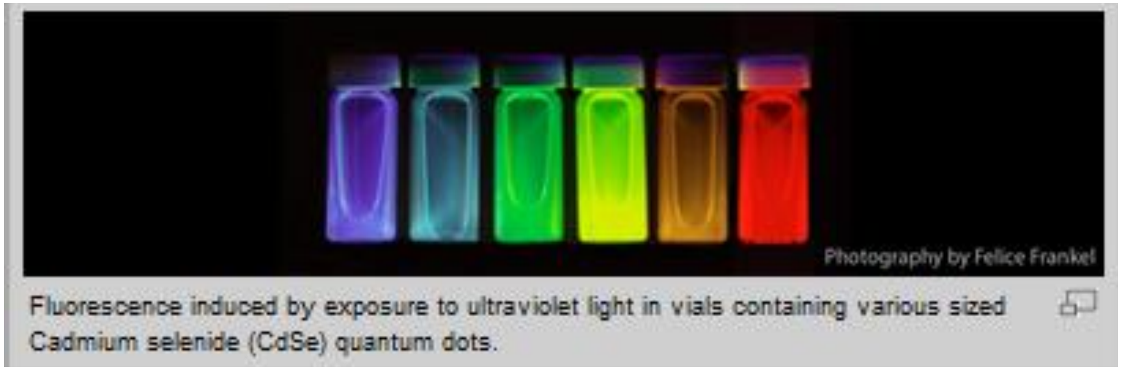

Fluorescence induced by exposure to ultraviolet light in vials containing various sized Cadmium selenide (CdSe) quantum dots.

http://nanocluster.mit.edu/research.php#Spectroscopy

Von MEMS zu NEMS

MEMS: **M**icro **E**lectro **M**echanical **S**ystems

NEMS: **N**ano **E**lectro **M**echanical **S**ystems

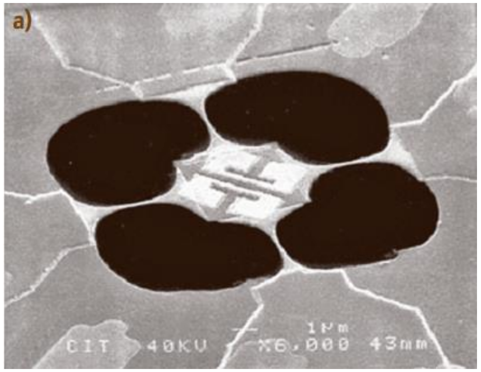

Suspended phonon device for measuring ballistic phonon transport. Four Si_3N_4 membranes (60 nm thick, < 200 nm wide) hold a 4x4 µm² „phonon cavity“. The big, bright „C“-shaped objects at the „phonon cavity“ are Cr/Au thin film heating and sensing resistors.

Source: Springer Handbook of Nanotechnolog

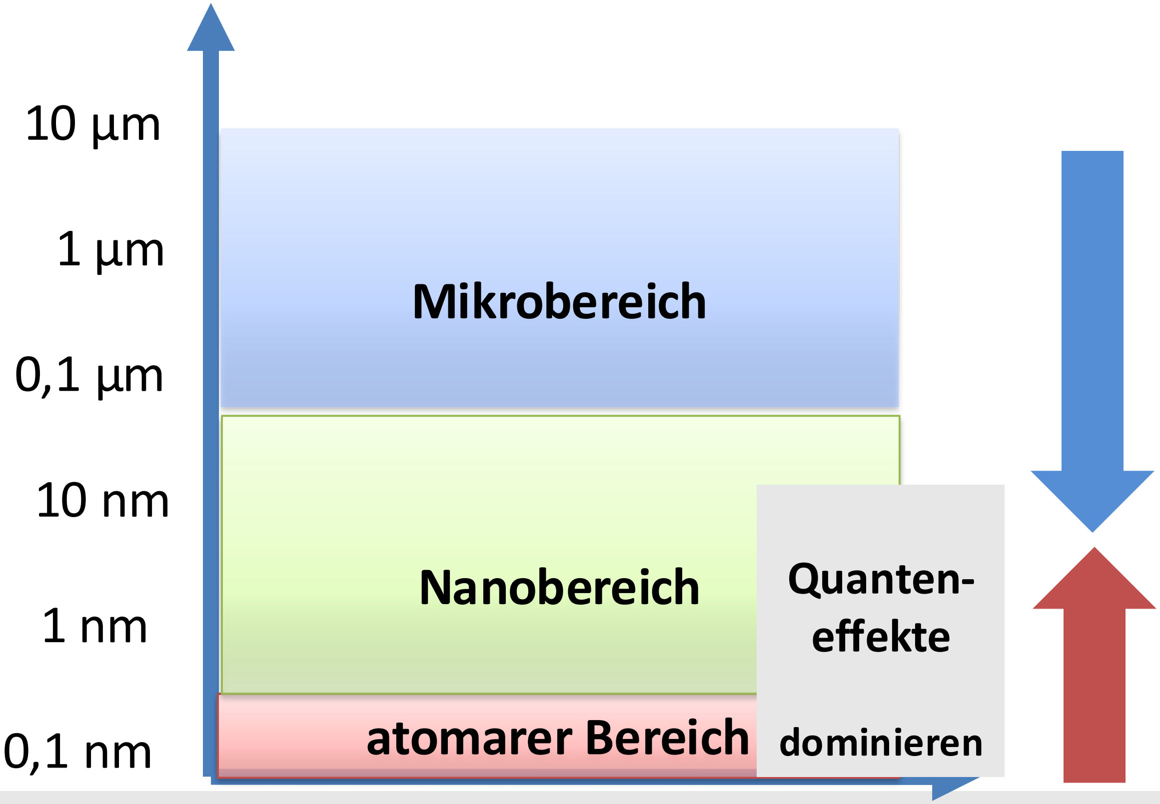

„top down“ Ansatz

Figure 4.4 The convergence of top-down and bottom-up production techniques (Whatmore 2001)

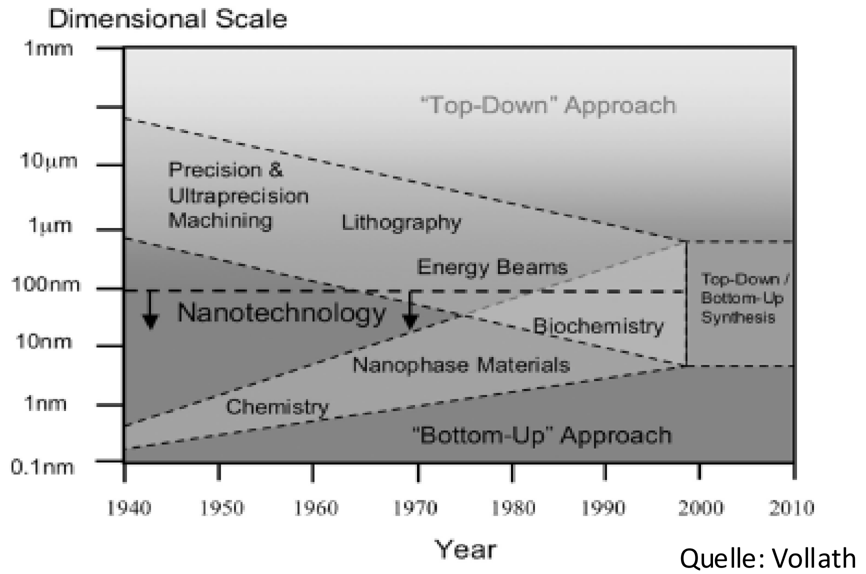

Quelle: Vollath

„bottom up“ Ansatz

Von MEMS zu NEMS

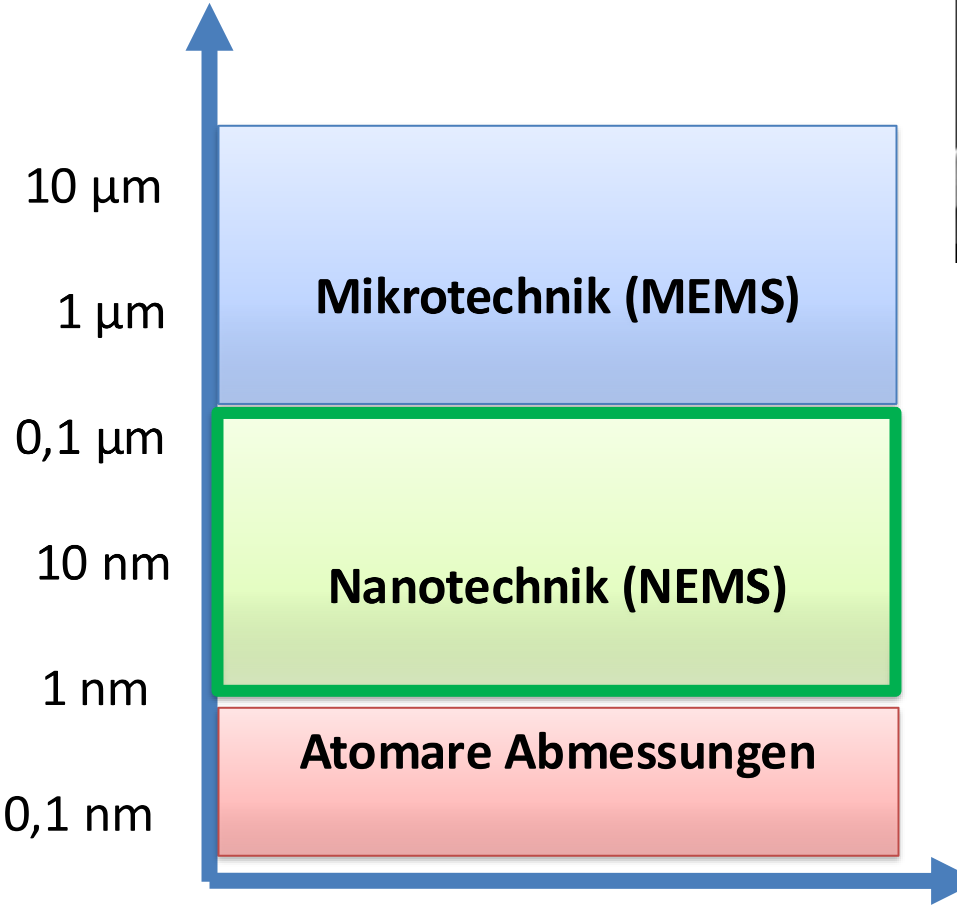

Mikrotechnik (MEMS)

Nanotechnik (NEMS)

Atomare Abmessungen

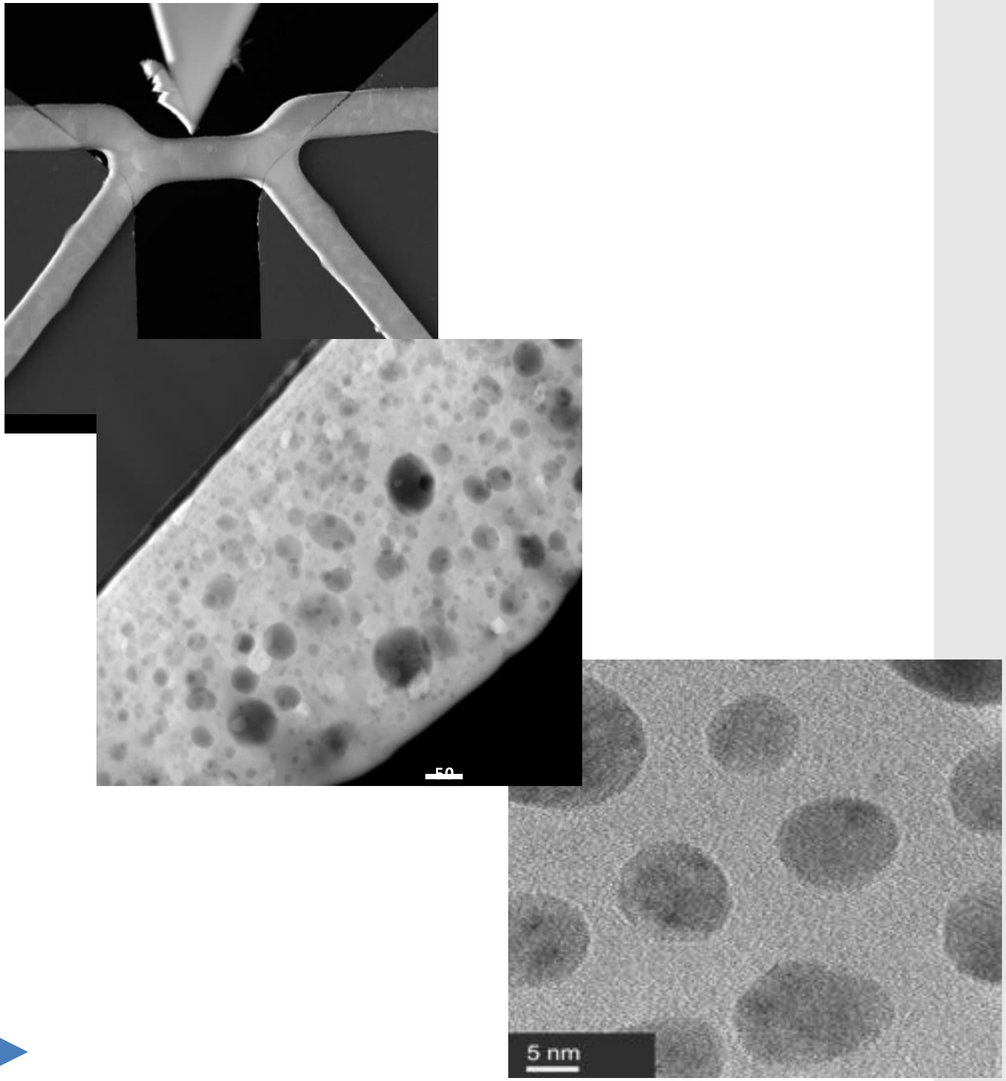

Konzepte der Nanotechnologie
„bottom up“ und „top down“ Ansätze

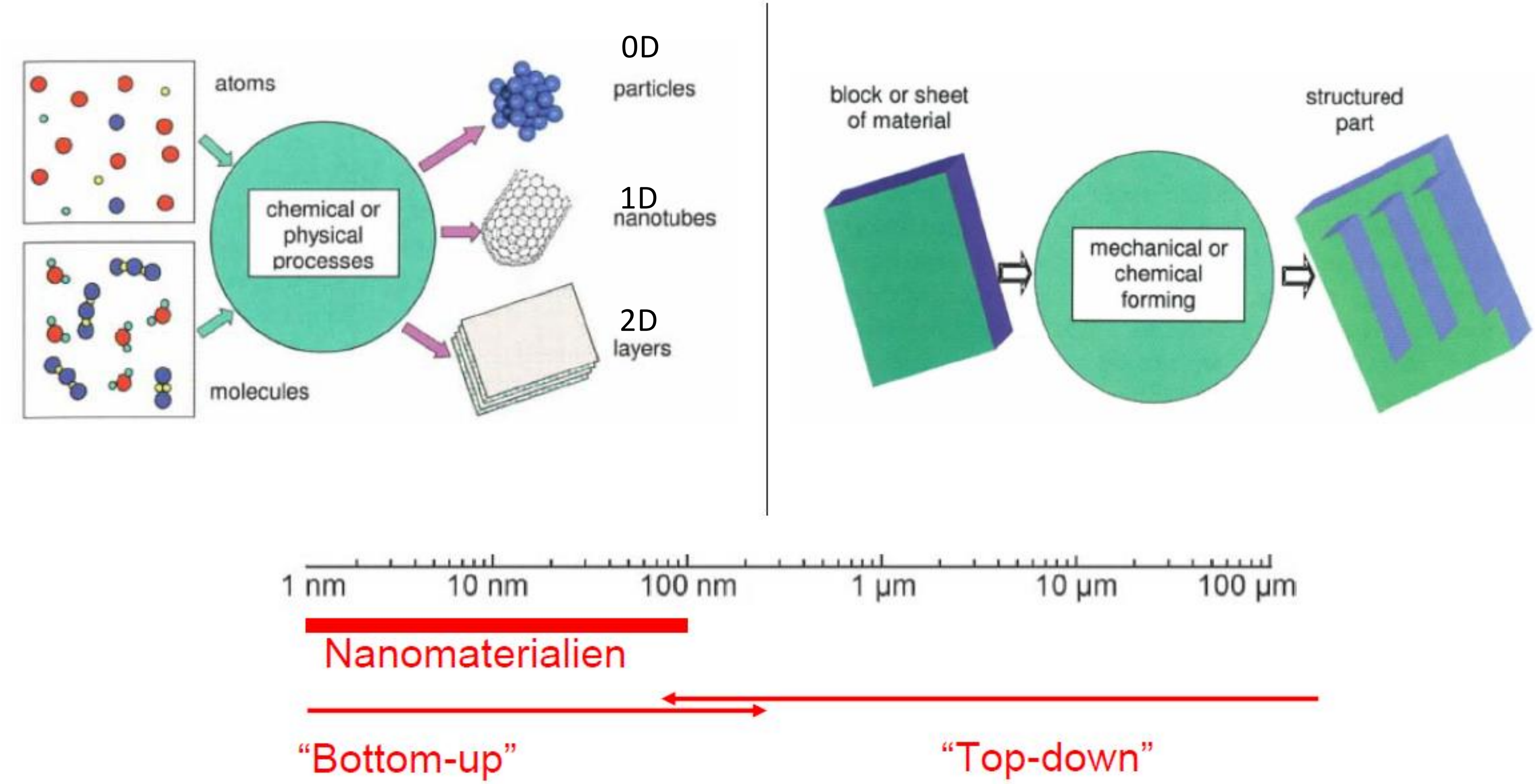

Quelle: Behrens

Nanotechnologie: Meilensteine und Personen

1930s:

Scanning electron microscopy and **transmission electron microscopy**:

E. Ruska, M. Knoll, M. von Ardenne

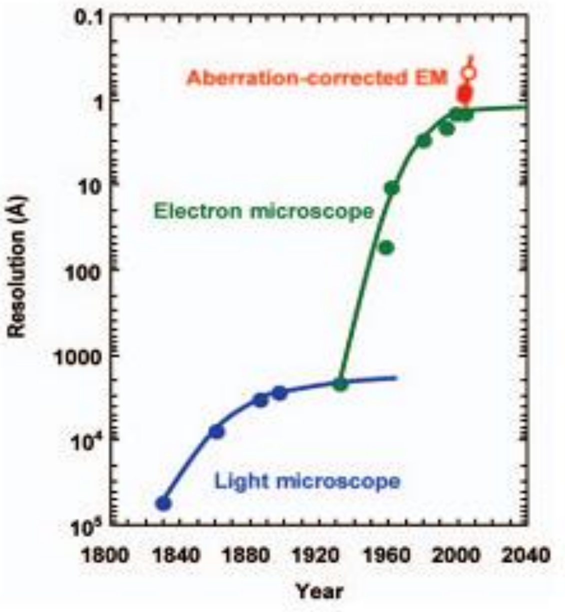

Figure 1. The evolution of resolution in microscopy (after H. Rose, adapted from Reference 2). The open circle is the predicted resolution for the next-generation fifth-order correctors currently under development.

MRS BULLETIN • VOLUME 31 • JANUARY 2006

Materials Advances through Aberration-Corrected Electron Microscopy

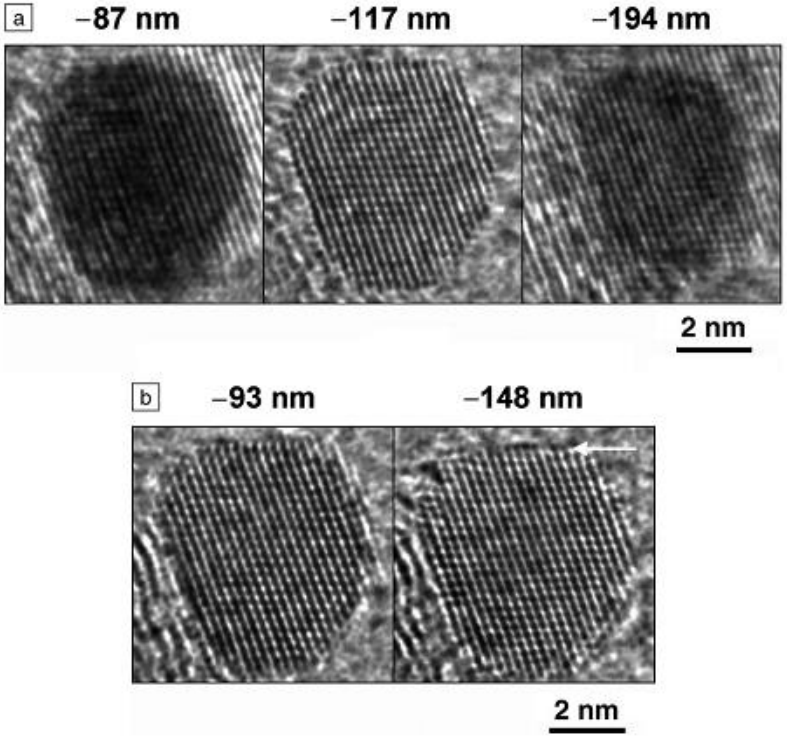

Figure 9. (a) Through-focal series of images of a nanocrystalline Pt particle supported on partially graphitized carbon with a spherical aberration of 450 µm. (b) Equivalent focal series of the same particle after aberration correction with a spherical aberration of −20 µm. In both (a) and (b), defocus values are indicated, with negative values corresponding to underfocus. In (a), extensive contrast delocalization as a function of defocus is observed, which is eliminated in (b). A partially complete surface layer is marked with an arrow in (b).

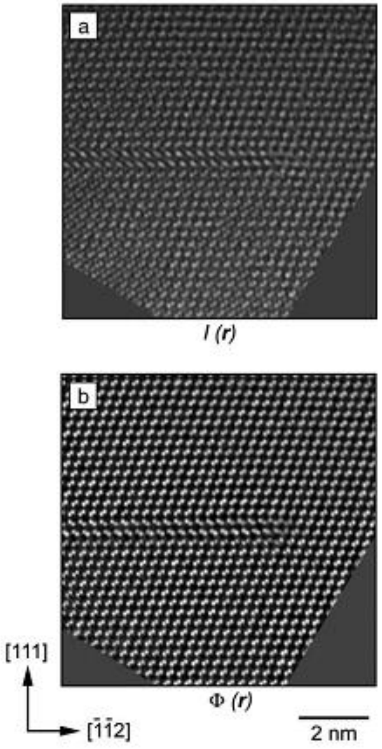

Figure 10. Multiple stacking fault in GaAs laterally bound by a partial dislocation. (a) Optimum defocus image, I(r). (b) Reconstructed exit plane phase, Φ(r), showing enhanced contrast and lower noise levels. (Reproduced with

Nanotechnologie: Meilensteine und Personen

Ideen und Konzepte

Richard Feynmann (USA):
1959: „There is plenty of room at the bottom“

“the problem of manipulating and controlling things on a small scale”

“Why cannot we write the entire 24 volumes of the Encyclopedia Brittanica on the head of a pin?”

“what is possible in principle---
in other words, what is possible according to the laws of physic”

Task: Read Feynmans speech and think about what has been realized untill today

Transcript of the classic talk that Richard Feynman gave on December 29th 1959 at the annual meeting of the American Physical Society at the California Institute of Technology (Caltech) was first published in the Feb. 1960 issue of Caltech's *Engineering and Science*, which owns the copyright. It is available at http://www.zyvex.com/nanotech/feynman.html.

http://www.youtube.com/watch?v=4eRCygdW--c

Nanotechnologie: Meilensteine und Personen

1974: Prof. Norio Taniguchi (Tokio): A definition of nanotechnology

„**Nanotechnology** mainly consists of the processing of separation, consolidation, and deformation of materials *by one atom or one molecule*.“

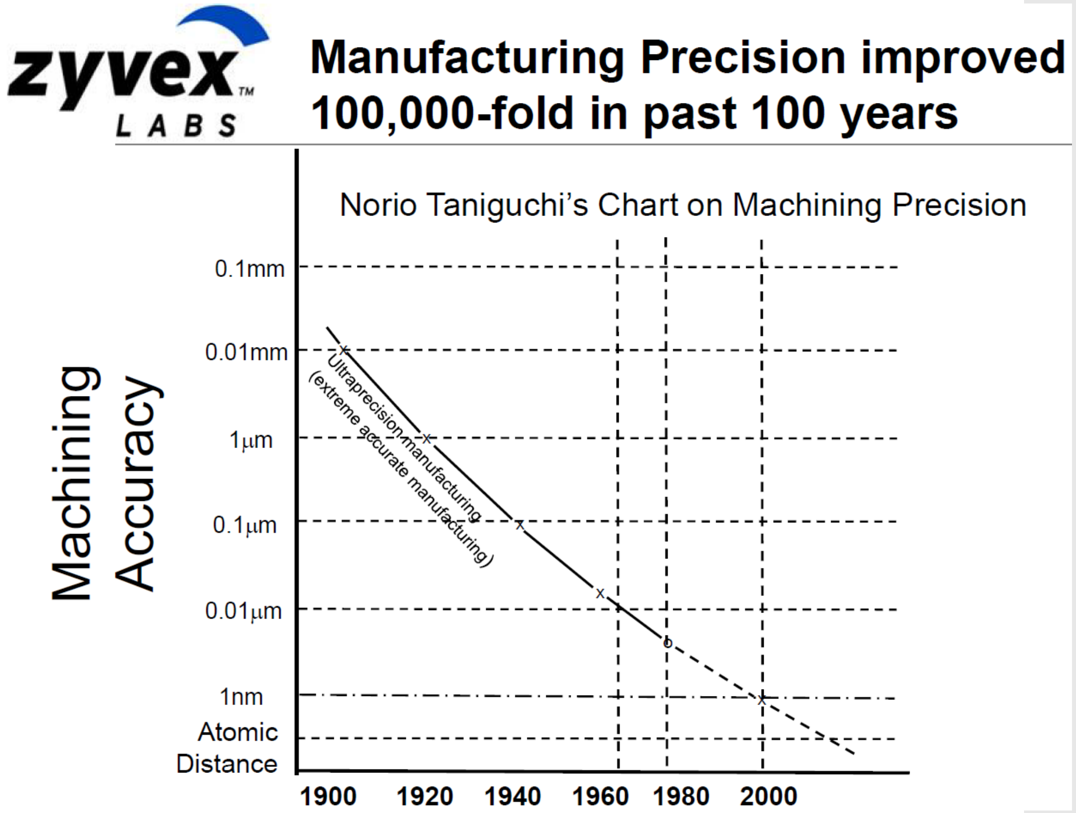

Nanotechnologie: Meilensteine und Personen

1981: **Scanning tunneling microscopy** (STM):
Gerd Binnig und Heinrich Rohrer, IBM Zürich

Technology

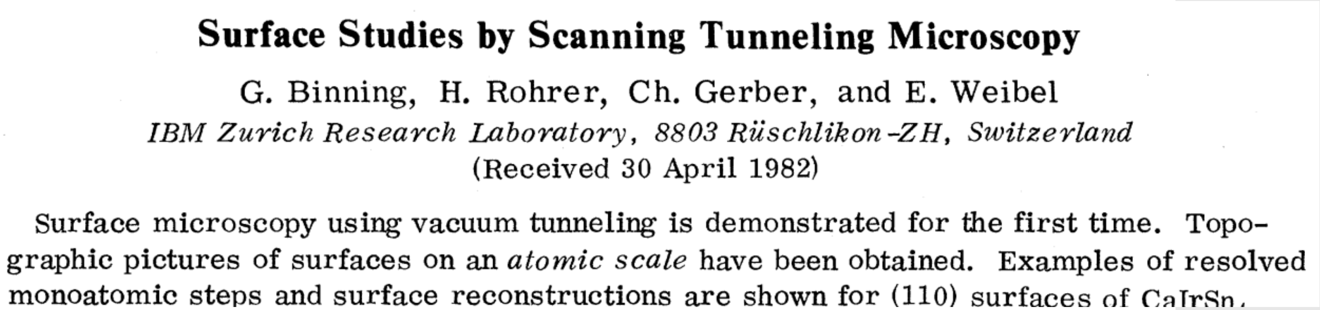

Surface Studies by Scanning Tunneling Microscopy

G. Binning, H. Rohrer, Ch. Gerber, and E. Weibel
IBM Zurich Research Laboratory, 8803 Rüschlikon-ZH, Switzerland
(Received 30 April 1982)

Surface microscopy using vacuum tunneling is demonstrated for the first time. Topographic pictures of surfaces on an *atomic scale* have been obtained. Examples of resolved monoatomic steps and surface reconstructions are shown for (110) surfaces of CaIrSn

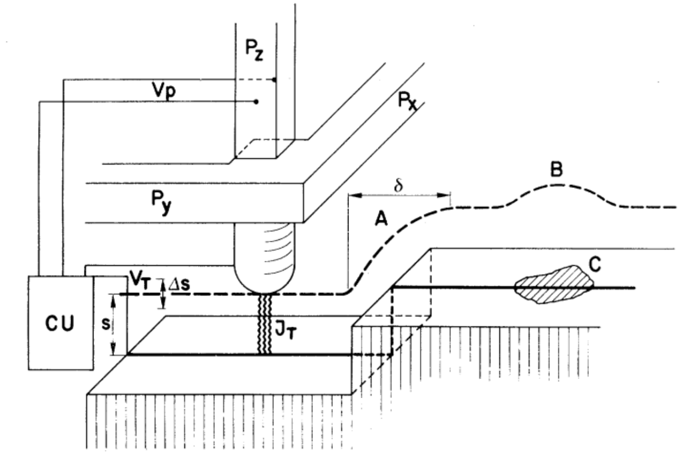

FIG. 1. Principle of operation of the scanning tunneling microscope. (Schematic: distances and sizes are not to scale.) The piezodrives P_x and P_y scan the metal tip M over the surface. The control unit (CU) applies the appropriate voltage V_p to the piezodrive P_z for constant tunnel current J_T at constant tunnel voltage V_T. For constant work function, the voltages applied to the piezodrives P_x, P_y, and P_z yield the topography of the surface directly, whereas modulation of the tunnel distance s by Δs gives a measure of the work function as explained in the text. The broken line indicates the z displacement in a y scan at (A) a surface step and (B) a contamination spot, C, with lower work function.

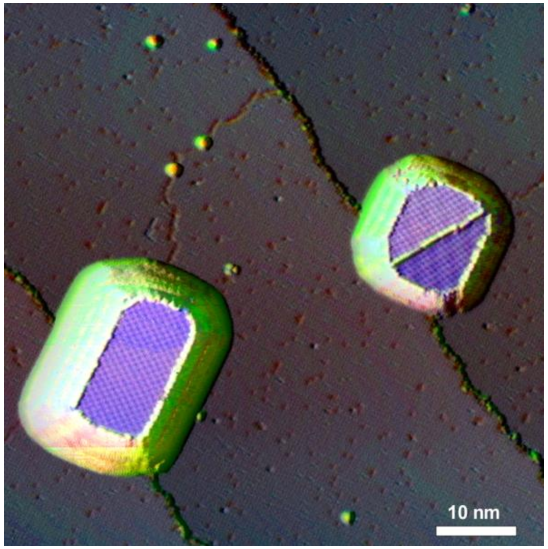

Samples need to be electrically conductive

Nanotechnologie: Meilensteine und Personen

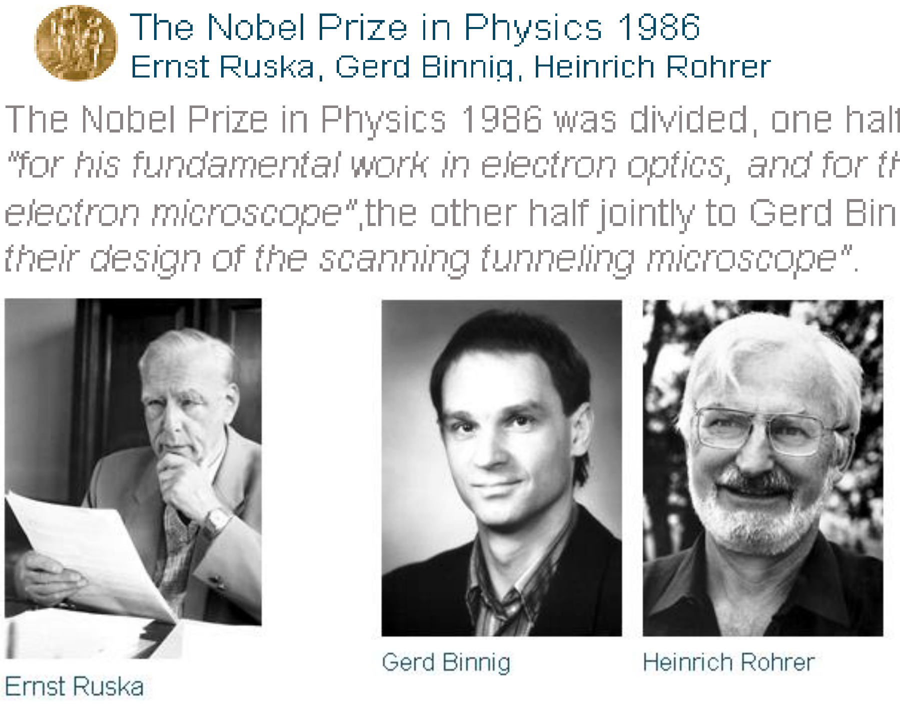

The Nobel Prize in Physics 1986
Ernst Ruska, Gerd Binnig, Heinrich Rohrer

The Nobel Prize in Physics 1986 was divided, one half awarded to Ernst Ruska *"for his fundamental work in electron optics, and for the design of the first electron microscope"*,the other half jointly to Gerd Binnig and Heinrich Rohrer *"for their design of the scanning tunneling microscope"*.

Ernst Ruska

Gerd Binnig

Heinrich Rohrer

http://nobelprize.org/nobel_prizes/physics/laureates/1986 /

Further Nobel Prizes related to Nanotechnology:
Chemistry 1996 – “*discovery of fullerenes*”,
molecules that approach the size of quantum dots ($C_{60} \approx 0.71$ nm)
Physics 2000 – “*developing semiconductor heterostructures used in highspeed-and opto-electronics*”
Physics 2010 – “*for groundbreaking experiments regarding the two-dimensional material graphene*”
Chemistry 2016 "*design and synthesis of molecular machines*"
Chemistry 2023 "*discovery and synthesis of quantum dots*"

Nanotechnologie: Meilensteine und Personen

Feynman spekulierte 1959 über die vermutliche Wirkung der Manipulation kleiner Teile verdichteter Materie

Gleiter macht 1981 in einem Vortrag auf das Arbeitsgebiet nanostrukturierter Materialien aufmerksam

Siegel bezeichnet 2001 diesen Vortrag als Wendepunkt, **Cahn** fügt 2001 hinzu, dass **Gleiter** das Arbeitsgebiet nanostrukturierter Materialien begründet hat

Der Wendepunkt wird gewöhnlich mit der Erfindung des STMs identifiziert, aber auch mit den Arbeiten von **Eigler** (willkürliche Verschiebung einzelner Atome) und **Drexler** (Visionär, Beginn der US-amerikanischen Nanotechnologie-Initiative)

Herbert Gleiter:
For discovery of **nanocrystalline materials** he received many prizes (Leibniz-Preis of DFG, Vinci of Excellence Award Hennessy-Vuitton-Stiftung, Max Planck Forschungspreis der Alexander-von-Humboldt-Stiftung, gold medal of Federation of European Materials Societies). 1998 director of the new Institute for Nanotechnology at KIT.

Nanomaterialien

Nanokristalline Metalle und Legierungen mit hohem Grenzflächenvolumen

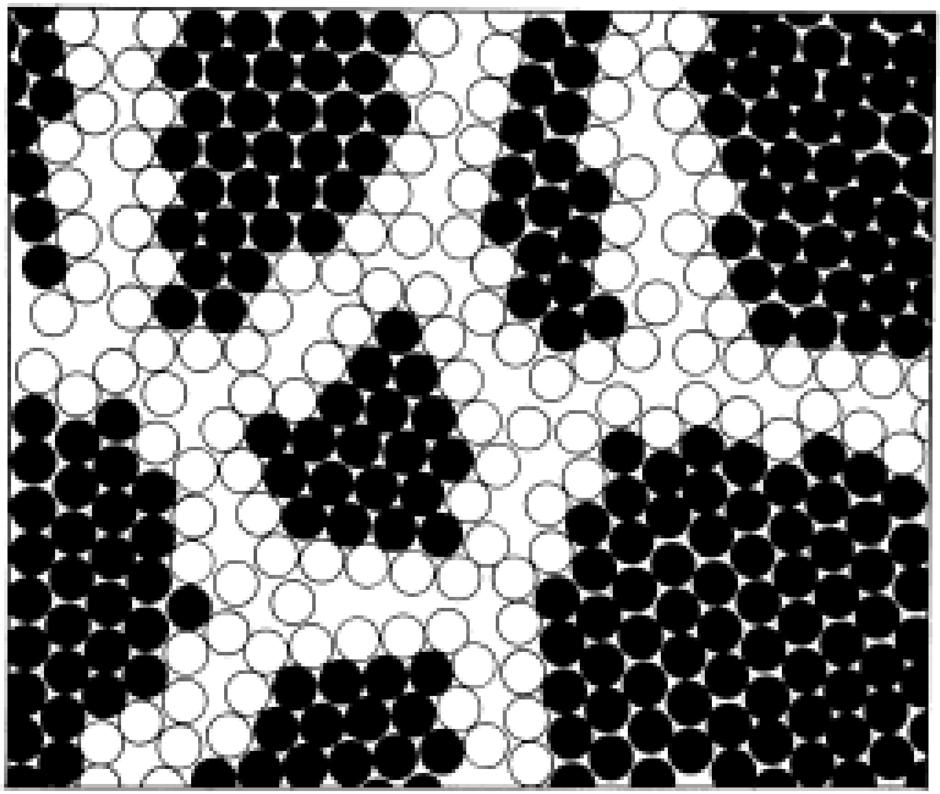

Fig. 2. Two-dimensional model of a nanostructured material. The atoms in the centers of the crystals are indicated in black. The ones in the boundary core regions are represented as open circles [13].

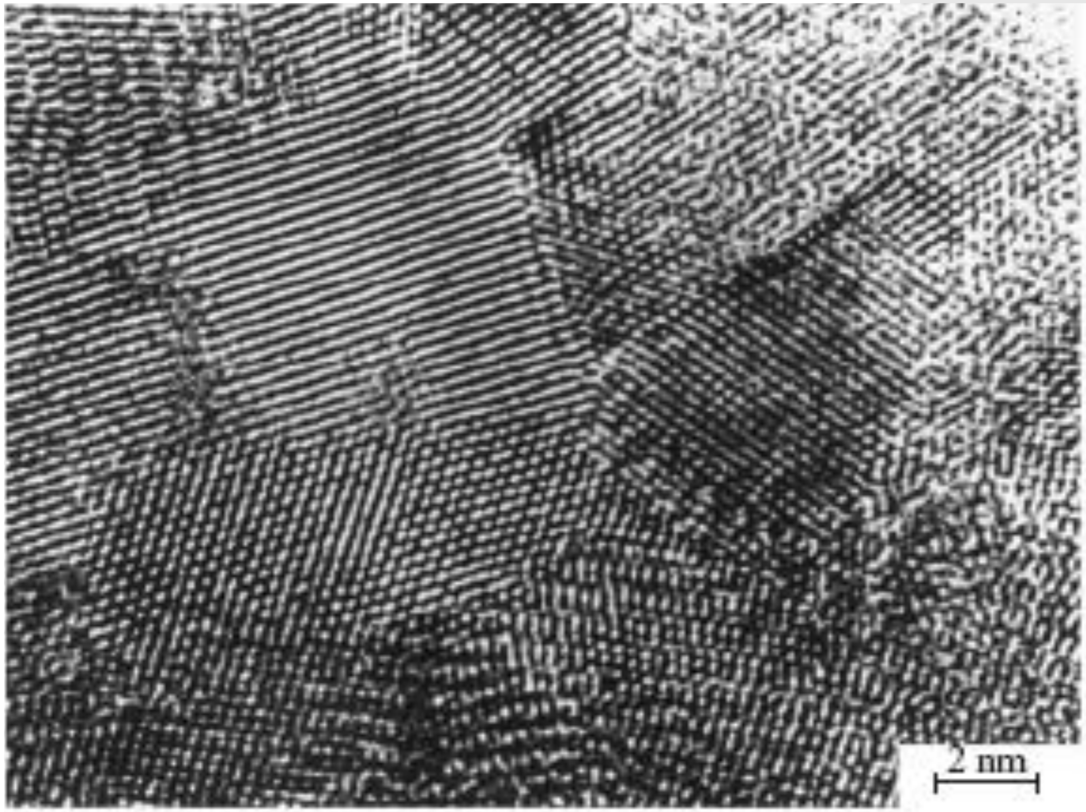

Figure 7
High-resolution TEM micrograph of nanocrystalline palladium.

Quelle: Gleiter

Nanotechnologie: Meilensteine und Personen

Ideas and concepts

1986:
K. Eric Drexler: Engines of Creation: The Coming Era of Nanotechnology
„Molecular nanotechnology“

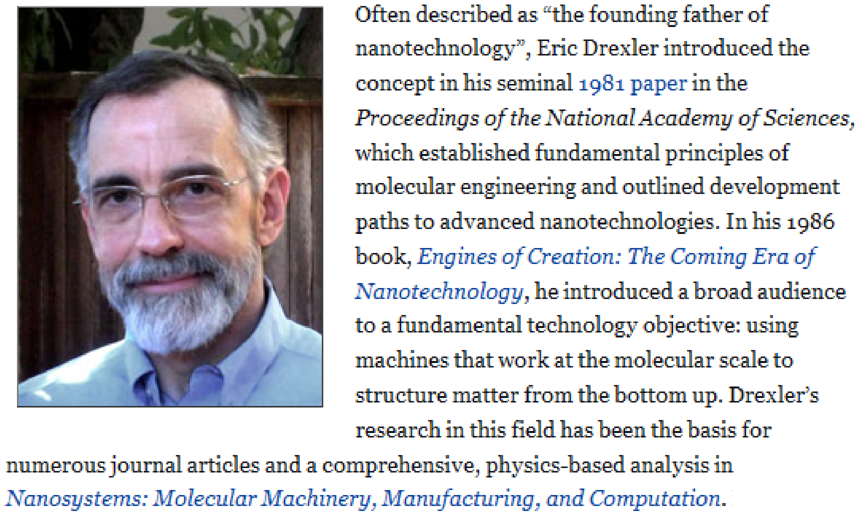

Often described as “the founding father of nanotechnology”, Eric Drexler introduced the concept in his seminal 1981 paper in the *Proceedings of the National Academy of Sciences*, which established fundamental principles of molecular engineering and outlined development paths to advanced nanotechnologies. In his 1986 book, *Engines of Creation: The Coming Era of Nanotechnology*, he introduced a broad audience to a fundamental technology objective: using machines that work at the molecular scale to structure matter from the bottom up. Drexler’s research in this field has been the basis for numerous journal articles and a comprehensive, physics-based analysis in *Nanosystems: Molecular Machinery, Manufacturing, and Computation*.

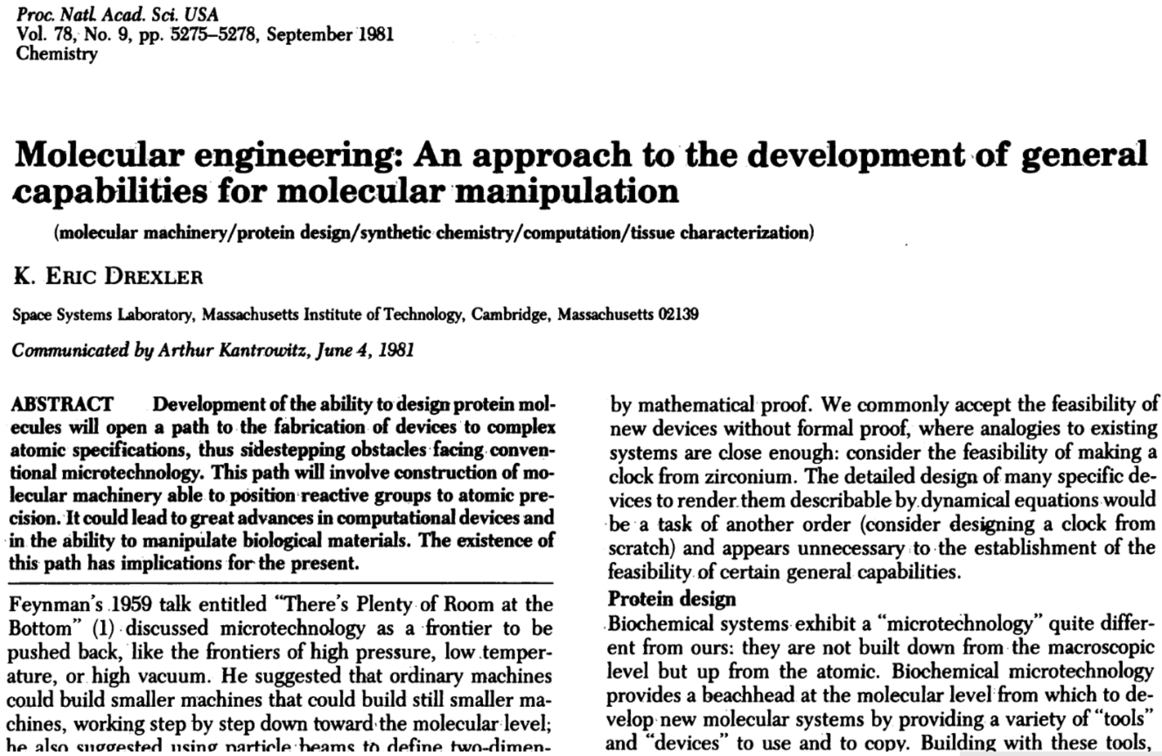

Proc. Natl. Acad. Sci. USA
Vol. 78, No. 9, pp. 5275–5278, September 1981
Chemistry

Molecular engineering: An approach to the development of general capabilities for molecular manipulation

(molecular machinery/protein design/synthetic chemistry/computation/tissue characterization)

K. Eric Drexler

Space Systems Laboratory, Massachusetts Institute of Technology, Cambridge, Massachusetts 02139

Communicated by Arthur Kantrowitz, June 4, 1981

ABSTRACT **Development of the ability to design protein molecules will open a path to the fabrication of devices to complex atomic specifications, thus sidestepping obstacles facing conventional microtechnology. This path will involve construction of molecular machinery able to position reactive groups to atomic precision. It could lead to great advances in computational devices and in the ability to manipulate biological materials. The existence of this path has implications for the present.**

Feynman’s 1959 talk entitled “There’s Plenty of Room at the Bottom” (1) discussed microtechnology as a frontier to be pushed back, like the frontiers of high pressure, low temperature, or high vacuum. He suggested that ordinary machines could build smaller machines that could build still smaller machines, working step by step down toward the molecular level; he also suggested using particle beams to define two-dimen-

by mathematical proof. We commonly accept the feasibility of new devices without formal proof, where analogies to existing systems are close enough: consider the feasibility of making a clock from zirconium. The detailed design of many specific devices to render them describable by dynamical equations would be a task of another order (consider designing a clock from scratch) and appears unnecessary to the establishment of the feasibility of certain general capabilities.

Protein design

Biochemical systems exhibit a “microtechnology” quite different from ours: they are not built down from the macroscopic level but up from the atomic. Biochemical microtechnology provides a beachhead at the molecular level from which to develop new molecular systems by providing a variety of “tools” and “devices” to use and to copy. Building with these tools,

http://e-drexler.com/ http://e-drexler.com/index.html#PNvideo

Atomically Precise Manufacturing Processes

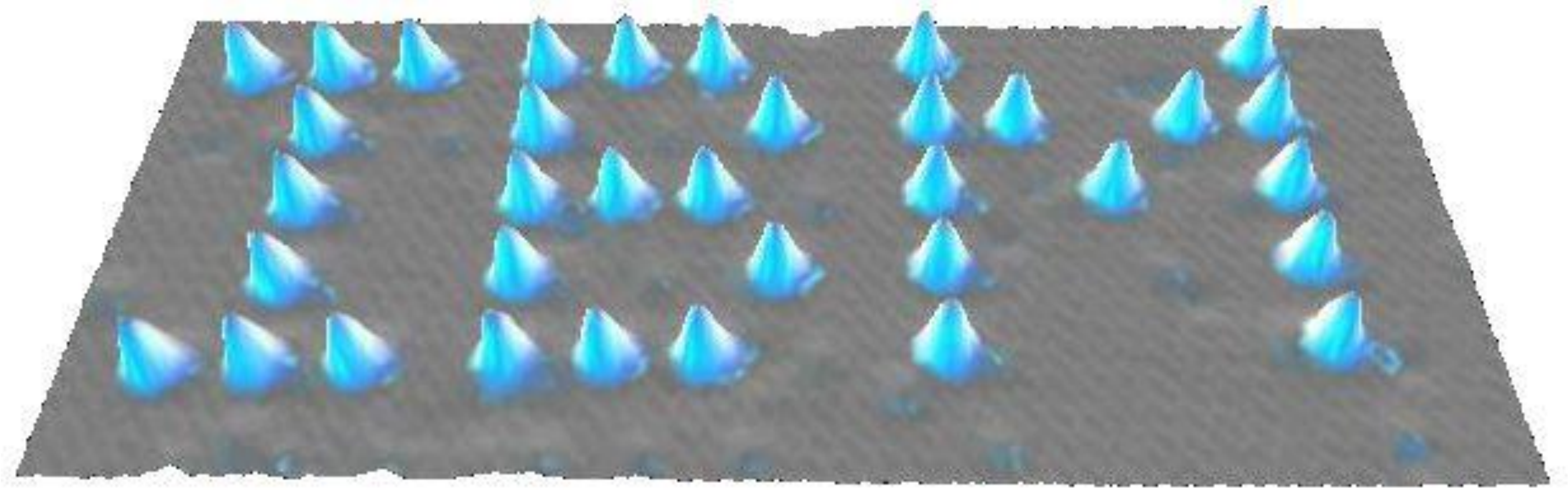

1989 Donald M. Eigler (physicist at IBM Almaden Research Center) demonstrated the ability to **manipulate individual atoms with atomic-scale precision**.
I-B-M was written on (110) Ni using 35 individual Xe atoms using a low temperature ultra high vacuum (UHV) scanning tunneling microscope that he designed and built.

Source: Wikipedia

Atomically Precise Manufacturing Processes

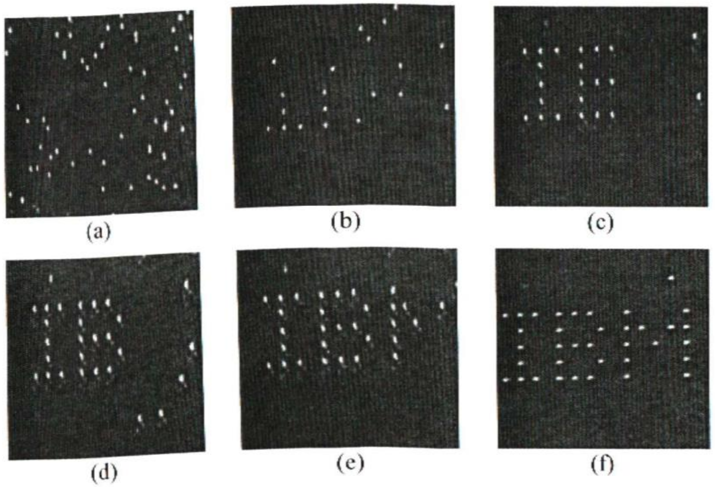

Manipulation of single surface atoms by STM

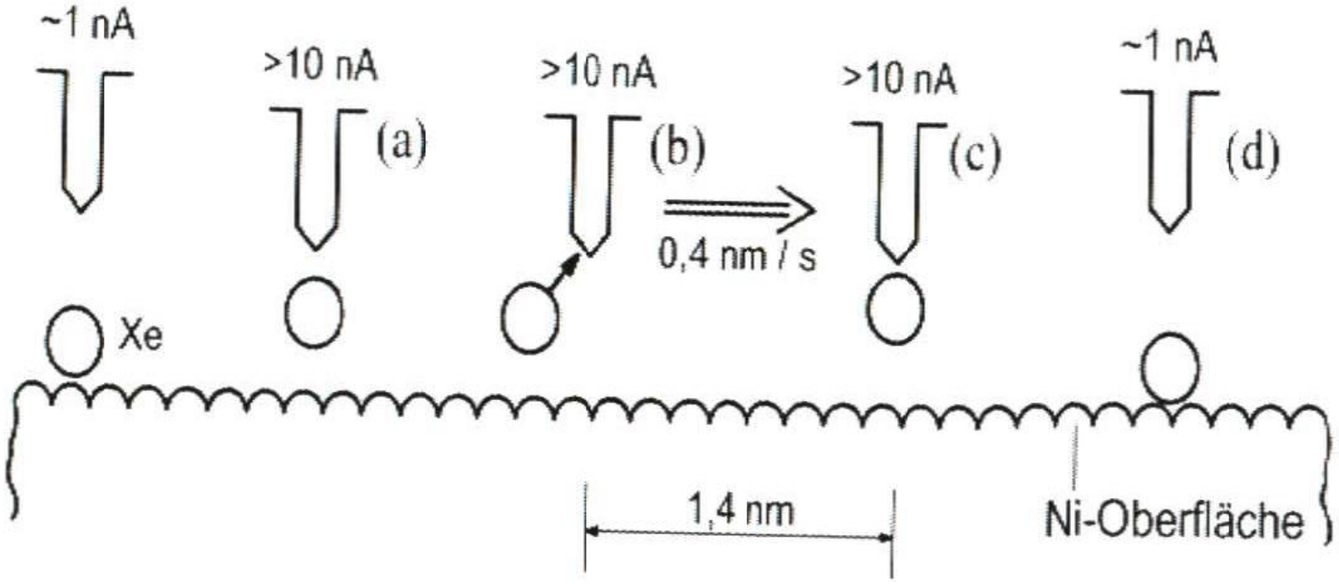

Source: Fahrner 2003

Introduction

Atomically Precise Manufacturing Processes

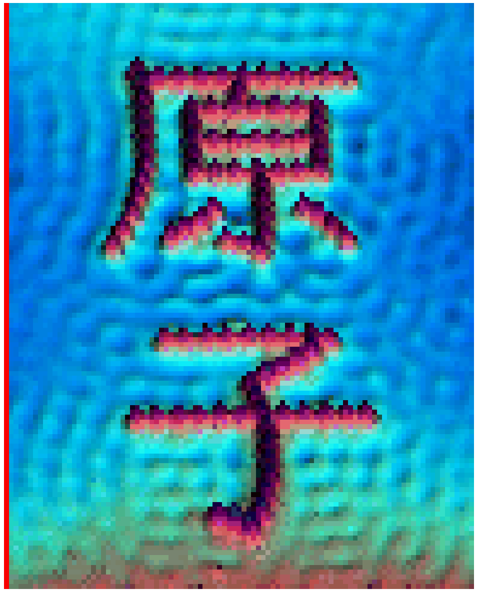

***Title**: Atom*
***Media**: Fe atoms on (111) Cu*

The Kanji characters for "atom." The literal translation is something like "original child."

http://www.almaden.ibm.com/vis/stm/atomo.html#stm11

http://news.rub.de/wissenschaft/2017-02-02-chemie-der-womoeglich-kleinste-rub-schriftzug-der-welt

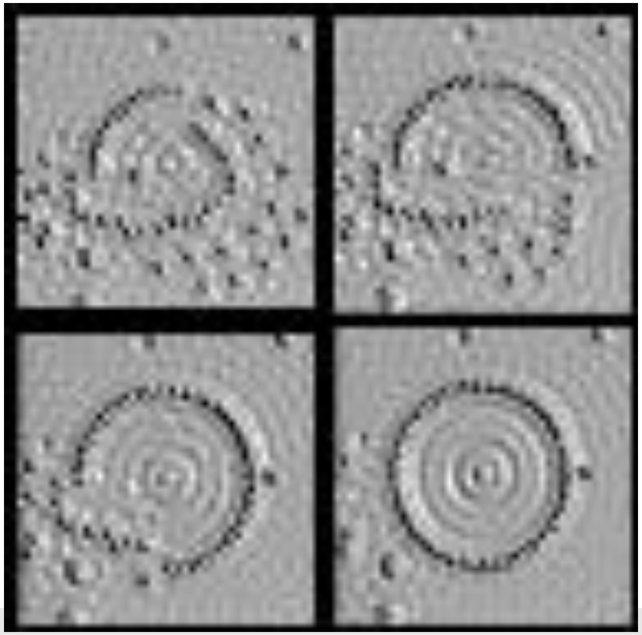

***Title** : The Making of the Circular Corral*
***Media** : Fe atoms on (111) Cu*

http://www.almaden.ibm.com/vis/stm/atomo.html#stm11

Nanotechnologie: Meilensteine und Personen

The Nobel Prize in Chemistry 2023 was awarded jointly to … Bawendi
"discovery and synthesis of ***quantum dots****"*

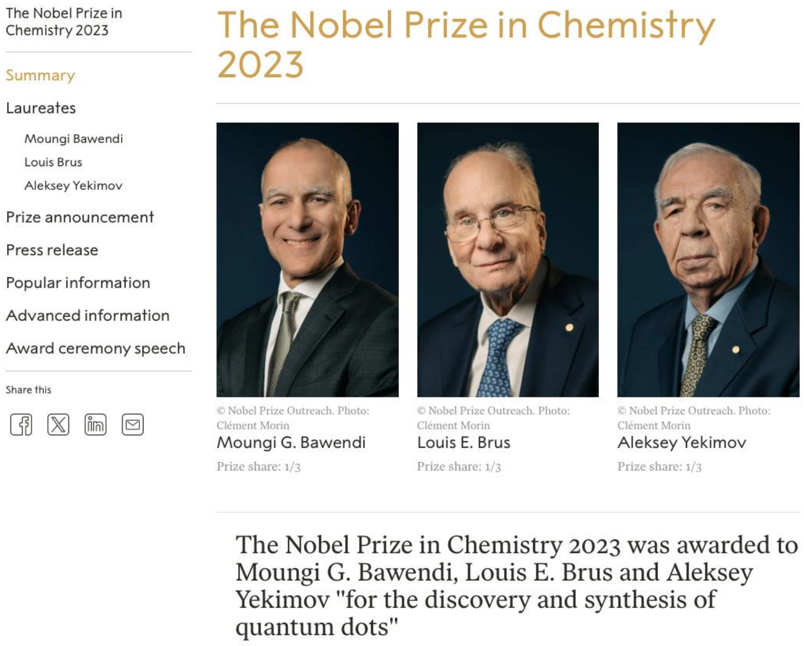

The Nobel Prize in Chemistry 2023

© Nobel Prize Outreach. Photo: Clément Morin
Moungi G. Bawendi
Prize share: 1/3

© Nobel Prize Outreach. Photo: Clément Morin
Louis E. Brus
Prize share: 1/3

© Nobel Prize Outreach. Photo: Clément Morin
Aleksey Yekimov
Prize share: 1/3

The Nobel Prize in Chemistry 2023 was awarded to Moungi G. Bawendi, Louis E. Brus and Aleksey Yekimov "for the discovery and synthesis of quantum dots"

https://youtu.be/S4IFjDugU5A?feature=shared

https://www.nobelprize.org/uploads/2023/10/advanced-chemistryprize2023-3.pdf

https://www.nobelprize.org/prizes/chemistry/2023/popular-information/

Nanotechnologie: Meilensteine und Personen

Quantum dots — seeds of nanoscience

The Royal Swedish Academy of Sciences has decided to award ***Moungi G. Bawendi, Louis E. Brus****, and* ***Aleksey Yekimov*** *the Nobel Prize in Chemistry 2023, for the discovery and synthesis of quantum dots.*

Introduction

This year's Nobel Prize in Chemistry recognizes the discovery and synthesis of nanometre-sized semiconductor crystals, the properties of which are determined by quantum size effects. Referred to as quantum dots, such nanoparticles are so small that their physical size determines the quantum mechanical states of the material's charge carriers.

Quantum dots constitute a new class of materials that is neither molecular nor bulk. They have the same structure and atomic composition as bulk materials, but their properties can be tuned using a single parameter, the particle's size. For example, the optical absorption and emission of CdSe quantum dots can be tuned across nearly the entire visible range of the optical spectrum. This is possible because the energy bandgap of CdSe quantum dots varies between 1.8 eV (its bulk value) to 3 eV (in the smallest quantum dots, see Fig. 1). Other material properties that are tuneable by quantum dot size include redox potentials[1], melting temperature[2], and solid-solid phase transitions,[3] to name just a few.

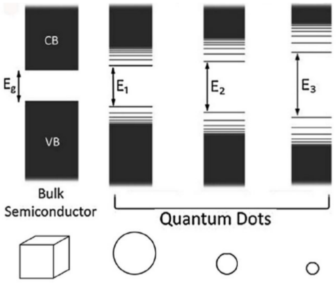

Fig. 1. Illustration of size-dependent bandgap. Reproduced from G. Dong et al., *Frontiers in Materials* **2**, 1 (2015).

The discovery of quantum dots, and the ability to synthesize such materials with high accuracy but relatively simple chemical methods, was an important step in the development of nanoscience and nanotechnology. The core principle of nanoscience is that, at the scale of nanometres, materials and particles attain new, size-dependent properties that can be harnessed and controlled for novel applications. The tools of chemistry are an indispensable enabler of nanotechnology, with applications in areas as diverse as biotechnology, catalysis, sensing, medical diagnostics, electronics, photonics, and quantum technology.

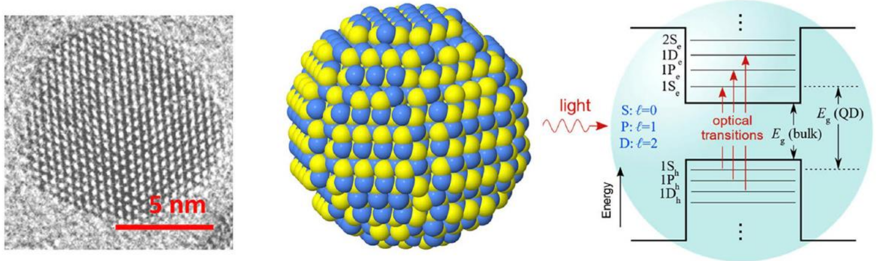

Fig. 3. Illustration of quantum dots. Left: transmission electron microscope image of a CdSe nanocrystal. Centre: Atomic structure of a nanocrystal. Right: Electronic states in a core-shell quantum dot, with the dot itself in the centre bracketed by a wide-bandgap shell. Reproduced from A. L. Efros and L.E. Brus, *ACS Nano* **15**, 6192 (2021).

https://youtu.be/S4IFjDugU5A?feature=shared

https://www.nobelprize.org/uploads/2023/10/advanced-chemistryprize2023-3.pdf
https://www.nobelprize.org/prizes/chemistry/2023/popular-information/

Nanotechnologie
Definitionen

Nanoscience is the study of phenomena and manipulation of materials at atomic, molecular and macromolecular scales, where properties differ significantly from those at larger scale.

Nanotechnologies are the design, characterization, production and application of structures, devices and systems by controlling shape and size at the nanometre scale

- Kontrolle des Gefüges und der Zusammensetzung von Werkstoffen auf atomarer Ebene mit Verfahren, die auch die makroskopische Herstellung von Produkten zulässt

Quelle: Royal Society, Royal Academy of Engineering

Nanotechnologie

Definitionen

„**Nanotechnology** comprises
the emerging application of nanoscience.

Nanoscience deals with functional systems
either based on the use of subunits with
specific **size-dependent properties**
or of individual or combined subunits“

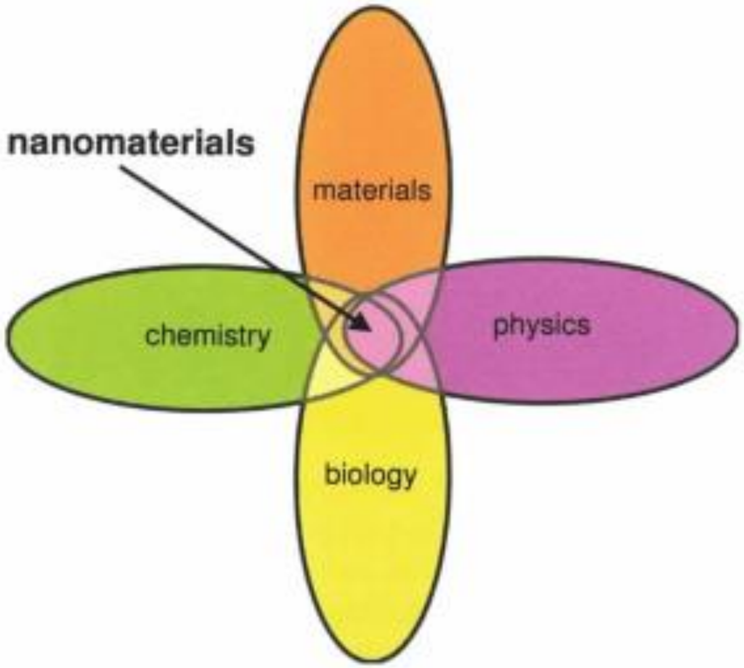

Figure 1.1 A basic understanding of physics and chemistry, and some knowledge of materials science, is necessary to understand the properties and behavior of nanomaterials. As many applications are connected with biology and medicine, some knowledge of these areas is also required.

Size-dependent nano-effects

„Size-dependent nano-effects“ versus „Scaling effects“

Sources: u.a. Vollath,Europäische Akademie Bad Neuenahr-Ahrweiler

Nanotechnologie

DIN Norm

Nanoscale objects:
Nanoparticles, Nanofibres, Nanowires, Nanoplates, Nanotubes, Nanorods, …

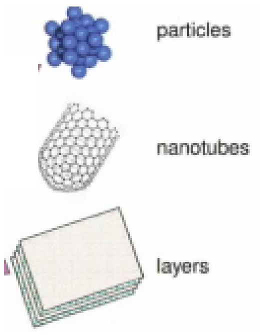

Nanoobjects:
at least one outer dimension between 1 and 100 nm

Nanoobjects, which are nanoscale in all three dimensions, are **nanoparticles**.

DIN SPEC 1121:2010-02
CEN ISO/TS 27687:2009 (D)

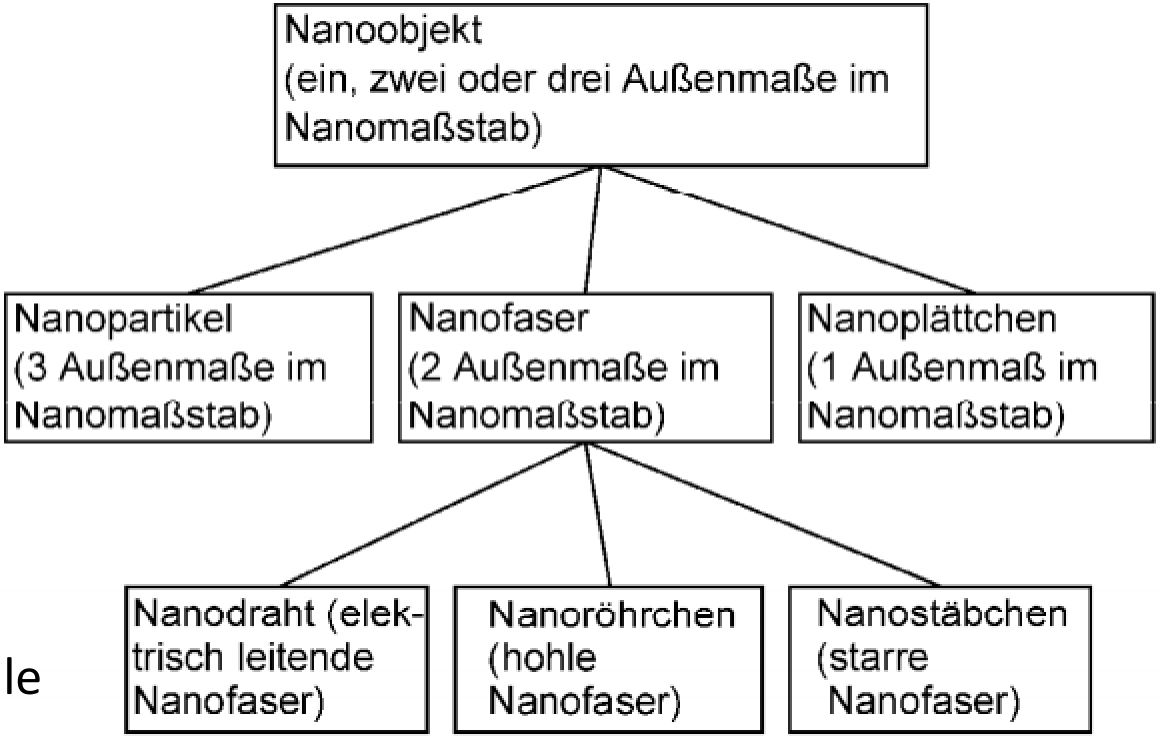

Nanoobjekt
(ein, zwei oder drei Außenmaße im Nanomaßstab)

Nanopartikel
(3 Außenmaße im Nanomaßstab)

Nanofaser
(2 Außenmaße im Nanomaßstab)

Nanoplättchen
(1 Außenmaß im Nanomaßstab)

Nanodraht (elektrisch leitende Nanofaser)

Nanoröhrchen
(hohle Nanofaser)

Nanostäbchen
(starre Nanofaser)

Advanced Materials Processing and Microfabrication

Nanotechnolgie: „0-D Strukturen“
Nanopartikel

Größenabhängige Nanoeffekte: Thermodynamische Eigenschaften (Phasenumwandlung)

Beispiel Au: Schmelzpunkt

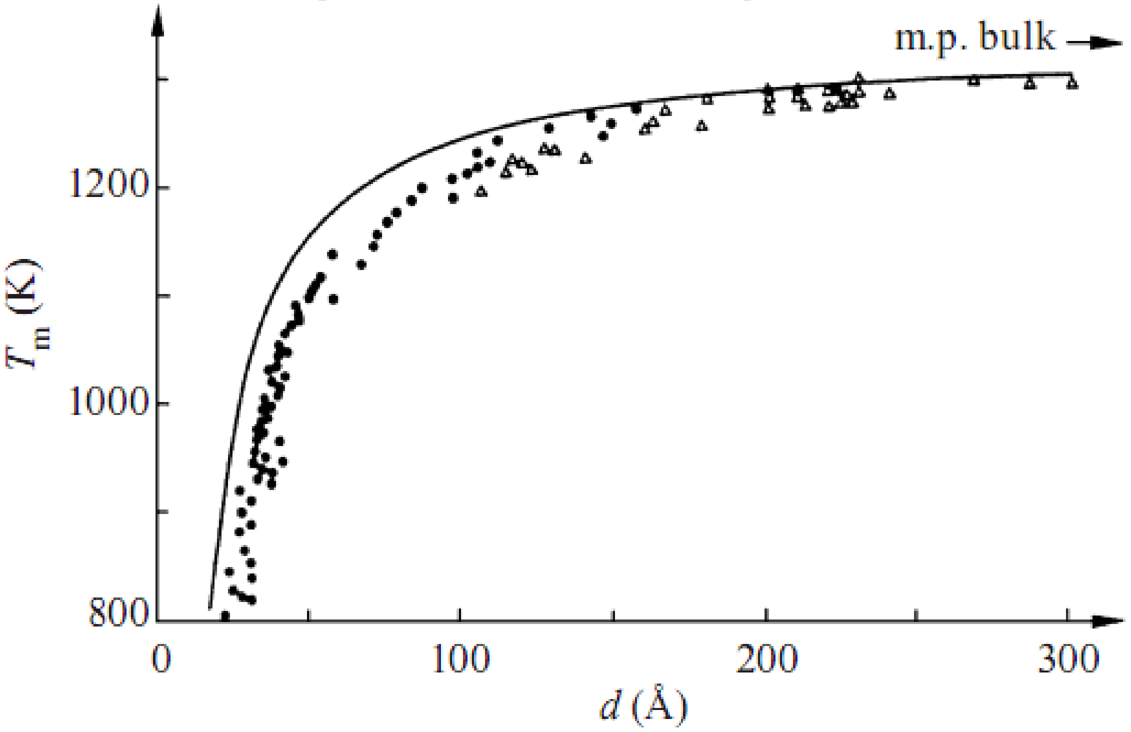

Figure 8
Reduction of the melting temperature of gold nanoparticles as a function of particle size; the solid line is the theoretical curve (after Borel 1981).

Eigenschaften von Nanomaterialien können sich von „bulk“-Eigenschaften unterscheiden:
z.B. niedrigerer Schmelzpunkt aufgrund eines hohen Oberflächenanteils in Nanopartikeln

Quelle: Encyl. Materials

Größenabhängige Nanoeffekte: Strukturelle Eigenschaften

Kleine Nanopartikel haben oft kleinere Gitterkonstanten als “bulk”

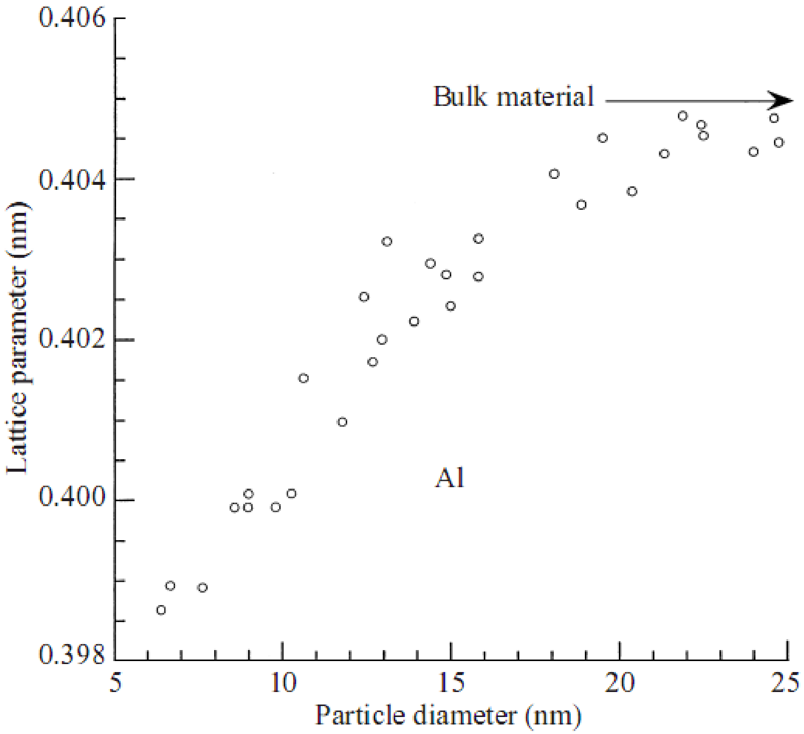

Figure 6
Reduction of the lattice constant of aluminum nanoparticles as a function of particle size (after Woltersdorf *et al.* 1981).

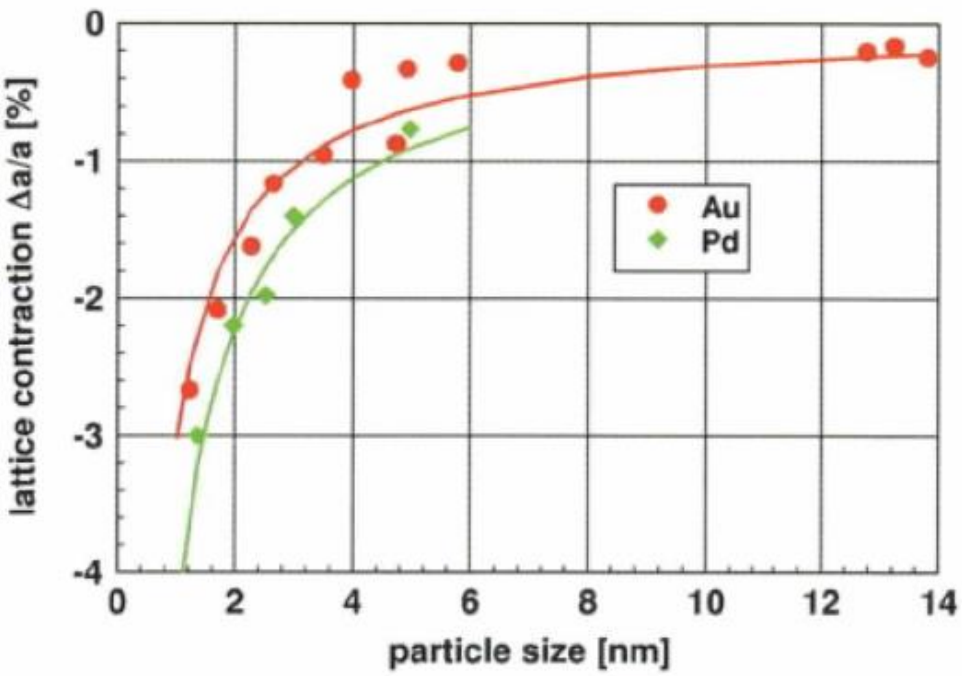

Figure 2.15 Experimental values for the lattice constant of gold [11] and palladium [12] nanoparticles. Due to hydrostatic pressure originating from surface tension, decreasing lattice parameters are observed with decreasing particle size.

Größere Partikel haben gewöhnlich gleiche Gitterkonstanten und Kristallstruktur wie “bulk”

Quelle: Encyl. Materials, Vollath

Größenabhängige Nanoeffekte: Strukturelle Eigenschaften

Kleine Nanopartikel können eine <u>andere Kristallstruktur</u> als im “bulk” haben.

<u>Erklärung:</u>
Gleichgewicht von Oberflächen- und elastischer Energie

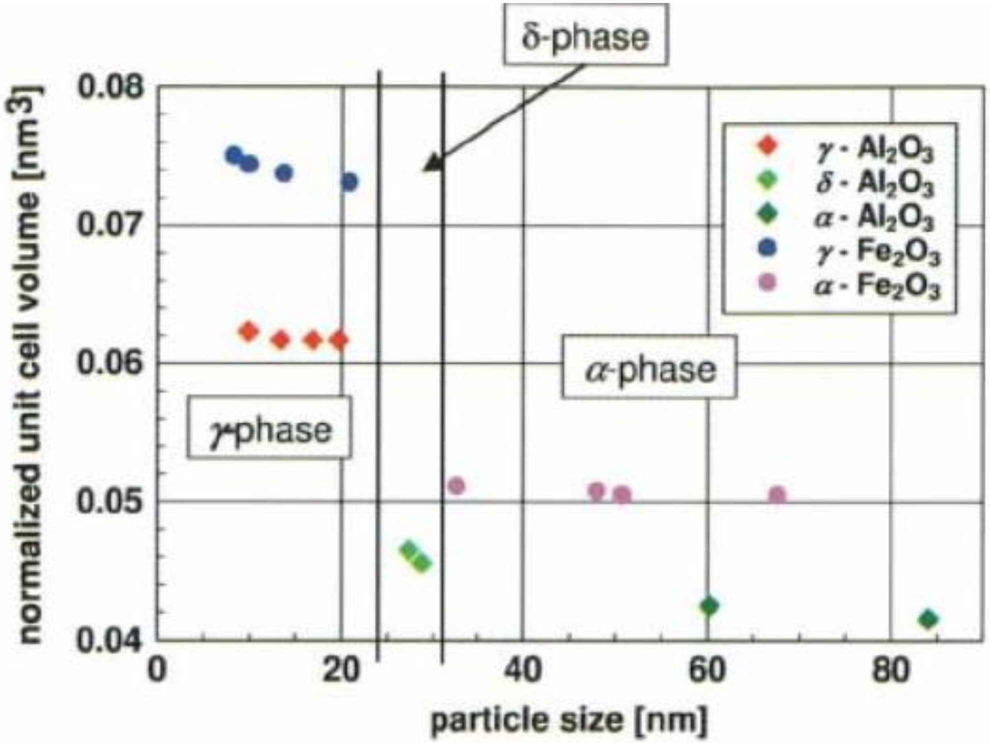

Figure 3.14 Normalized unit cell volume for different Al_2O_3 and Fe_2O_3 phases as a function of grain size [15]. Normalization provides a constant number of formula units per unit cell; otherwise, comparison is impossible. In the γ-phase, the unit cell volume is increased as the particle size decreases. A preference for high-temperature structures as the particle size decreases is clearly visible.

Quelle: Vollath

Größenabhängige Nanoeffekte
Au: Farbe

Typische größenabhängige Nanoeffekte können auftreten, sobald eine kritische Abmessung bei der Verkleinerung von Partikeln unterschritten wird. Diese kritische Abmessung ist eigenschaftsabhängig und kann für dasselbe Element für unterschiedliche Eigenschaften unterschiedlich sein.

Beispiel Au: in bulk Form ist die Goldfarbe durch einen relativistischen Effekt begründet (spezielle Relativitätstheorie).

Au-Nanopartikel zeigen keine Goldfarbe.
Unter einer Größe von 50 nm erst blau,
dann lila,
bei 15-20 nm rot
Ursache: Plasmonenresonanz

Figure 6.29 A beaker covered with gold ruby glass, a composite consisting of gold nanoparticles. Note the faint blue hue in the color, which is typical of pigments based on gold nanoparticles.

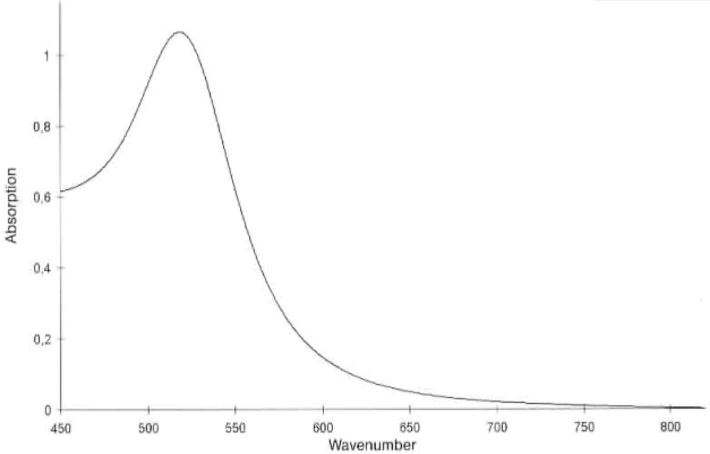

Figure 2.3 UV–visible spectrum of 18-nm gold particles.

Plasmonen: quantisierte Wellen der freien Elektronen
Phononen: quantisierte Gitterschwingungen

Quellen: u.a. Schmid , Vollath, 2008

Konzepte der Nanotechnologie

Monodisperse Nano-Objekte

Für viele Anwendungen ist es wichtig,
Nano-Objekte mit monodisperser Größenverteilung zu haben

monodispers

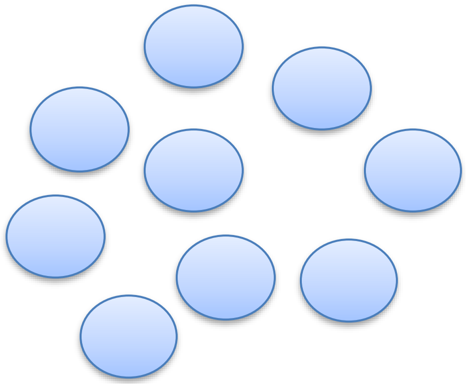

polydispers

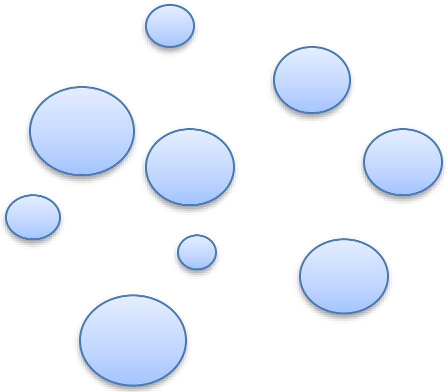

Konzepte der Nanotechnologie
Agglomeration von Nanoobjekten

Nanoobjekte treten häufiger in Gruppen auf, als isoliert.
Aufgrund der hohen Oberflächenenergie ist es wahrscheinlich, dass koexisitierende Nanoobjekte wechselwirken.

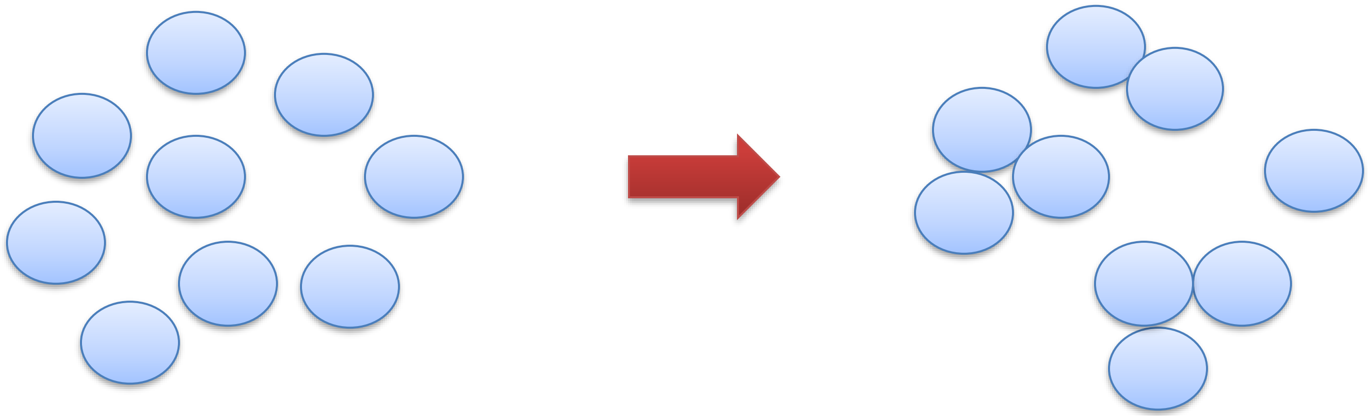

Verhinderung der Agglomeration von Nanoobjekten?

Konzepte der Nanotechnologie

Agglomeration von Nanoobjekten

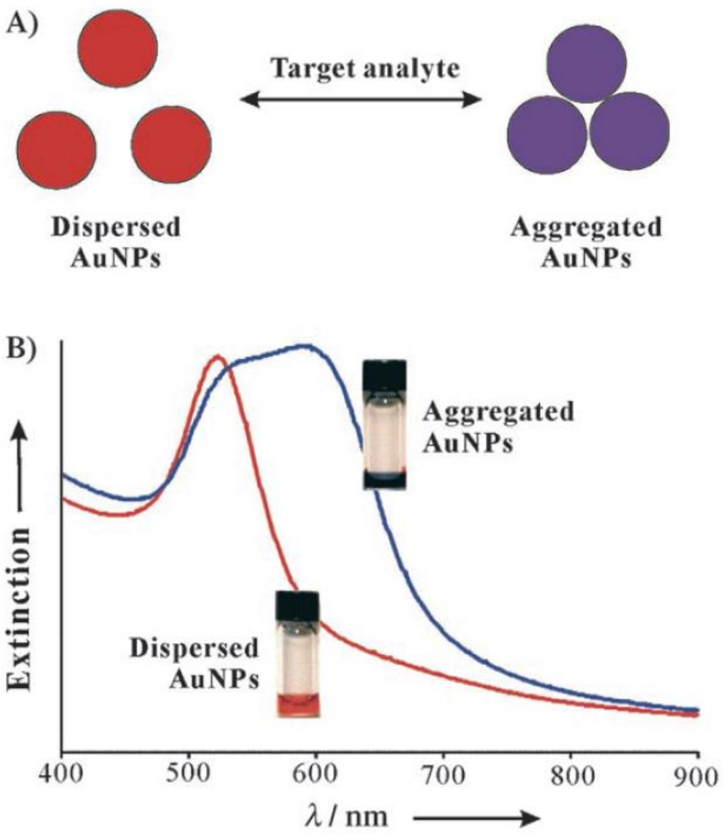

Figure 1. A) General schematic representation of absorption-based colorimetric AuNP biosensing assays by using AuNP aggregation and dispersion. B) Typical surface plasmon absorption bands for 13 nm AuNPs in the visible light region. The red and blue curves correspond to dispersed and aggregated AuNPs, respectively.

Colorimetric biosensing

Dispersion vs. aggregation

ChemBioChem **2008**, *9*, 2363 – 2371

Konzepte der Nanotechnologie
Agglomerationen und Aggregate von Nano-Objekten

Agglomerate
Nanoobjekte haben die starke Tendenz, sich zusammenzulagern und mikro- oder millimetergroße Agglomerate zu bilden, etwa in pulverförmigen Materialien. Diese Agglomerate können mechanisch, zum Beispiel durch starkes rühren, wieder zerkleinert werden, da deren Einzelteile durch relativ schwache Kräfte miteinander verbunden sind.

Aggregate
Aggregate sind Zusammenlagerungen von Nanoobjekten, die durch starke Kräfte, z.B. durch chemische Bindungen, zusammengehalten werden. Diese können nicht mehr in ihre Einzelteile zerfallen, es sei denn, es würde enorme Energie aufgewendet.

Größen-und-Form-abhängige Nanoeffekte
Z.B.: Farbe von Nanopartikellösungen

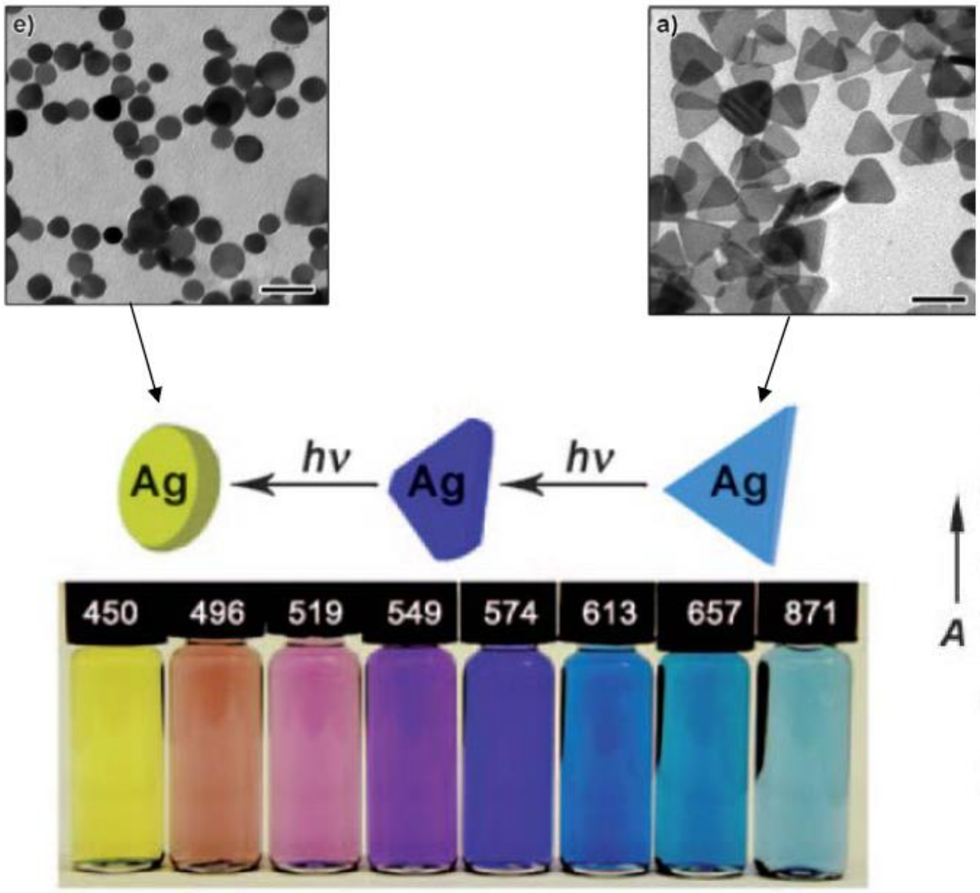

„tailoring optical properties“

Extinction spectra

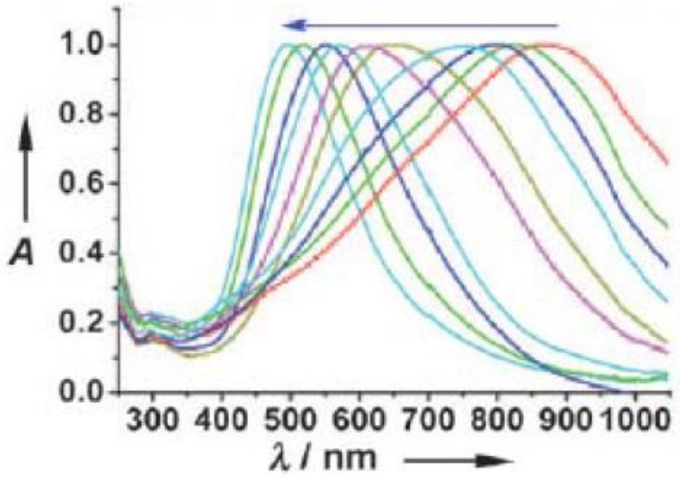

a) Schematic illustration of the evolution process of Ag nanoplates under UV irradiation: the sharp corners of triangular plates disappear, while the thickness of the nanoplates increases. b) Digital photographs and c) extinction spectra showing a backward tuning of the plasmon bands of the silver nanoplates by irradiation with UV light for different lengths of time. From right to left, the samples displayed in the photo were irradiated for 0, 60, 70, 80, 90, 100, 110, and 125 min. The numbers above the samples give the wavelength of plasmon resonance in nanometers. The spectra in c) were taken after irradiating the nanoplate solutions for 0, 20, 40, 60, 70, 80, 90, 100, 110, and 125 min.

Source: Zhang et al., Angew. Chem. Int. Ed. 2009, 48, 3156

Chemische Synthese von Nanopartikeln

Precursor

solid
liquid
gaseous

Generation →

Primary and secondary generation

Reaction

liquid
vaporous

Chemistry

Conversion →

Drying
Calcination

Product

Separation →

Separation

final solid material colloides

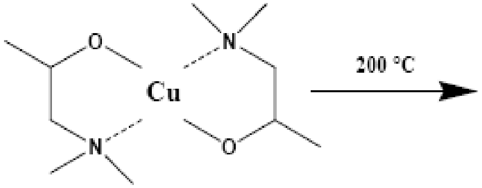

Cu(dmap)$_2$

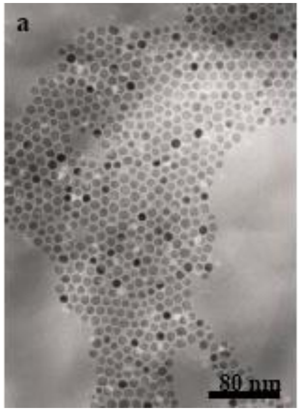

Cu nanoparticles

Chemische Synthese von Nanopartikeln: Heißinjektionsmethode

In 1993, **Moungi Bawendi** and co-workers developed a method for the synthesis of quantum dots with much more well-defined size and with high optical quality.[62] This discovery opened the door to the development of applications of colloidal quantum dots. Their synthesis begins with the injection and immediate pyrolysis of organometallic reagents (the precursors for the desired nanoparticles) into a hot coordinating solvent with a high boiling point. The rapid increase of reagent concentrations results in abrupt supersaturation and in nucleation that takes place at a well-defined moment. Injection is accompanied by a sudden drop in temperature and dilution of the precursors such that growth stops. After reheating to the desired growth temperature, a slow growth and annealing process takes place in the coordinating solvent that helps to stabilize the resulting colloidal dispersion. This principle of temporally discrete nucleation followed by controlled growth was known from the production of monodisperse lyophobic colloids.[63] Finally, particles can be selected using purification and size-dependent precipitation. The result is macroscopic quantities of nanoparticles with regular core structure and shape, with consistent surface derivation and electronically passivated semiconductor surface, and with a well-defined size that is determined by dynamic temperature control during the growth phase.[62] Relatively sharp optical absorption (Fig. 4) and emission spectra were observed at room temperature, with a luminescence quantum yield up to 10%. By removing aliquots during the growth process, an entire series of particle sizes can be obtained during a single growth run.[62]

The hot-injection synthesis method developed by **Bawendi** and co-workers constituted an adaptable and reproducible chemical strategy for synthesizing monodisperse nanoparticles using a wide range of material systems. It thus opened the door to the development of large-scale applications of quantum dots.

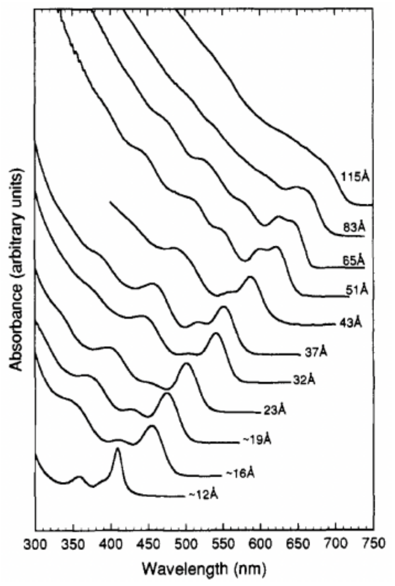

Fig. 4. Room-temperature optical absorption spectra of CdSe nanocrystallites dispersed in hexane and ranging in size from ~12 to 115 Å. Reproduced from C.B. Murray, D.J. Norris, and M.G. Bawendi, *J. Am. Chem. Soc.* **115**, 8706 (1993).

https://www.nobelprize.org/uploads/2023/10/advanced-chemistryprize2023-3.pdf
https://www.nobelprize.org/prizes/chemistry/2023/popular-information/

Chemische Synthese von Nanopartikeln: Heißinjektionsmethode

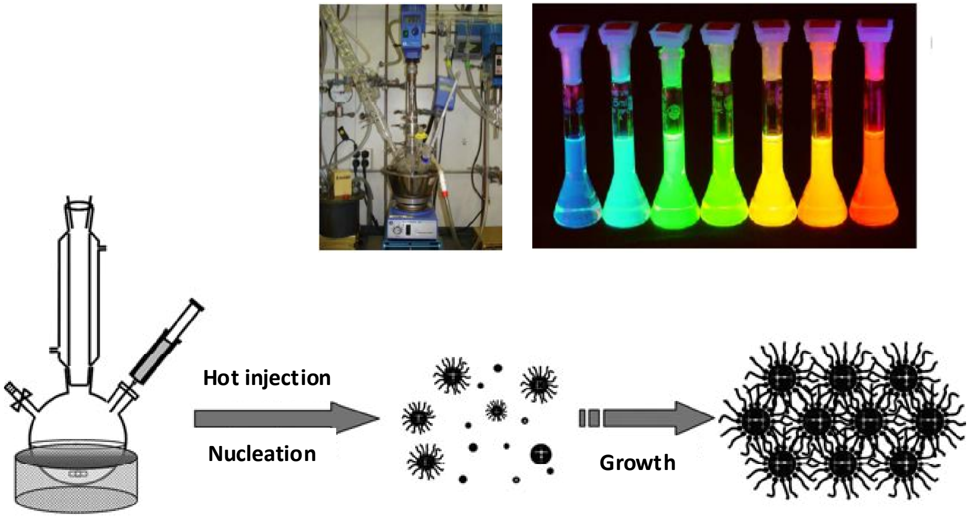

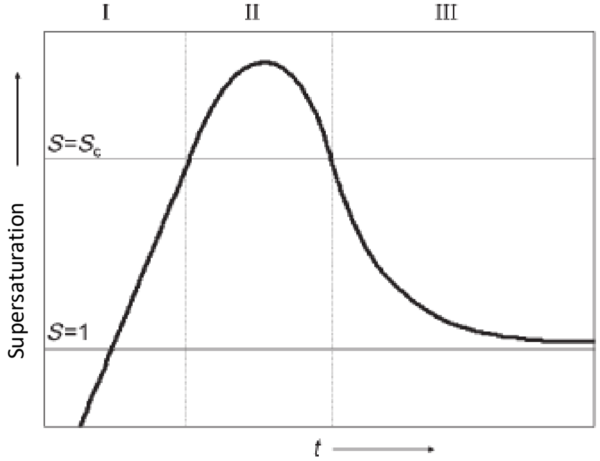

LaMer-Diagramm for changing of the supersaturation during reaction.

General steps for „hot injection“ method:

- **Injection of precursor into hot inert solvents containing reducing agents**
- **Nucleation and growth of particles**
- **Addition of capping agent (surfactant) to stop particle growth at desired size**

Phase I: Increasing the concentration of “monomers” after injection. In this stage no particle formation occurs due to high nucleation energy.
Phase II: Formation of nuclei (Critical concentration S_c).
Phase III: Growth phase of particles. Crystallisation of new grains returns to zero (Saturation concentration S=1)

→ **Homogeneous particle size distribution**

Vortrag Bawendi, ab 2. Minute zu hot injection:
https://www.youtube.com/watch?v=S4IFjDugU5A

Source: J. Park, J. Joo, S. Kwon, Y. Jang, T. Hyeon, *Angew. Chem.* **2007**, *119*, 4714 – 4745.

Stabilisierung von Nanopartikeln

A **surfactant** is a surface-active substance
which binds on surface and supports the stability of a nanoparticle

Choice of surfactant is important; examples:

Outer surface determines the solubility in solvent

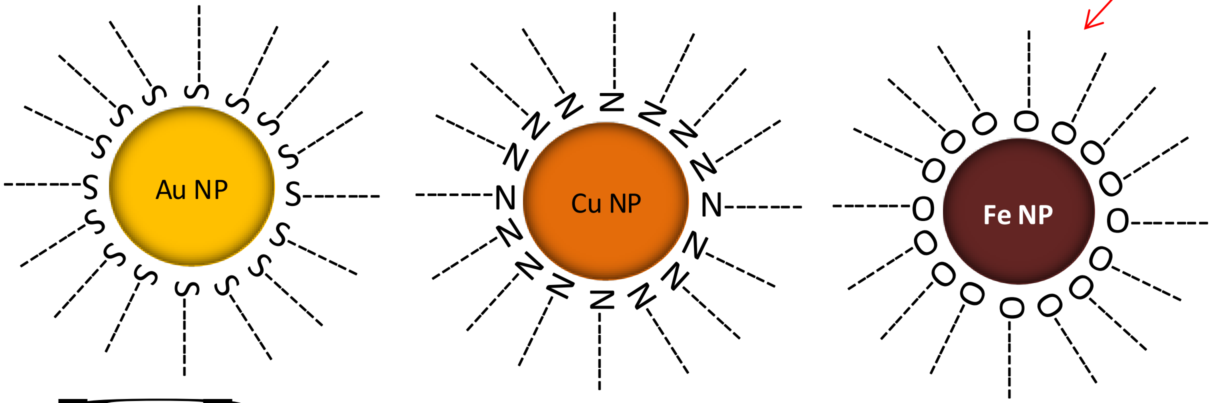

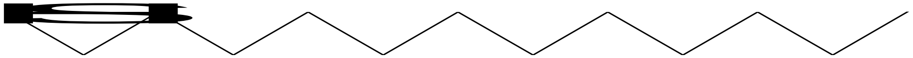

1-Dodecanthiole: S-Au Binding energy: 428 kJ/mol

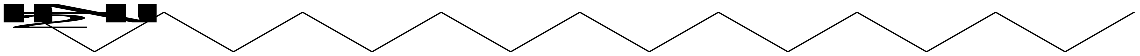

1-Hexadecylamine

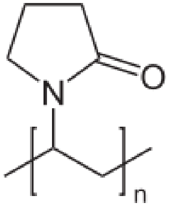

Polyvinylpyrrolidon (PVP)

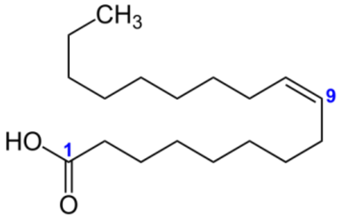

Oleic acid : O-Fe Binding energy: 400 kJ/mol

Legierungsnanopartikel

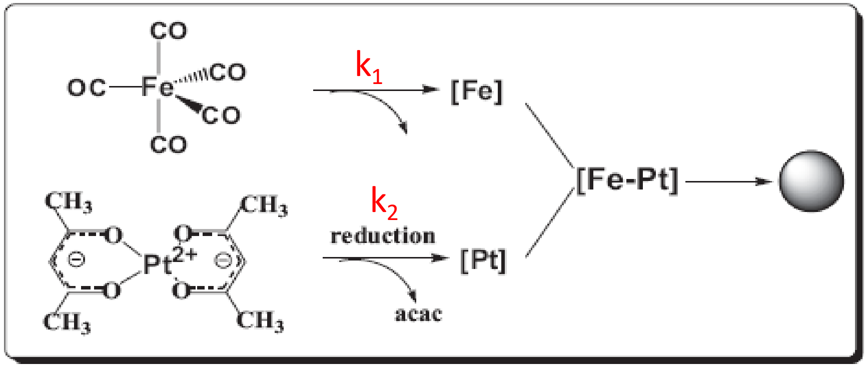

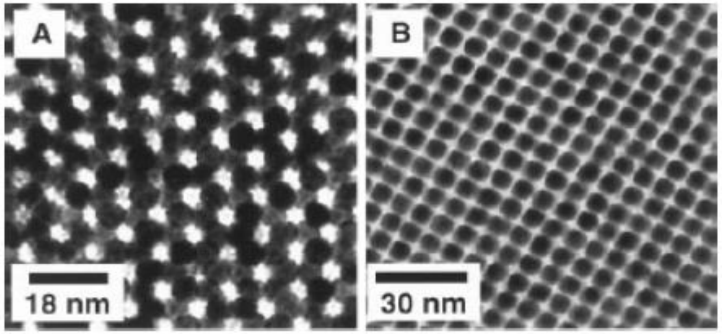

Fe/Pt alloy particles, oleic acid capped

Preparation of bimetallic nanoparticles by simultaneous reduction of ironpentacarbonyle $Fe(CO)_5$and platin-bis(acetylacetonate).
Reducing agents: H_2; $NaBH_4$; H_2N_2…….

To obtain homogeneous alloy particles,
reaction kinetic of both precursers must be the same.

Source: S. Sun, *Adv. Mater.***,** Vol. 18, 2004, pp. 393.

Hybride Nanopartikel

Growth mechanism:

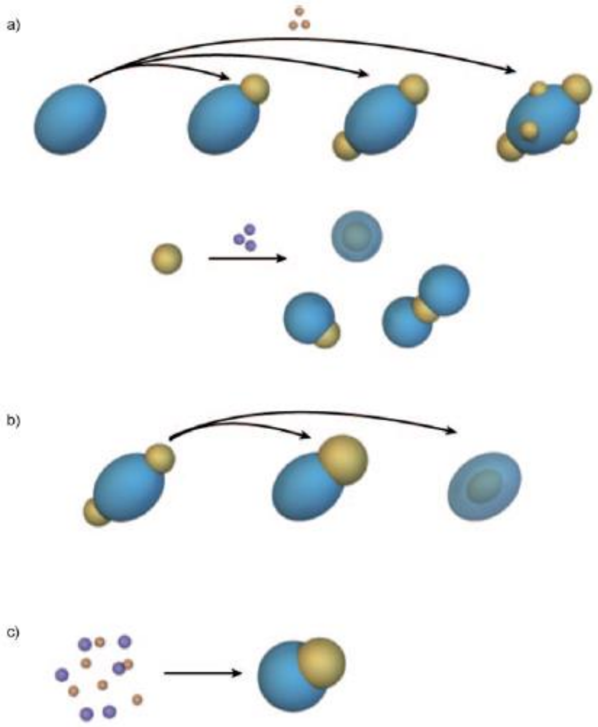

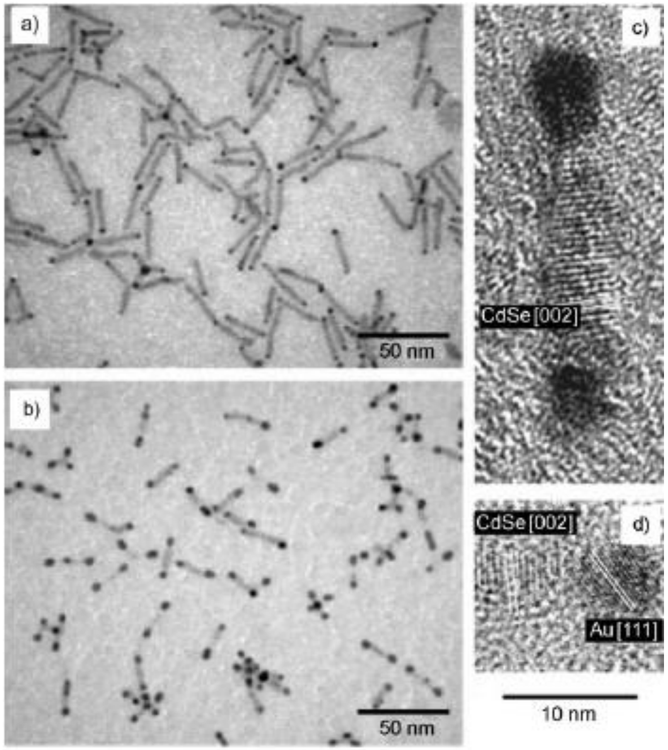

Sheme of different growth mechanism for hybrid nanoparticles:
a) Surface nucleation and island growth on primary particle. b) Surface necleation and diffusion of into the core. c) Simulaneous nucleation and growth.

T. Mokari, E. Rothenberg, I. Popov, R. Costi, U. Banin, Science **2004**, 304, 1787.
Angew. Chem. **2010**, 122, 2–23

Iron oxide particles / ferrofluids

Ferrofluids: Mainly magnetite Fe_3O_4 $(Fe^{2+}(Fe^{3+})_2O_4$

1. $2\ Fe(III)Cl_3 + Fe(II)Cl_2 + 8\ NH_3 + 4H_20 \rightarrow Fe_3O_4 + 8\ NH_4Cl$
2. *Cis*-oleic acid as capping agent $H_3(CH_2)_7CH{=}CH(CH_2)_7COOH$, in oil
3. Removing of water

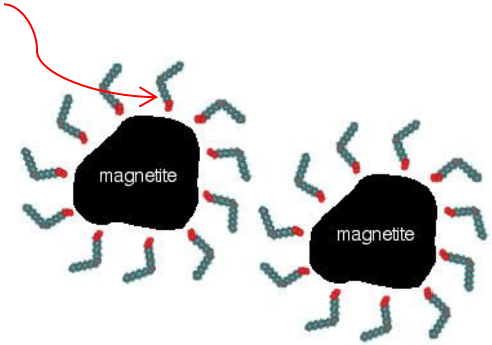

Thermal decomposition of precursors:

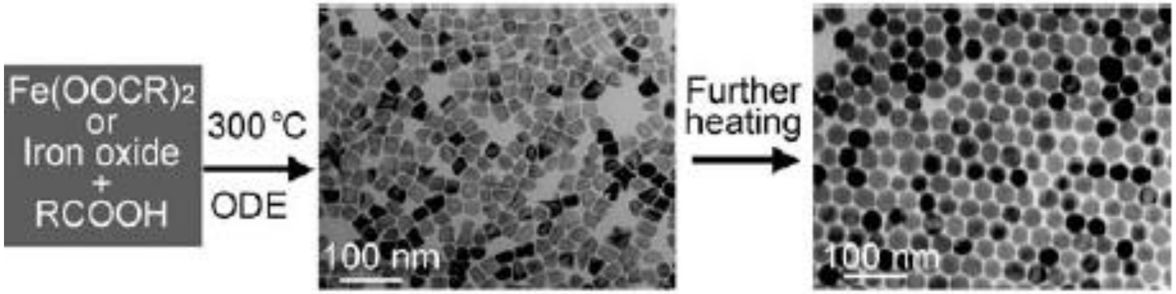

The formation of Fe_3O_4 nanocrystals. The middle and right panels are TEM images of the as-synthesized nanocrystals taken at different reaction times. ODE: Octadecene

N. R. Jana, Y. Chen, X. Peng, Chem. Mater. 2004, 16, 3931.

Nanopartikel und „self assembly“

- “self assembly”
- “self organisation” of nanoparticles in regular structures

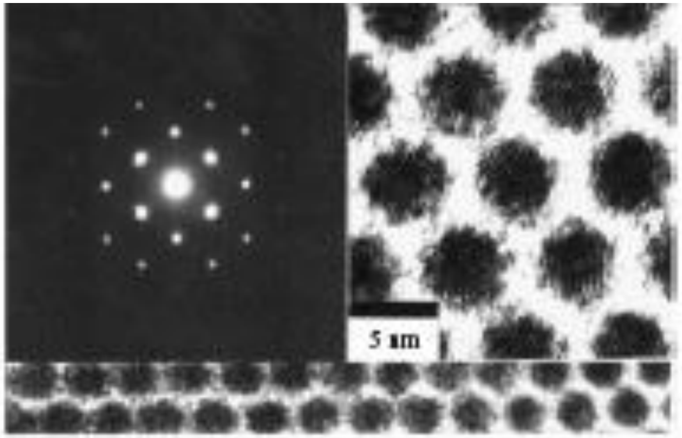

Bright field TEM image of self-assembled structure of CdSe nanoparticles (right) and their diffraction pattern (left). *Murray et al.*

MOF: metal organic coordination polymer by conecting metal linkers (oxo-cluster) with organic linkers into a 3D framework. Useful as catalyst, gas storage……

Organic SAMs (self assebbled monolayer)

1. Bonding of head-groups to substrate due to high binding energy, e.g. sulfur on gold substrate

2. Self ordering of molecules on surface. Formation of monolayers

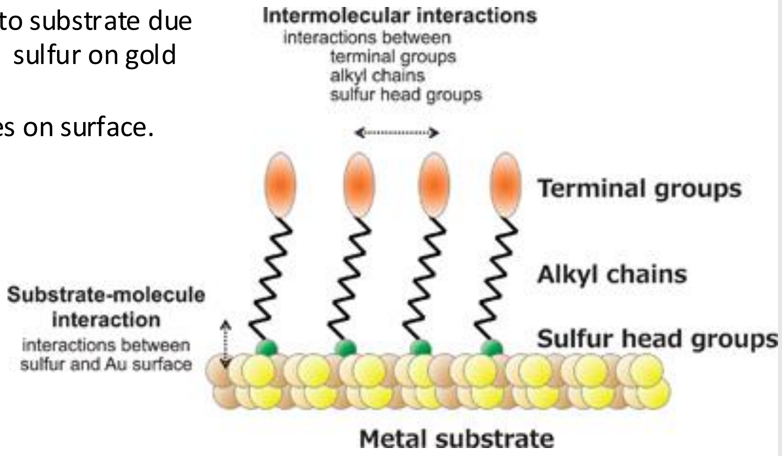

3. Further modification of terminal groups.
E.g. Linking of MOFs on SAMs

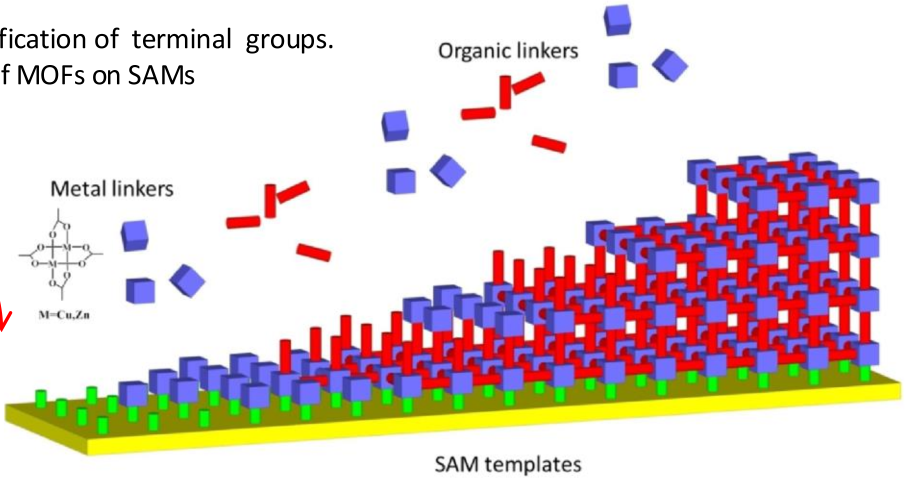

Growth of metal organic frameworks (MOFs) on SAM structure : SURMOF

Source:
Encl. Mat. Sci. Karlsruher Institute of Technology (KIT)
www.ifg.kit.edu

Herstellung von Nanopartikeln durch Sputtern in ionische Flüssigkeiten, ionic liquids (IL)

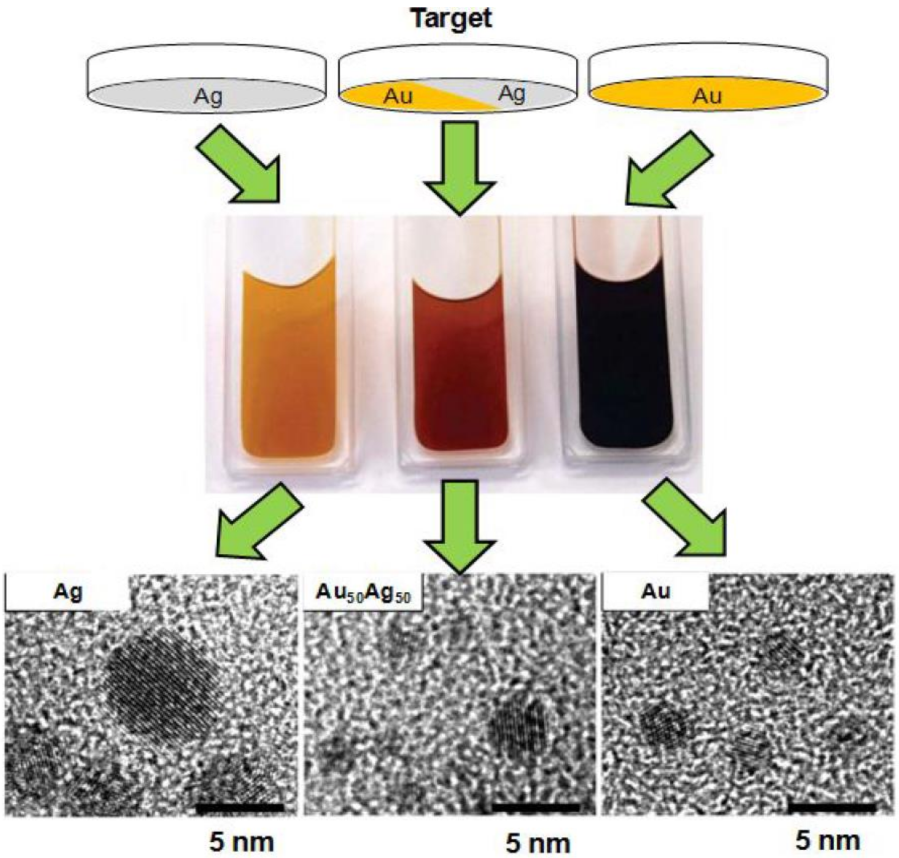

Fabrication of elemental and alloy NPs by adjusting the area fraction of the target.

$[BuMeIm][PF_6]$
loaded with sputtered Ag, $Ag_{50}Au_{50}$ or Au NPs

Okazaki K., Kiyama T., Hirahara K., Tanaka N., Kuwabata S., Torimoto T.,
Single-step synthesis of gold-silver alloy nanoparticles in ionic liquids by a sputter deposition technique,
Chem. Commun. 691-693, (2008).

Screening stability of nanoparticle-IL suspensions

base cation:

1-Butyl-3-methylimidazolium [Bmim]

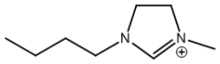

1

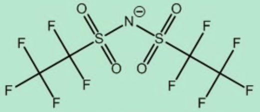

Bis-(perfluoroethylsulfonyl)imide [$(Pf)_2N$]

2

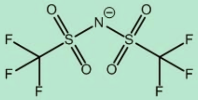

Bis-(trifluoromethylsulfonyl)imide [$(Tf)_2N$]

3

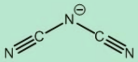

Dicyanamide [$(CN)_2N$]

4 $PF_6^{\ominus}$

Hexafluorophosphate [PF_6]

5 $BF_4^{\ominus}$

Tetrafluoroborat [BF_4]

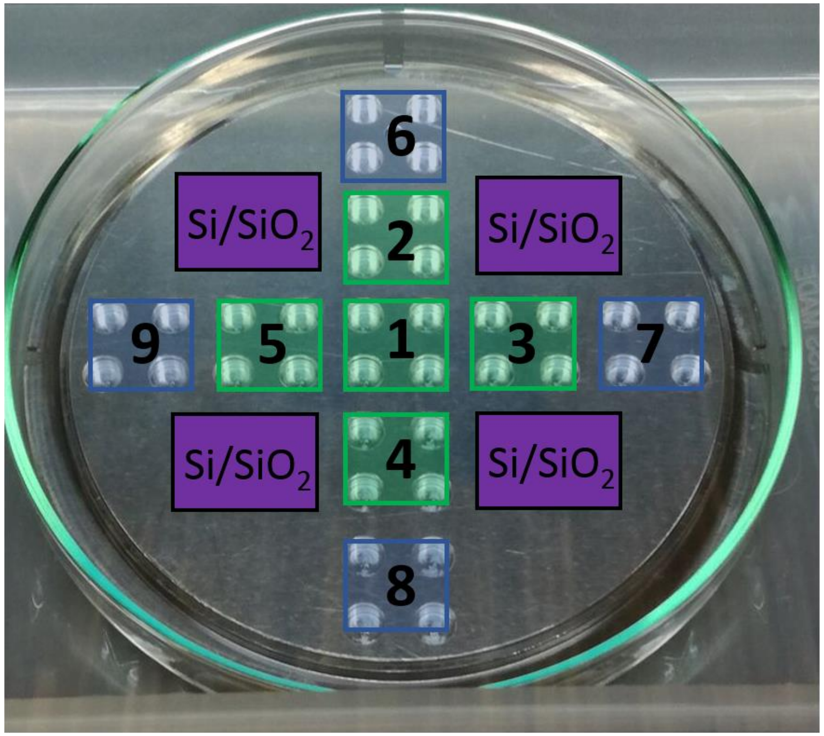

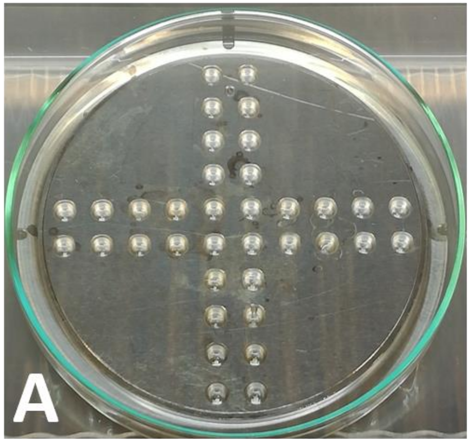

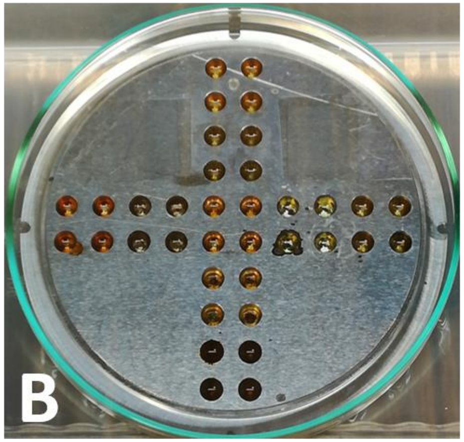

base anion:

Bis-(trifluoromethylsulfonyl)imide
[$(Tf)_2N$]

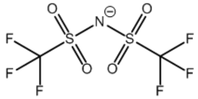

6

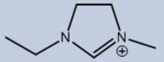

1-Etyl-3-methylimidazolium [Emim]

7

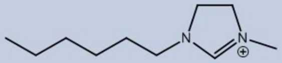

1-Hexyl-3-methylimidazolium [Hmim]

8

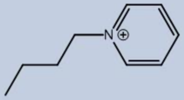

1-Butylpyridinium [BuPy]

9

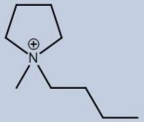

1-Butyl-1-methylpyrrolidinum [BmPyr]

A = before Ag sputtering
B = after Ag sputtering

H. Meyer, M. Meischein, A. Ludwig, ACS Comb. Sci. 2018, 20, 243−250

Combinatorial fabrication of nanoparticles by sputter deposition in ionic liquids (IL)

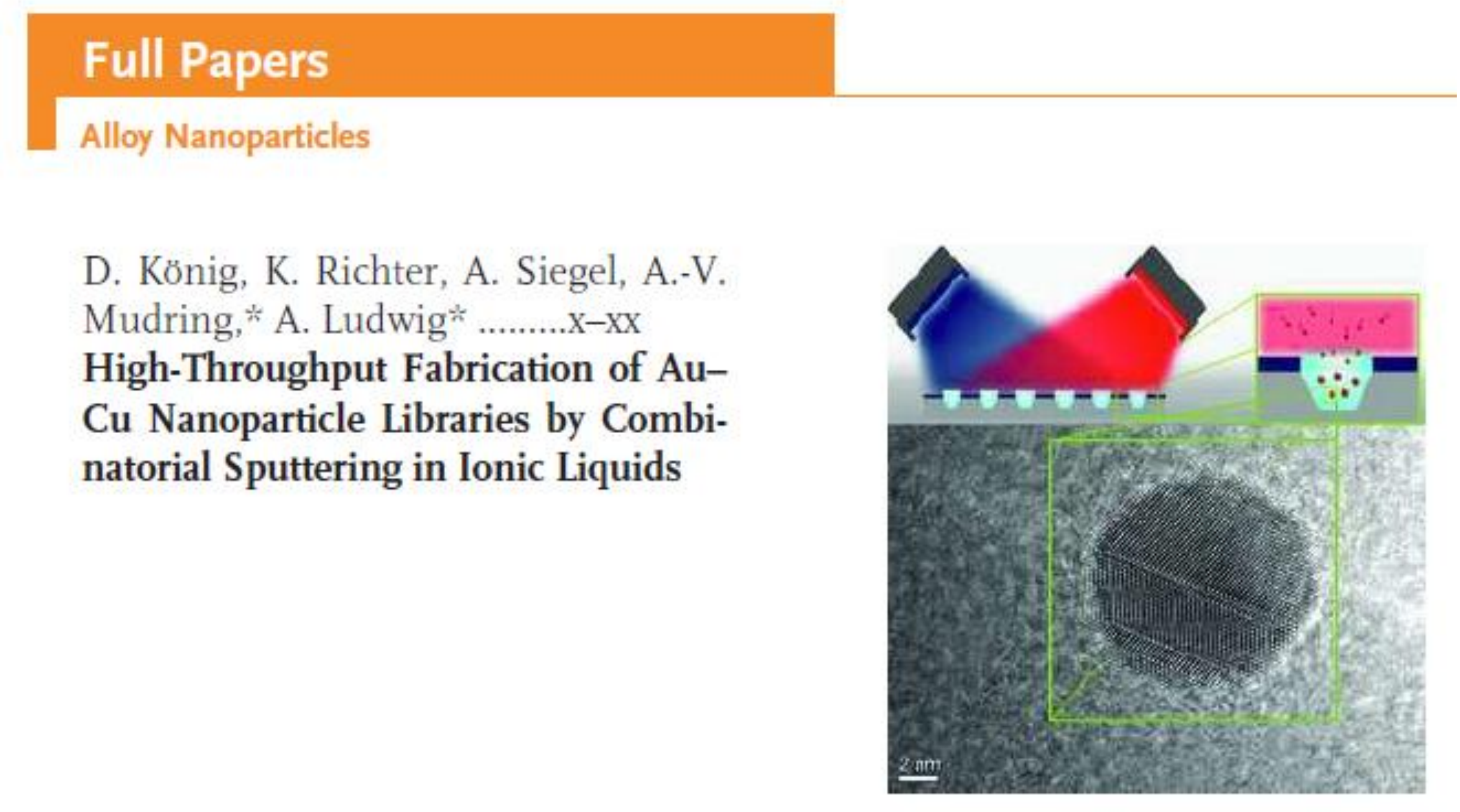

Full Papers

Alloy Nanoparticles

D. König, K. Richter, A. Siegel, A.-V. Mudring,* A. Ludwig* ....x–xx

High-Throughput Fabrication of Au–Cu Nanoparticle Libraries by Combinatorial Sputtering in Ionic Liquids

Combinatorial sputtering in ionic liquids

Sputtered Cu nanoparticles in ionic liquids
TEM in IL

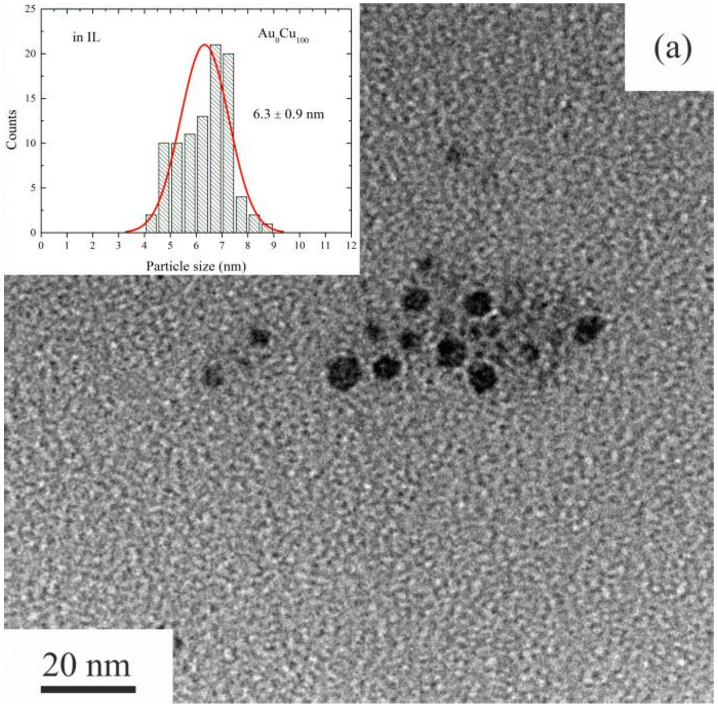

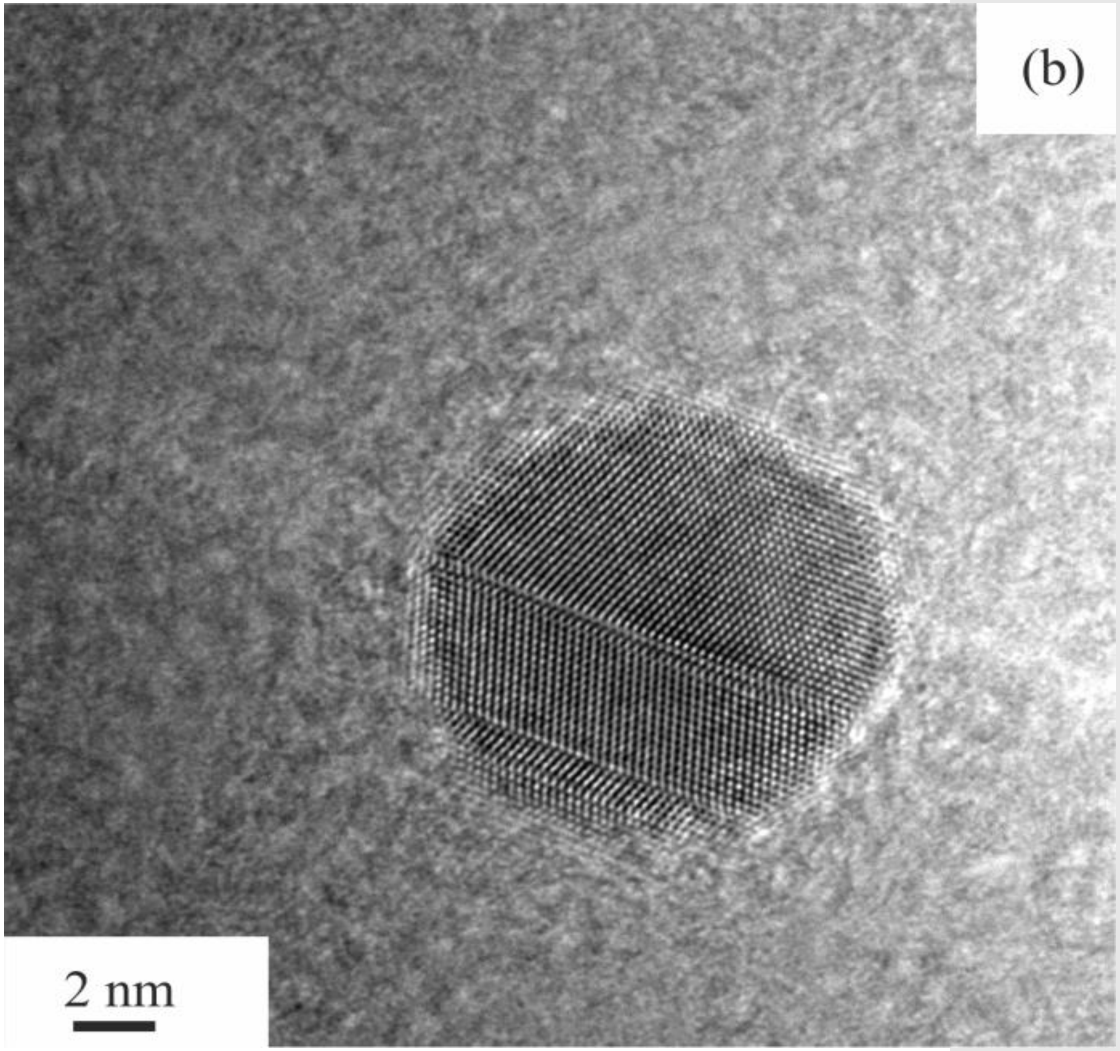

(a) TEM of Cu NPs in $[C_1C_4im][Tf_2N]$
(b) HRTEM of a single Cu NP in IL

Combinatorial sputtering in ionic liquids

Cu nanoparticles measured in ionic liquids and as extracted NPs

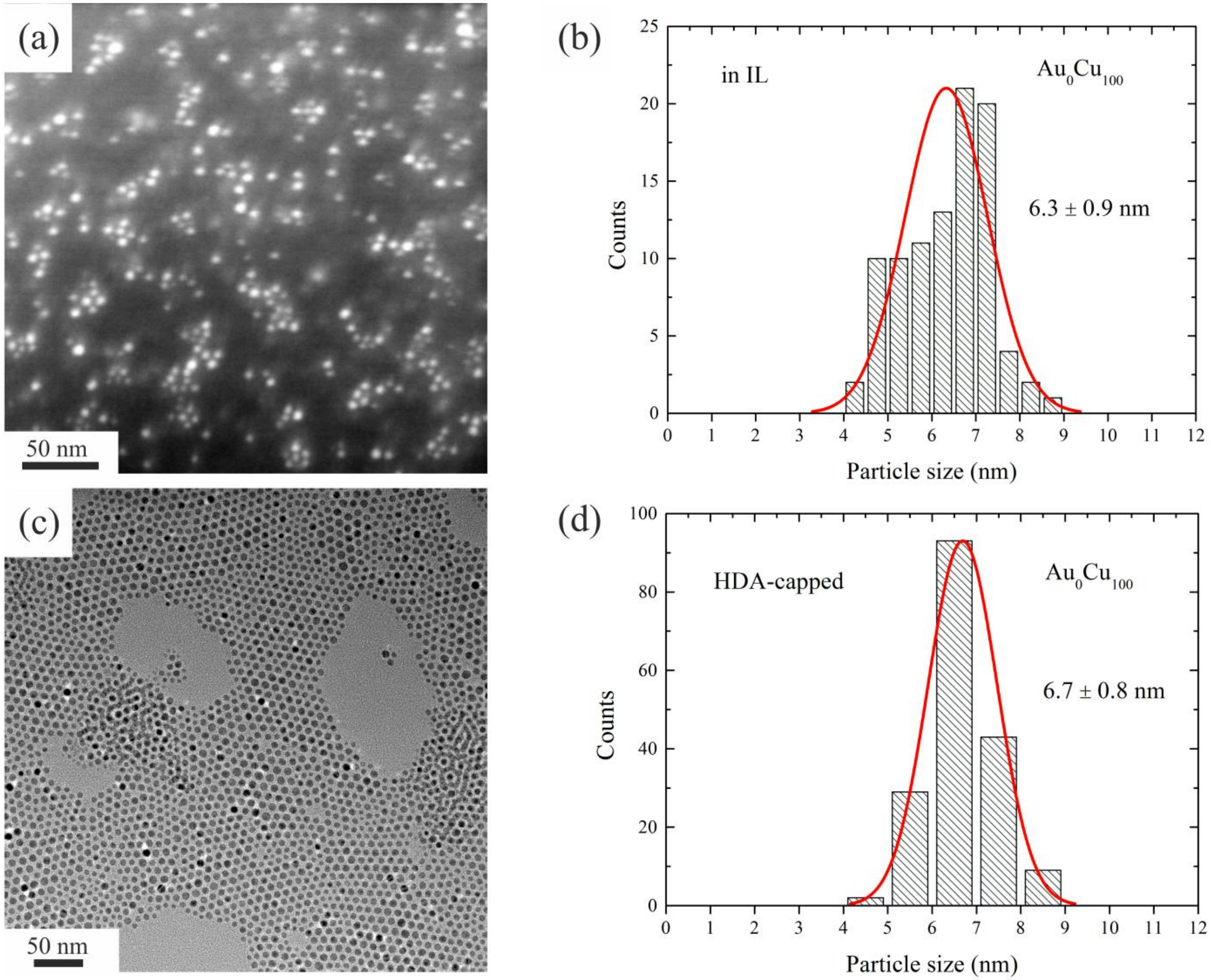

Fabrication of elemental, binary and ternary nanoparticles by combinatorial sputtering into ionic liquids

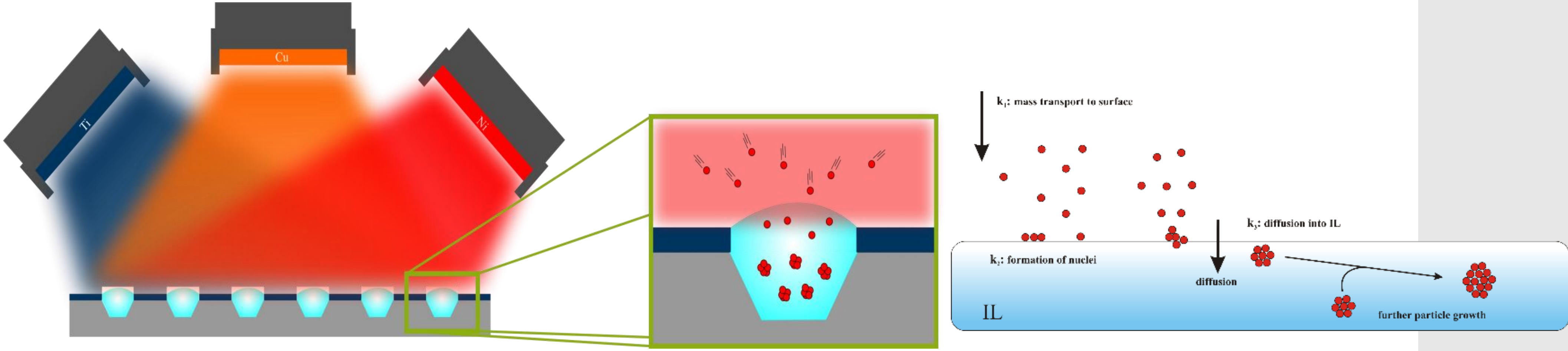

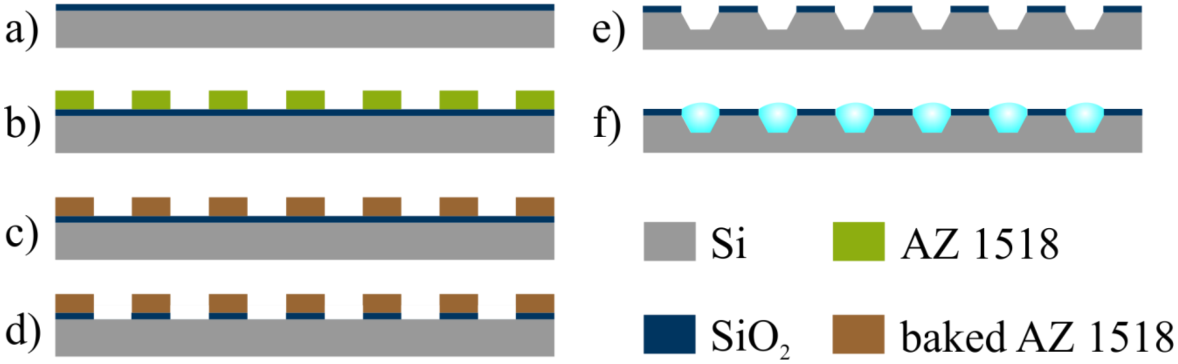

Fabrication of elemental, binary and ternary nanoparticles by combinatorial sputtering into ionic liquids

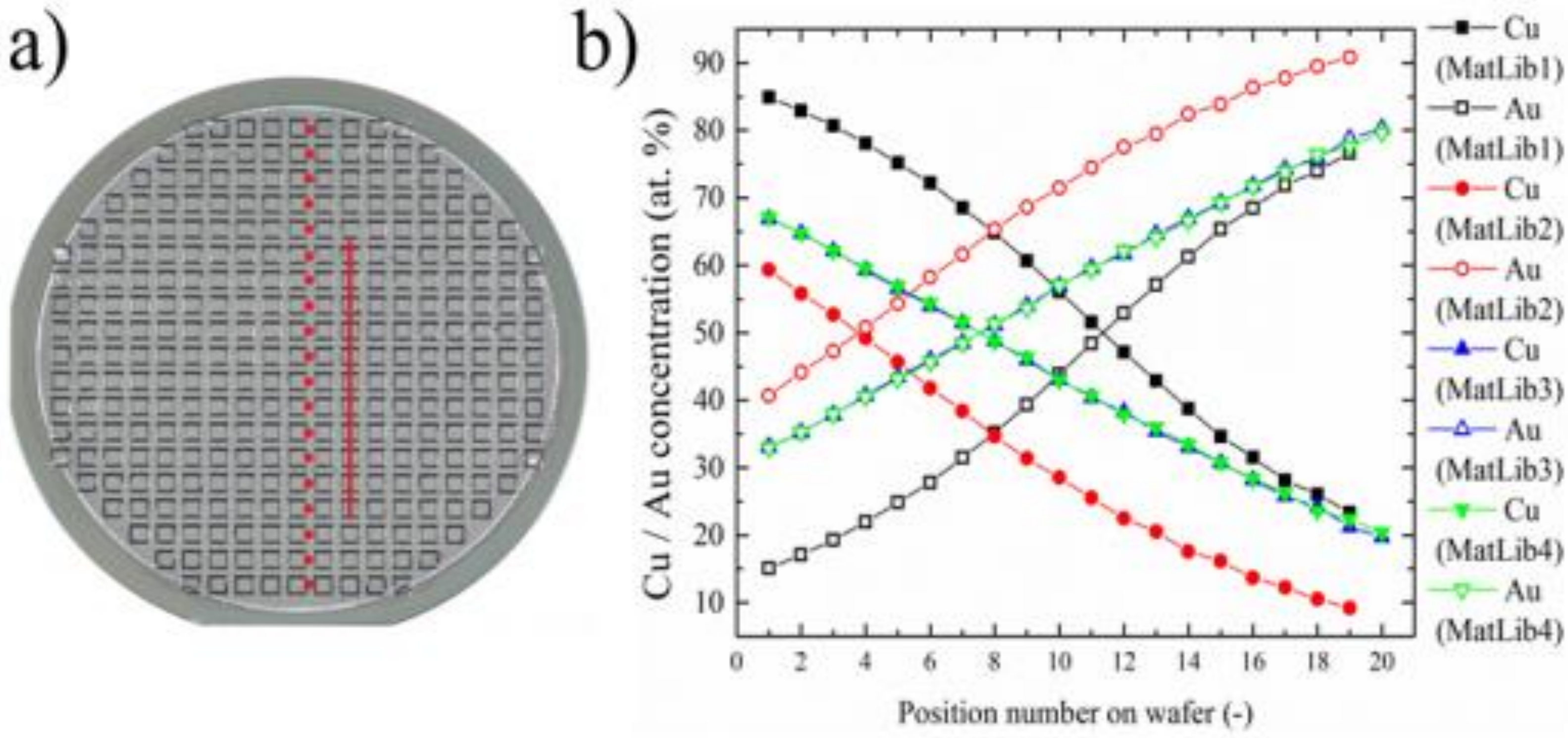

Development of new materials using high-throughput experimentation

Combinatorial sputtering in ionic liquids

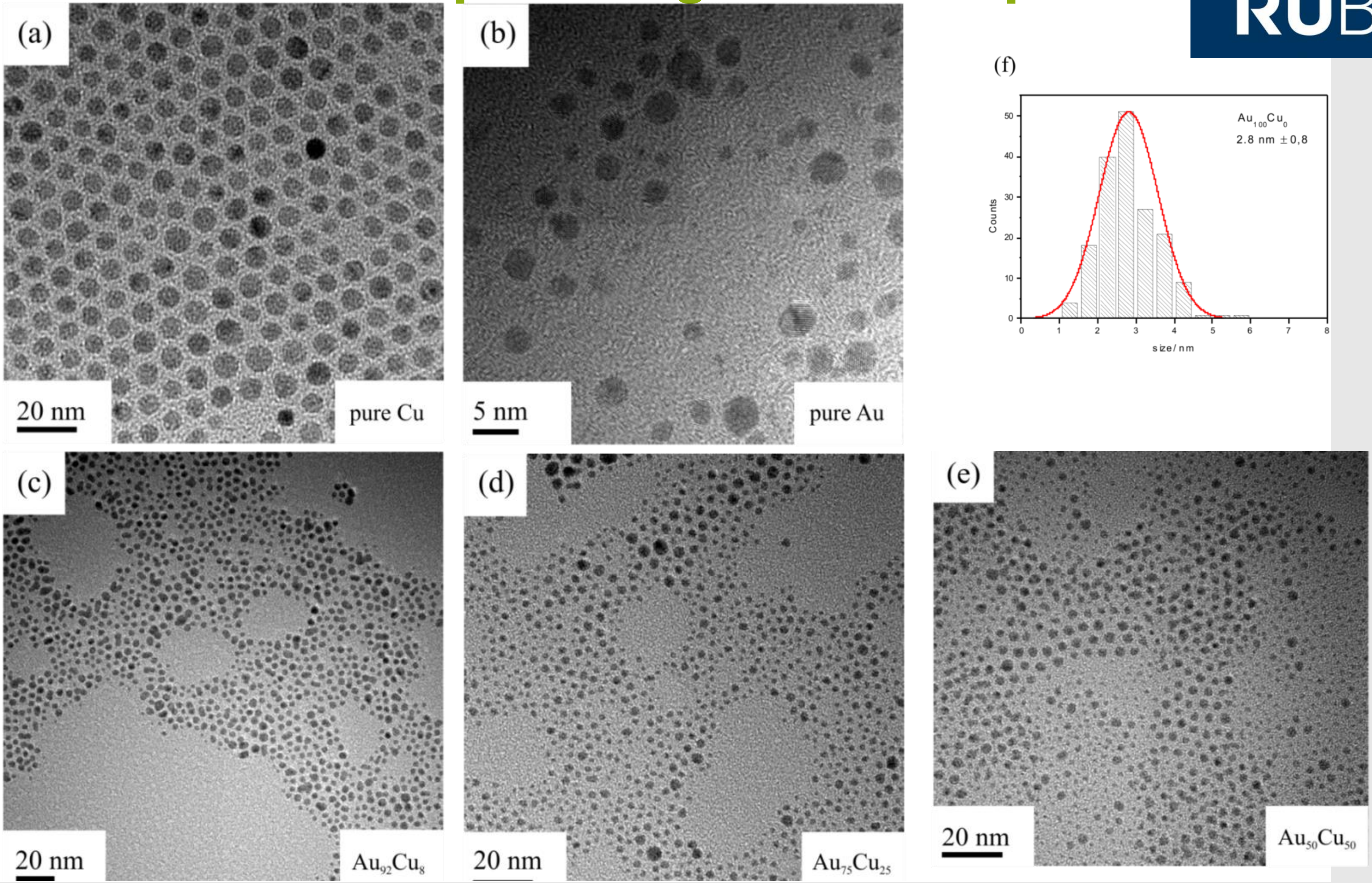

Discovery of a multinary noble metal free oxygen reduction catalyst: Strategy for evaluation of intrinsic activity of multinary alloy NPs

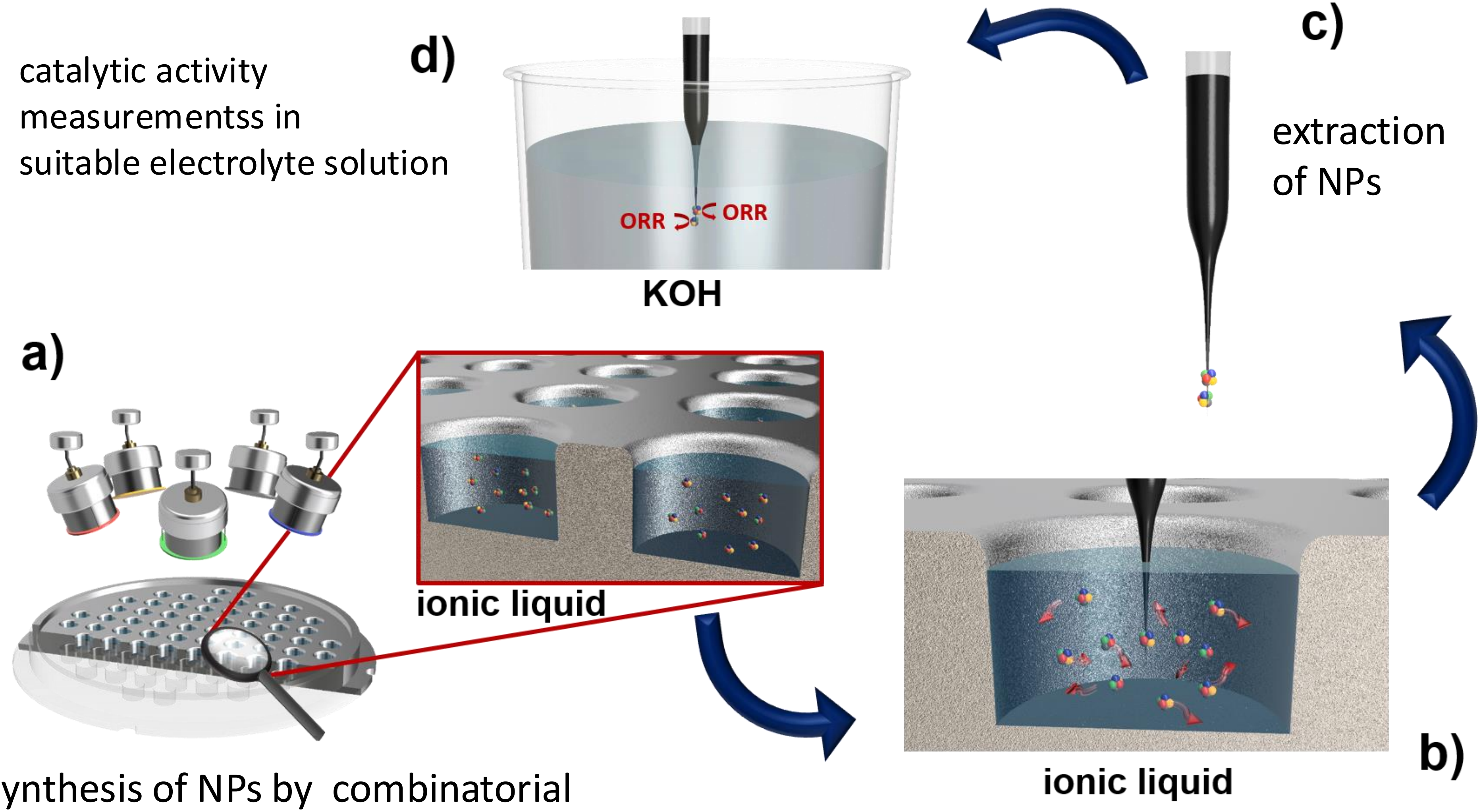

catalytic activity measurementss in suitable electrolyte solution

extraction of NPs

synthesis of NPs by combinatorial co-sputtering into an ionic liquid [Bmim][Tf2N]

potential-assisted immobilization at an etched carbon nanoelectrode utilizing nanoimpacts

T. Löffler, H. Meyer, A. Savan, P. Wilde, A. Garzón Manjón, Y.-T. Chen, E. Ventosa, C. Scheu, A. Ludwig, W. Schuhmann (2018) Discovery of a Multinary Noble Metal Free Oxygen Reduction Catalyst, Advanced Energy Materials1 802269

„High entropy“ alloy nanoparticle libraries: Cr-Mn-Fe-Co-Ni

BMBF Project NEMEZU

noble metal–free
multinary transition metal nanoparticle libraries

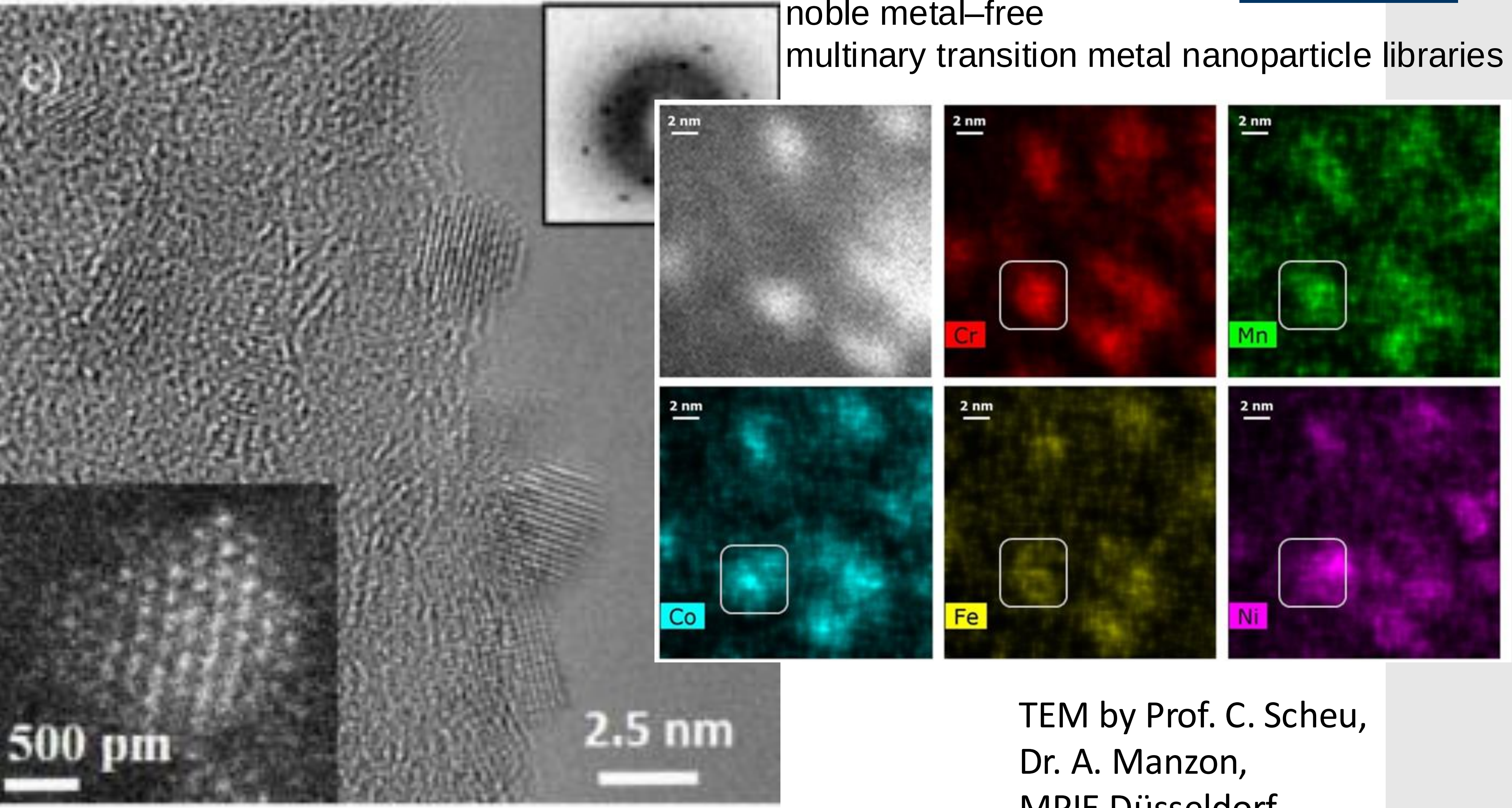

TEM by Prof. C. Scheu,
Dr. A. Manzon,
MPIE Düsseldorf

A. Garzón-Manjón, H. Meyer, D. Grochla, T. Löffler, W. Schuhmann, A. Ludwig, C. Scheu (2018)
Controlling amorphous and crystalline state of multinary alloy nanoparticles in an ionic liquid, Nanomaterials 2018, 8, 903

Cr-Mn-Fe-Co-Ni nanoparticle libraries: ORR catalysts

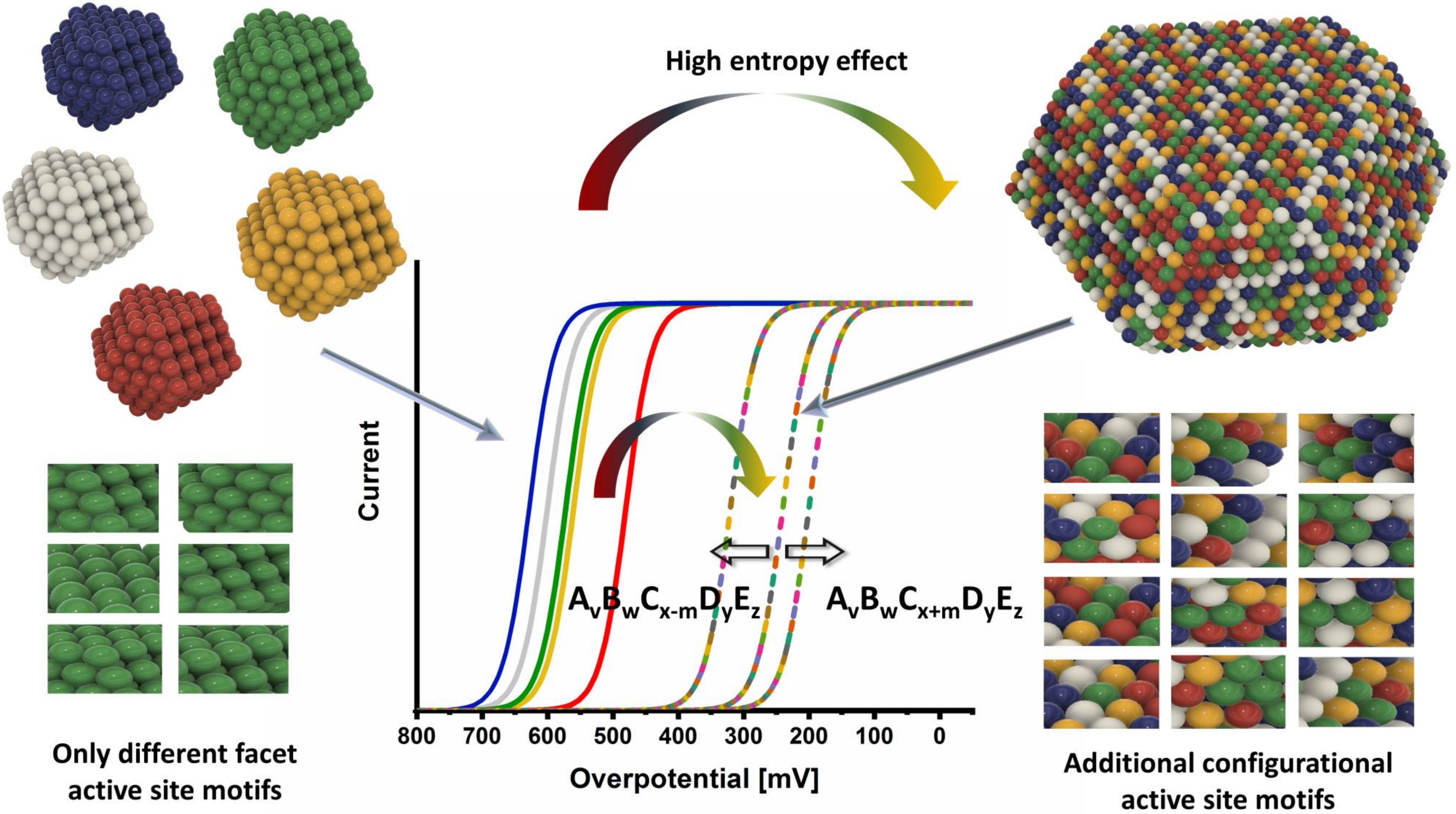

T. Löffler, H. Meyer, A. Savan, P. Wilde, A. Garzón Manjón, Y.-T. Chen, E. Ventosa, C. Scheu, A. Ludwig, W. Schuhmann (2018) Discovery of a Multinary Noble Metal Free Oxygen Reduction Catalyst, Advanced Energy Materials1 802269

Patent application 10 2017 128 058.8

„High entropy“ alloy nanoparticle libraries: Cr-Mn-Fe-Co-Ni

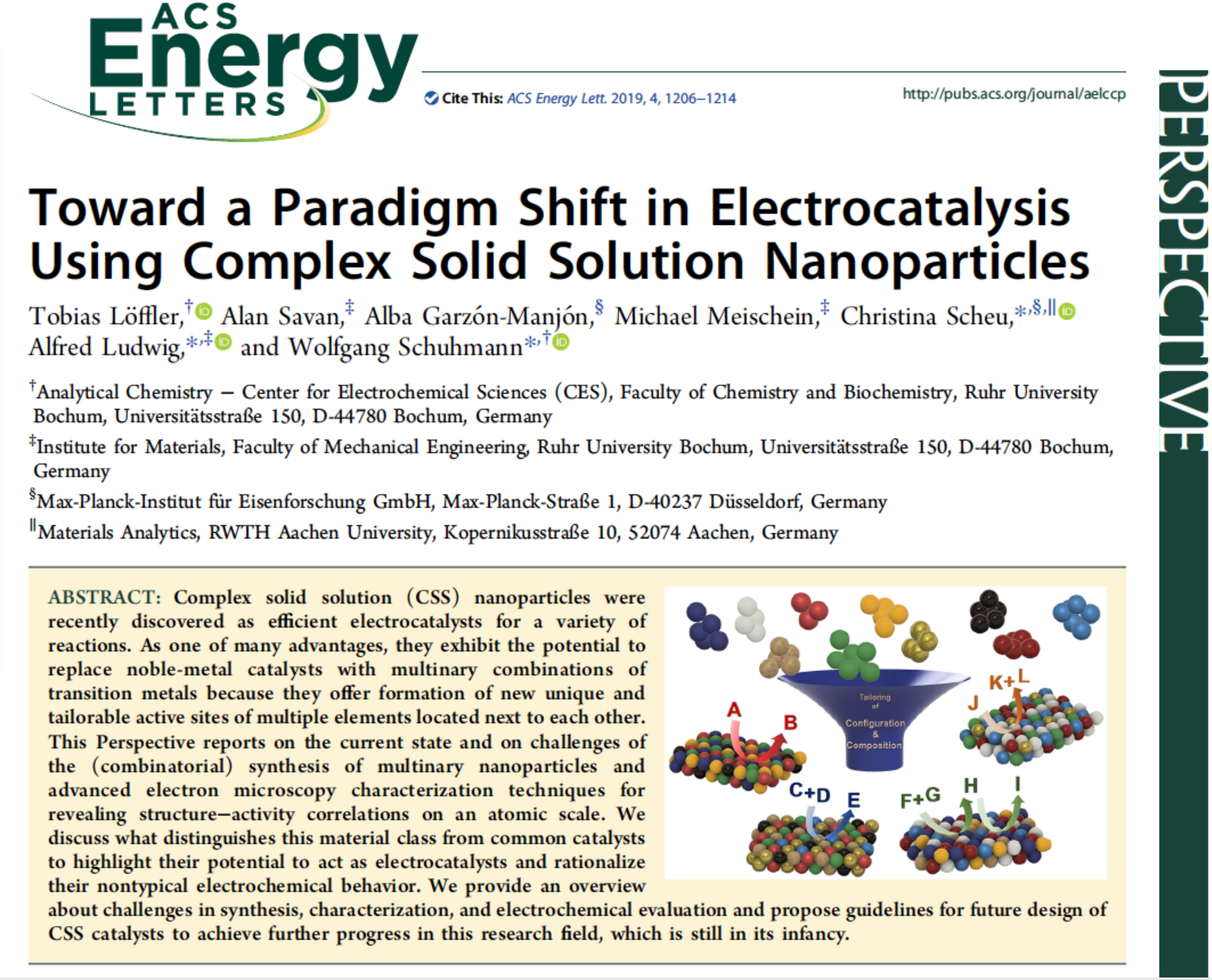

ACS Energy LETTERS

Cite This: ACS Energy Lett. 2019, 4, 1206−1214 http://pubs.acs.org/journal/aelccp

PERSPECTIVE

Toward a Paradigm Shift in Electrocatalysis Using Complex Solid Solution Nanoparticles

Tobias Löffler,[†] Alan Savan,[‡] Alba Garzón-Manjón,[§] Michael Meischein,[‡] Christina Scheu,[*,§,∥] Alfred Ludwig,[*,‡] and Wolfgang Schuhmann[*,†]

[†]Analytical Chemistry − Center for Electrochemical Sciences (CES), Faculty of Chemistry and Biochemistry, Ruhr University Bochum, Universitätsstraße 150, D-44780 Bochum, Germany

[‡]Institute for Materials, Faculty of Mechanical Engineering, Ruhr University Bochum, Universitätsstraße 150, D-44780 Bochum, Germany

[§]Max-Planck-Institut für Eisenforschung GmbH, Max-Planck-Straße 1, D-40237 Düsseldorf, Germany

[∥]Materials Analytics, RWTH Aachen University, Kopernikusstraße 10, 52074 Aachen, Germany

ABSTRACT: Complex solid solution (CSS) nanoparticles were recently discovered as efficient electrocatalysts for a variety of reactions. As one of many advantages, they exhibit the potential to replace noble-metal catalysts with multinary combinations of transition metals because they offer formation of new unique and tailorable active sites of multiple elements located next to each other. This Perspective reports on the current state and on challenges of the (combinatorial) synthesis of multinary nanoparticles and advanced electron microscopy characterization techniques for revealing structure−activity correlations on an atomic scale. We discuss what distinguishes this material class from common catalysts to highlight their potential to act as electrocatalysts and rationalize their nontypical electrochemical behavior. We provide an overview about challenges in synthesis, characterization, and electrochemical evaluation and propose guidelines for future design of CSS catalysts to achieve further progress in this research field, which is still in its infancy.

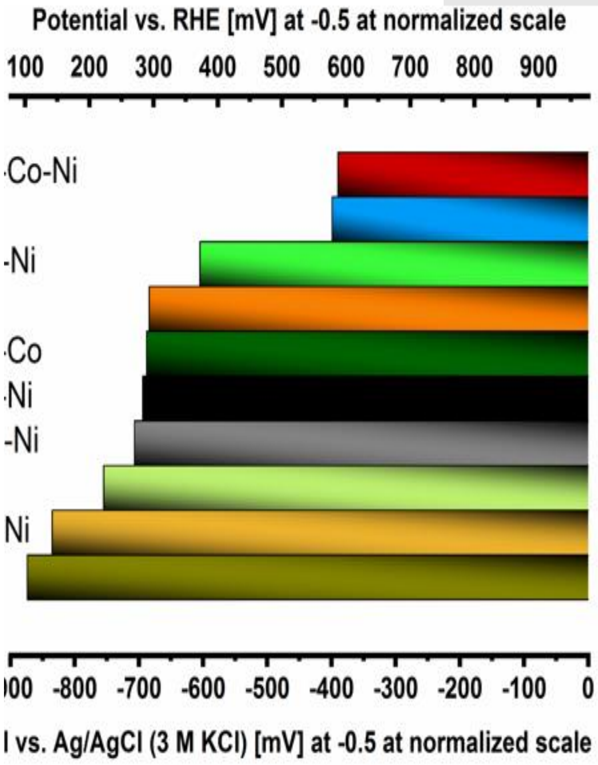

s a significant drop
e synergistic
solid solution
; of single elements

T. Löffler, H. Meyer, A. Savan, P. Wilde, A. Garzón Manjón, Y.-T. Chen, E. Ventosa, C. Scheu, A. Ludwig, W. Schuhmann (2018) Discovery of a Multinary Noble Metal Free Oxygen Reduction Catalyst, Advanced Energy Materials1 802269

Advanced Materials Processing and Microfabrication

Nanotechnolgie: „1-D Strukturen“

Nanodrähte, Nanosäulen

Synthese nanostrukturierter dünner Schichten: Glancing angle deposition (GLAD)

Thin films by physical vapor deposition (PVD)

PVD: evaporation, sputtering, PLD, …

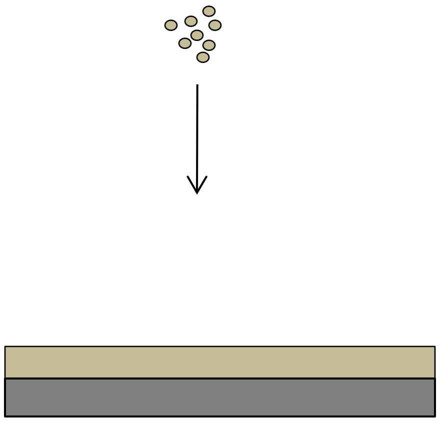

normal angle incidence

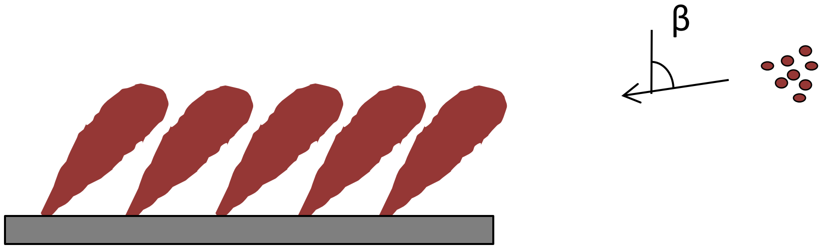

oblique angle incidence

→ particle flux under normal angle incidence leads to thin compact, dense film (compare structure zone diagrams)

→ under oblique angle (glancing angle) particle flux columnar nanostructures can be grown

(directional) material flux arrives at the surface of a substrate at an oblique angle

Laktakia and Messier, Sculptured thin films- nanoengineered morphology and optics, SPIE, Bellingham, WA, (2005)

Synthese nanostrukturierter dünner Schichten
Glancing angle deposition (GLAD)

Thin film deposition under oblique angle incidence (OAD)

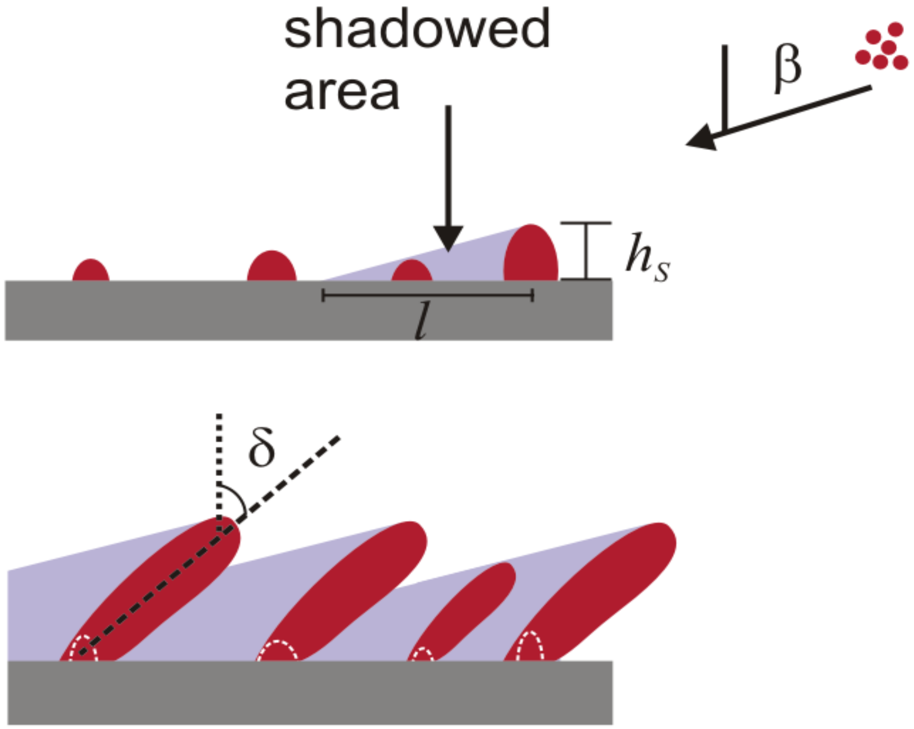

C.Khare, PhD thesis, Universität Leipzig (2011)

self-shadowing mechanism

- early stage mound formation
- limited surface diffusion
- shadowing length $l = h_s \cdot \tan \beta$
- β ≥ 80°
- competitive growth
- Volmer-Weber growth most favourable*

Kundt et al., *Annalen der Physik* 59 (1886)
Robbie et al. , *Nature* 384 (1996)
*Hawkeye and Brett J. Vac. Sci. Technol. A 25 (2007)

Synthese nanostrukturierter dünner Schichten
Glancing angle deposition (GLAD)

Thin film deposition under oblique angle incidence

86 *A. Barranco et al. / Progress in Materials Science 76 (2016) 59–153*

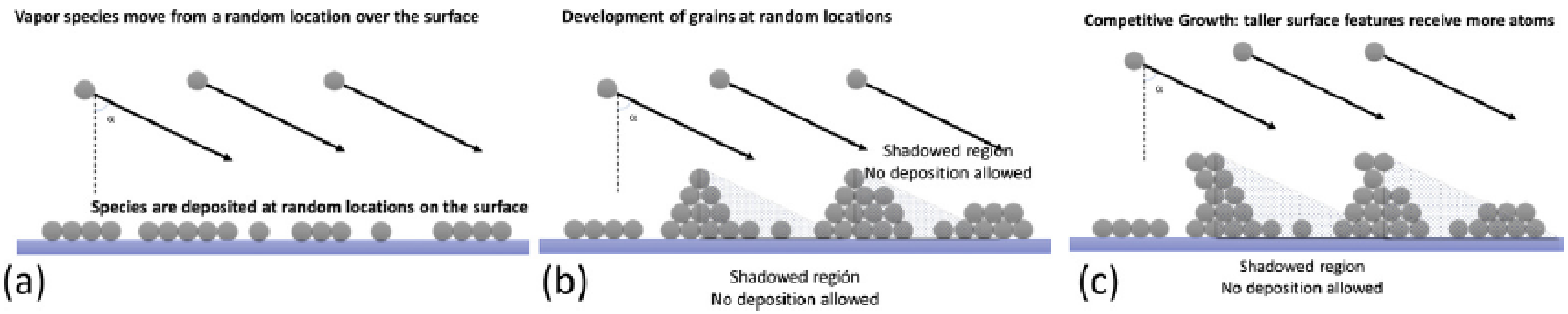

Fig. 4.1. First stages of growth during the OAD of thin films. (a) Individual vapor species arrive at random locations on the surface with a given tilt angle. (b) Deposited particles accumulate within certain regions in the form of grains of material that then cast shadows over other surface zones where vapor species cannot be deposited. (c) Taller surface features are more likely to grow, initiating a competitive growth process in which the taller a feature is the larger its shadow, thus forming tilted columnar structures.

Synthese nanostrukturierter dünner Schichten
Glancing angle deposition (GLAD)

Structure zone diagrams

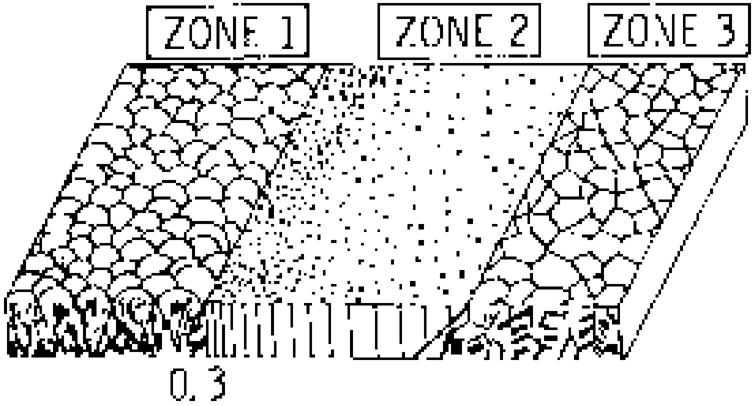

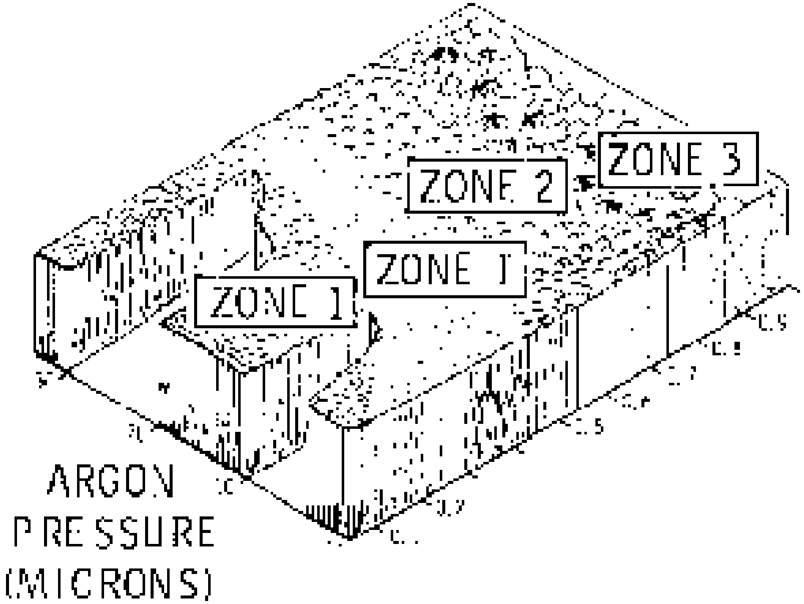

- surface diffusion
- substrate temperature
- sputter parameters (pressure, bias)

JA Thornton ,J. Vac. Sci. Technol., 11 (1974)
JA Thornton, Ann. Rev. Mater. Sci. 7 (1977)

Synthese nanostrukturierter dünner Schichten
Glancing angle deposition (GLAD)

Thin film deposition under oblique angle incidence

- *OAD coupled with substrate rotation by Young and Kowal in 1959* Nature 183, 104 (1959)

  - deposition of optically active fluorite films

- *Breakthrough: "GLAD" by Robbie et al. in 1995-96* Nature 384, 616 (1996)

(with the availibilty of powerful imaging technique " scanning electron microscopy ")

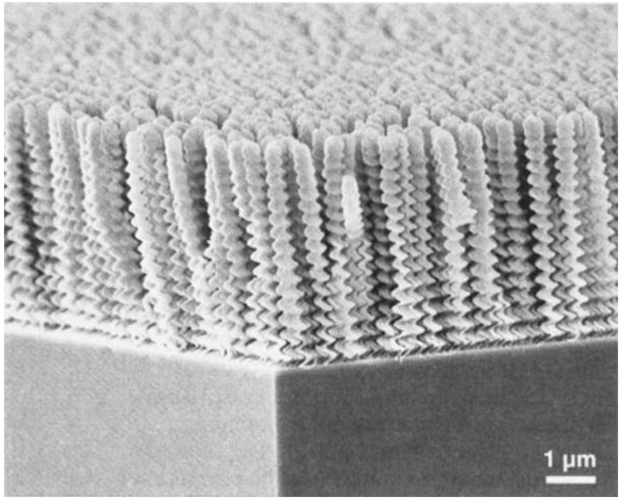

Robbie et al. Nature 384, 616 (1996)

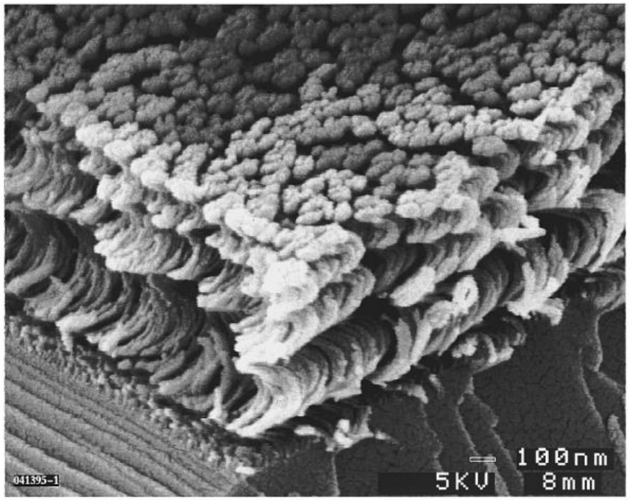

Robbie et al. J. Vac. Sci. Technol. A 13 (1995)

Synthese nanostrukturierter dünner Schichten
Glancing angle deposition (GLAD)

Oblique angle deposition and Glancing angle deposition

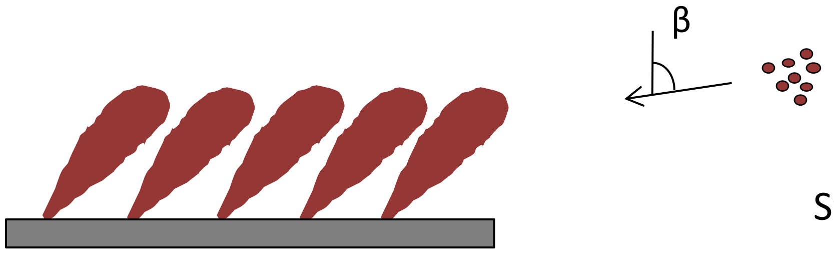

Stationary substrate: **Oblique angle incidence (OAD)**

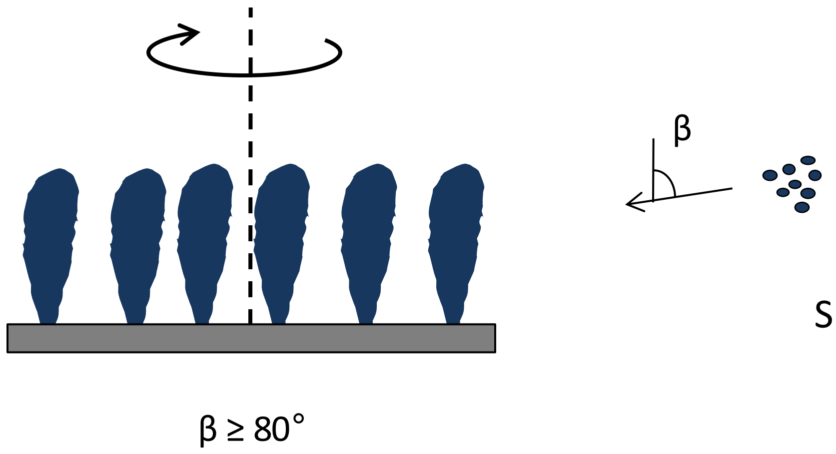

Substrate rotation: **Glancing angle deposition (GLAD)**

Robbie et al. J. Vac. Sci. Technol. A 13 (1995)
Robbie and Brett, J. Vac. Sci. Technol. A 15 (1997)
Hawkeye and Brett J. Vac. Sci. Technol. A 25 (2007)

Synthese nanostrukturierter dünner Schichten
Glancing angle deposition (GLAD)

Substrate rotation: **Glancing angle deposition (GLAD)**

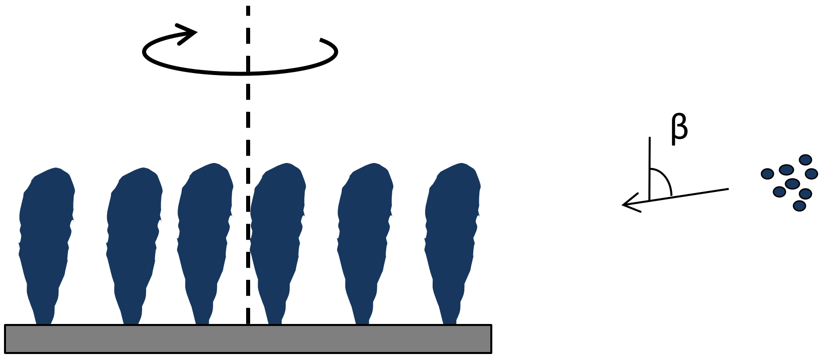

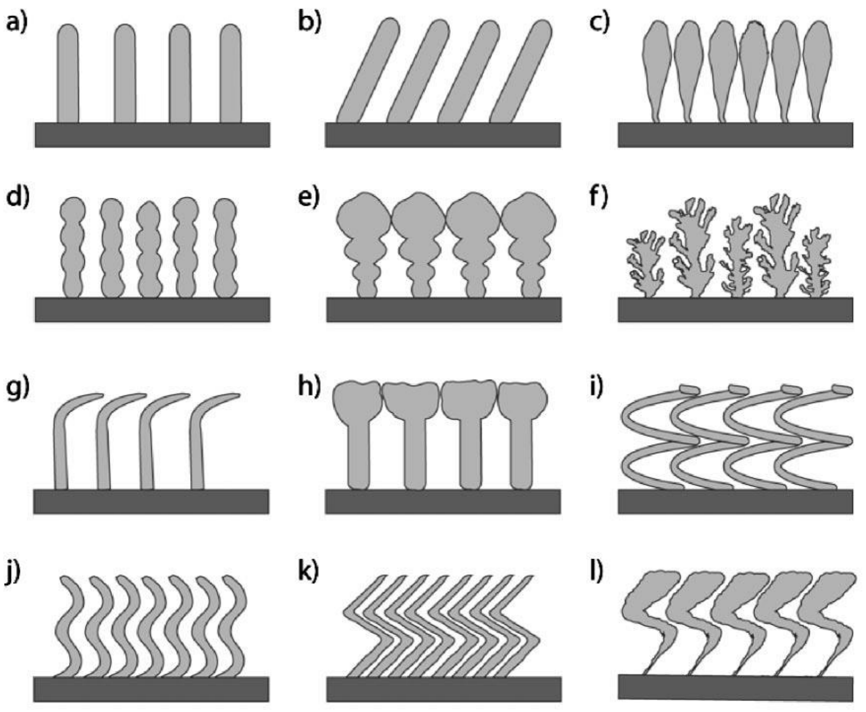

- continous rotation
- stepwise substrate rotation

Robbie et al. Nature 384, 616 (1996)
Robbie et al., Rev. Sci. Instrum. 75 (2004)
Hawkeye and Brett, J. Vac. Sci. Technol. A 25 (2007)

Synthese nanostrukturierter dünner Schichten
Glancing angle deposition (GLAD)

many nanostructures possible

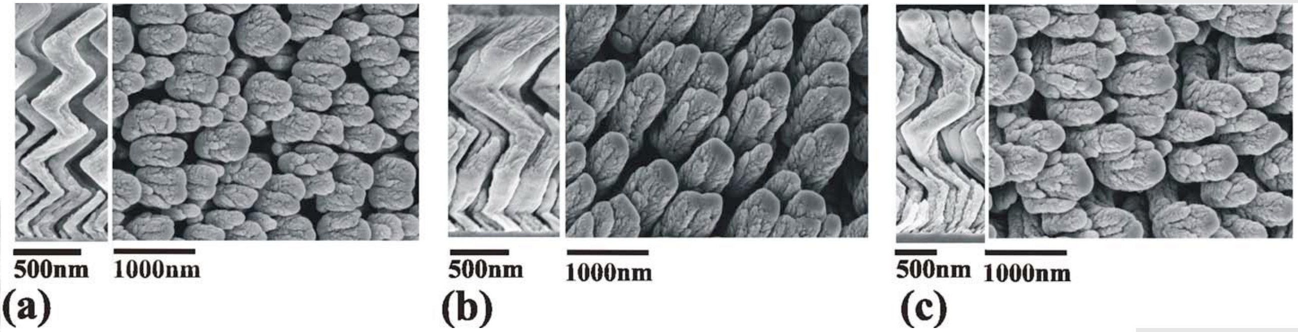

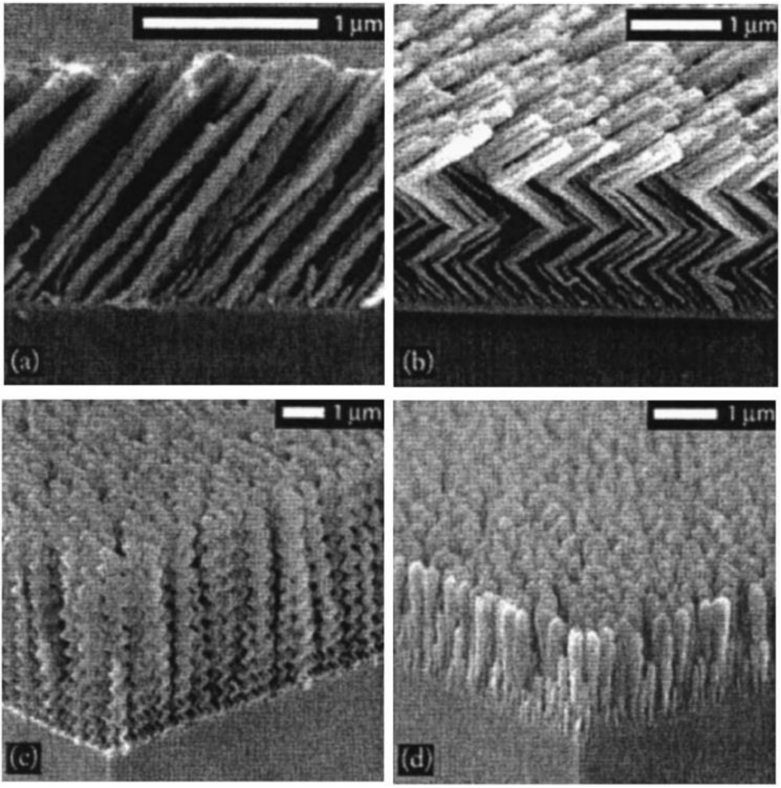

C. Patzig and B. Rauschenbach et al., J. Vac. Sci. Technol. B 25 (2007), C. Patzig, PhD thesis, Universität Leipzig, (2009)
Hawkeye and Brett, J. Vac. Sci. Technol. A 25 (2007)

Synthese nanostrukturierter dünner Schichten
Glancing angle deposition (GLAD)

scaling behaviour of nanostructures

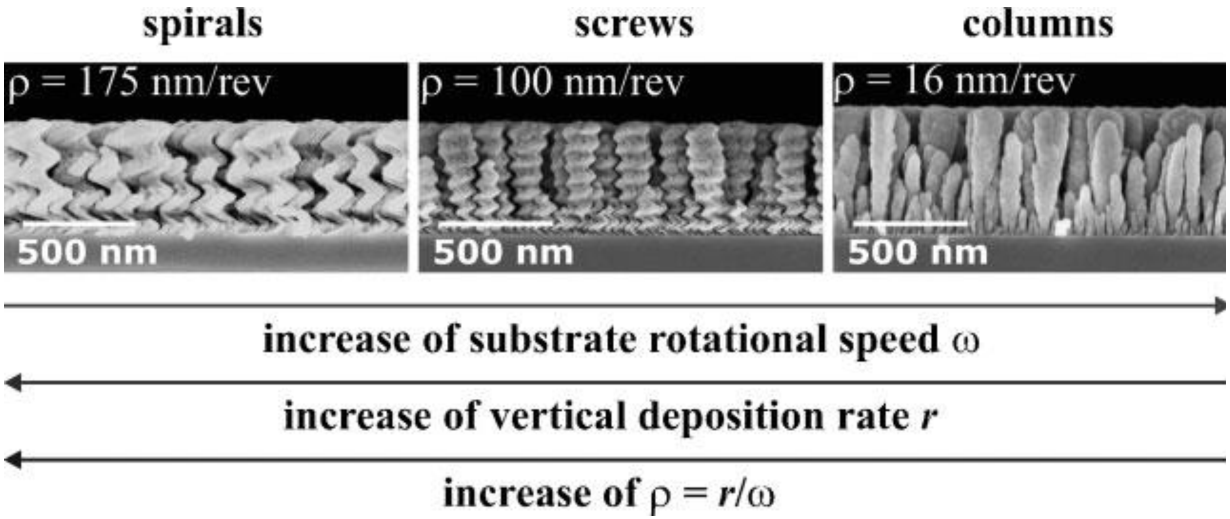

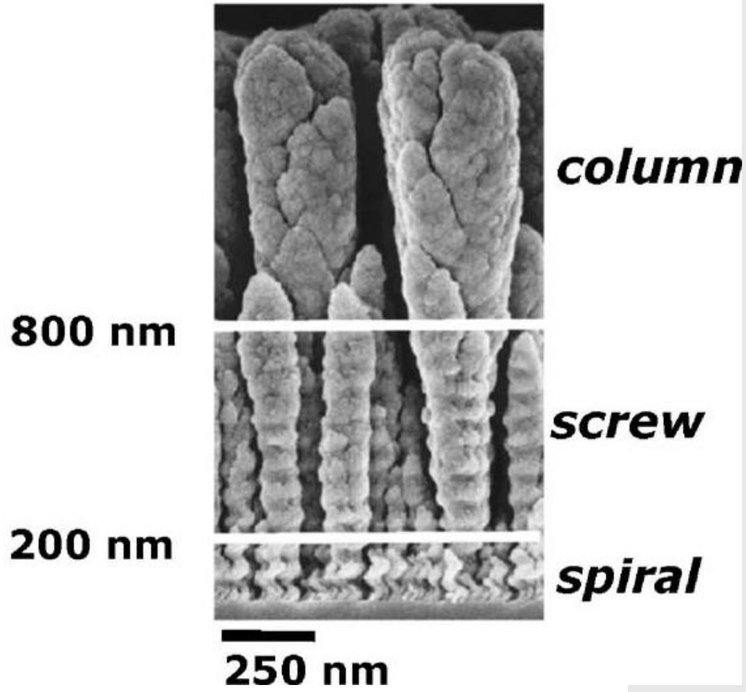

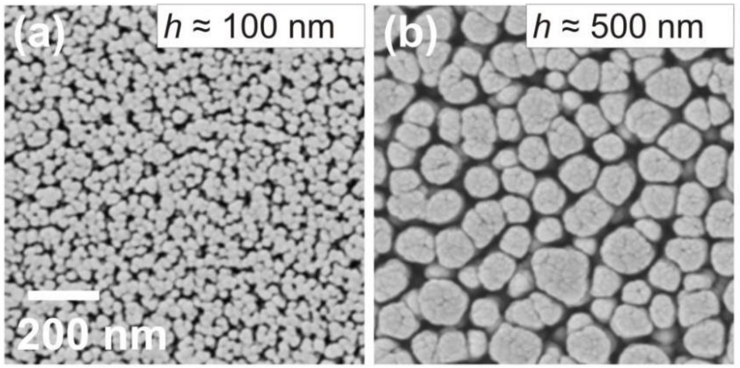

- stochastic process
- predominant seeds overgrow due to temporarily existing local non-uniform particle flux
- competitive growth

C. Patzig and B. Rauschenbach et al., J. Vac. Sci. Technol. B 25 (2007)
C. Patzig, PhD thesis, Universität Leipzig, (2009)
C. Khare, PhD thesis, Universität Leipzig (2012)
Hawkeye and Brett, J. Vac. Sci. Technol. A 25 (2007)

Synthese nanostrukturierter dünner Schichten
Glancing angle deposition (GLAD)

pre-patterned substrates

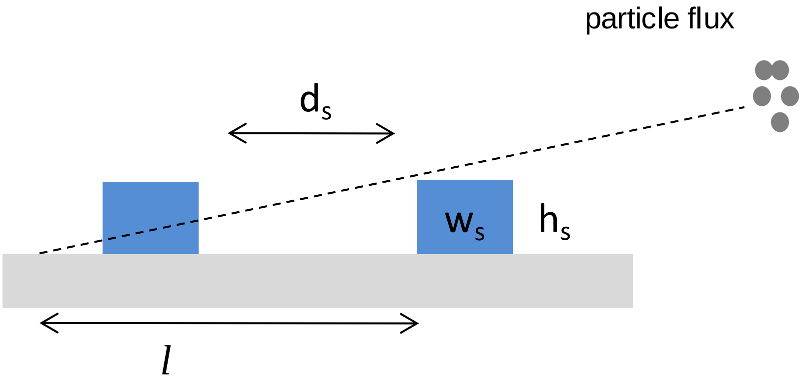

- depletion of inter-seed condensation
  $d_S \leq h_S \cdot \tan(\beta)$
- planar density
  $w_S \geq d_S - h_S \cdot tan\, \beta$
- seed dimension

Examples of pre-patterned substrates

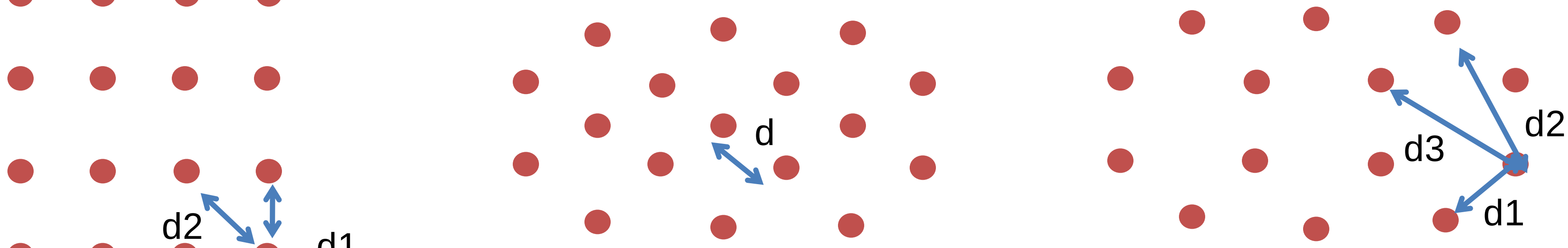

square pattern

planar hexagonal pattern

honeycomb pattern

Synthese nanostrukturierter dünner Schichten
Glancing angle deposition (GLAD)

periodic nanostructure arrays

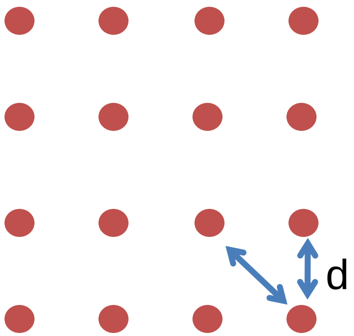

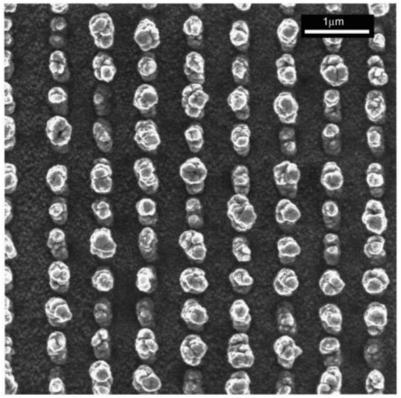

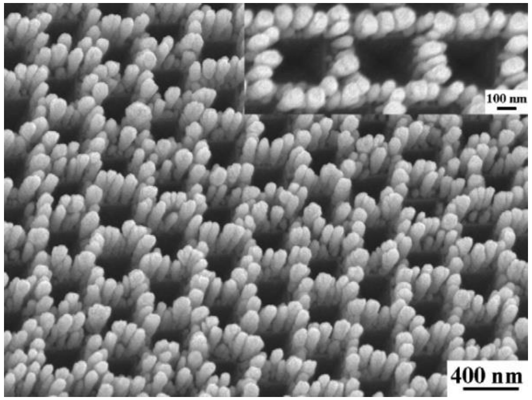

Pre-patterned substrates

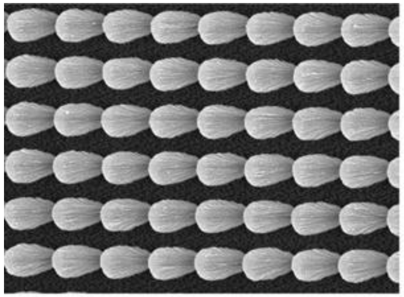

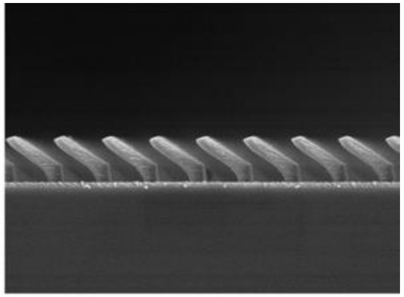

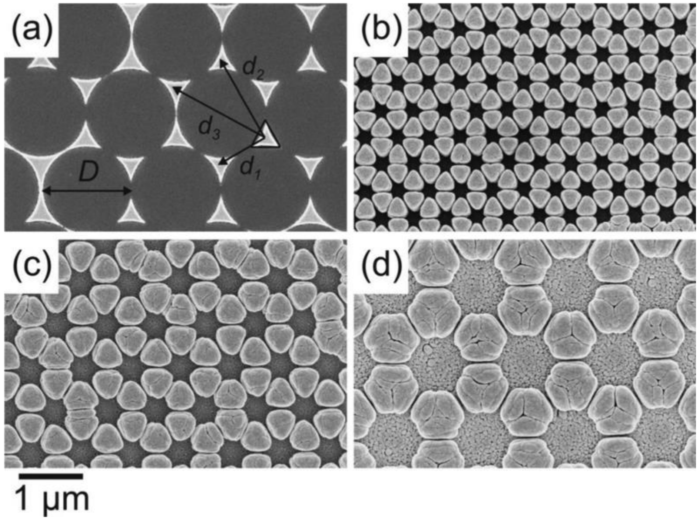

Malac and Brett et al. J. Vac. Sci. Technol. B 17 (1999)
Ye and Lu et al. Nanotechnology 16 (2005)
Zhou and Gall, Thin Solid Films 516, (2007)
Khare and Rauschenbach et al. . J. Vac. Sci. Technol. A 29 (2011)

Synthese nanostrukturierter dünner Schichten
Glancing angle deposition (GLAD)

Temperature influence (surface diffusion)

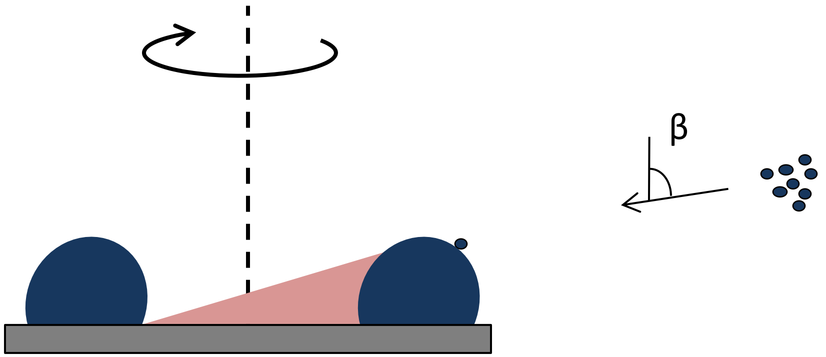

ballistic deposition at low T

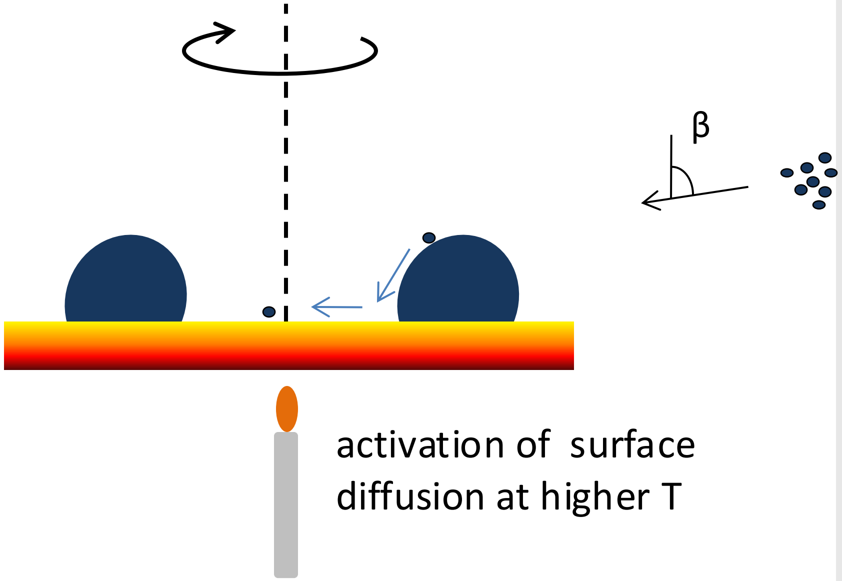

activation of surface diffusion at higher T

Surface diffusion: Fick‘s law

$$D \sim \exp\left(\frac{-E_a}{k_b T_s}\right)$$

Resulting morphology is considerably influenced by surface diffusion

Hawkeye and Brett, J. Vac. Sci. Technol. A 25 (2007)

Synthese nanostrukturierter dünner Schichten
Sculptured thin films (STF)

Different STFs can be obtained by changing
either alternatively or simultaneously the zenithal, azimuthal and/or polar (h) angle to alter the incoming direction of the deposition flux during growth

e.g. oblique matchsticks, chevrons, multiple zigzags, S's, C's, helices, superhelices
in response to moving the substrate during deposition

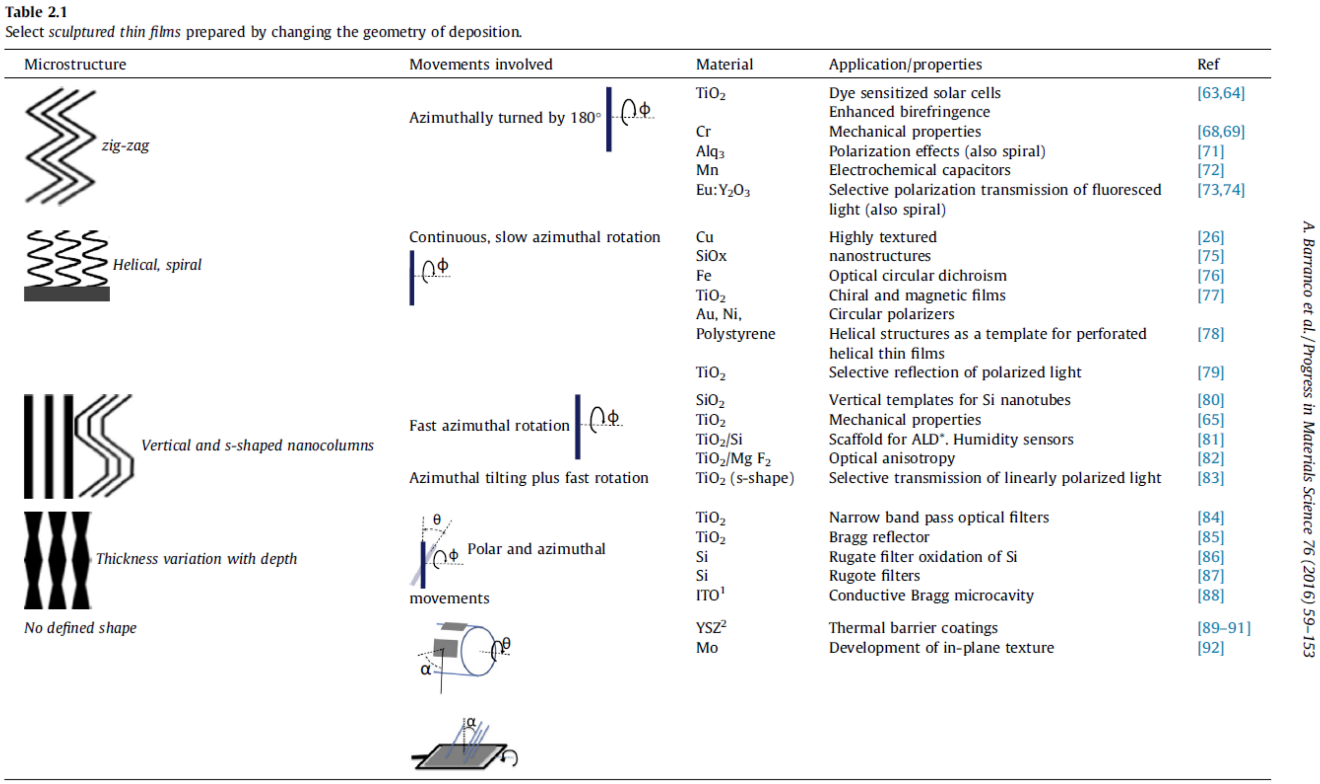

Table 2.1
Select *sculptured thin films* prepared by changing the geometry of deposition.

Microstructure	Movements involved	Material	Application/properties	Ref
zig-zag	Azimuthally turned by 180° ϕ	TiO_2	Dye sensitized solar cells Enhanced birefringence	[63,64]
		Cr	Mechanical properties	[68,69]
		Alq_3	Polarization effects (also spiral)	[71]
		Mn	Electrochemical capacitors	[72]
		$Eu{:}Y_2O_3$	Selective polarization transmission of fluoresced light (also spiral)	[73,74]
Helical, spiral	Continuous, slow azimuthal rotation ϕ	Cu	Highly textured	[26]
		SiOx	nanostructures	[75]
		Fe	Optical circular dichroism	[76]
		TiO_2	Chiral and magnetic films	[77]
		Au, Ni,	Circular polarizers	
		Polystyrene	Helical structures as a template for perforated helical thin films	[78]
		TiO_2	Selective reflection of polarized light	[79]
Vertical and s-shaped nanocolumns	Fast azimuthal rotation ϕ	SiO_2	Vertical templates for Si nanotubes	[80]
		TiO_2	Mechanical properties	[65]
		TiO_2/Si	Scaffold for ALD*. Humidity sensors	[81]
		TiO_2/MgF_2	Optical anisotropy	[82]
	Azimuthal tilting plus fast rotation	TiO_2 (s-shape)	Selective transmission of linearly polarized light	[83]
Thickness variation with depth	θ ϕ Polar and azimuthal movements	TiO_2	Narrow band pass optical filters	[84]
		TiO_2	Bragg reflector	[85]
		Si	Rugate filter oxidation of Si	[86]
		Si	Rugote filters	[87]
		ITO^1	Conductive Bragg microcavity	[88]
No defined shape	α θ α	YSZ^2	Thermal barrier coatings	[89–91]
		Mo	Development of in-plane texture	[92]

A. Barranco et al. / Progress in Materials Science 76 (2016) 59–153

Quelle: Barranco et al.
Progr. in Mat. Sc. 76 (2016) 59–153

Synthese nanostrukturierter dünner Schichten
Sculptured thin films (STF)

Sculptured thin films (STF):

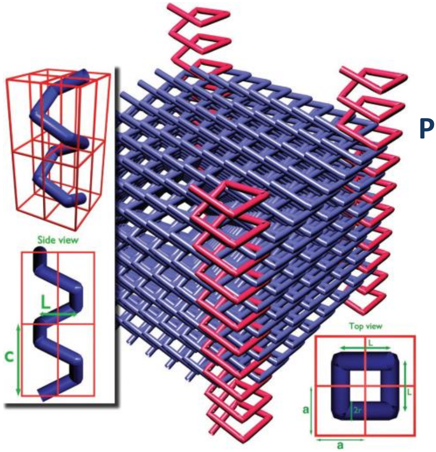

Photonic crystals[*]

‡ ‡ Solar cells: TiO_2 nanocolumn

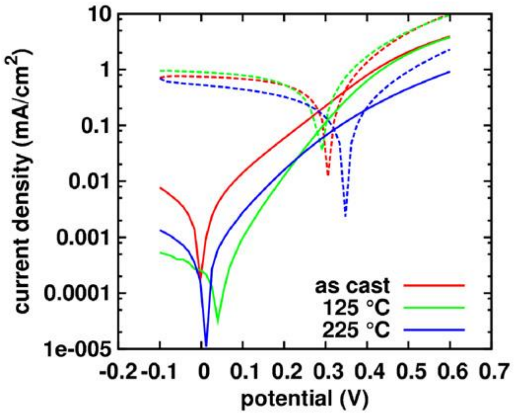

humidity sensing

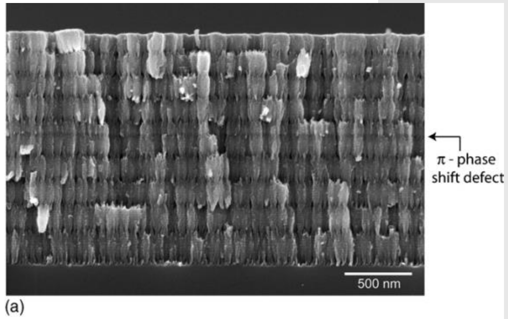

Pt nanorod electrodes for fuel cells[+]

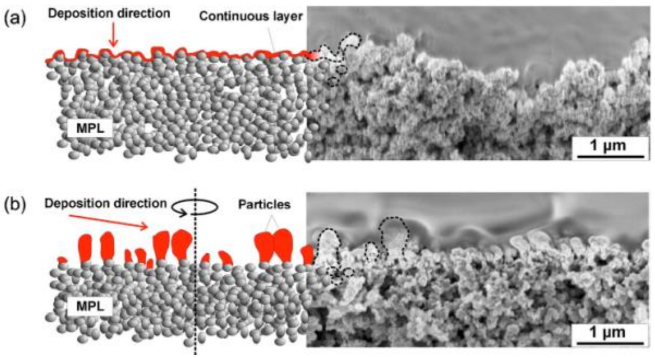

‡ Li-ion batteries: Si nanospirals

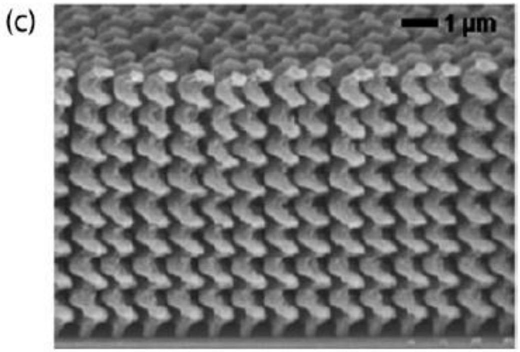

 # Hydrogen storage: Mg nanoblades decorated with V

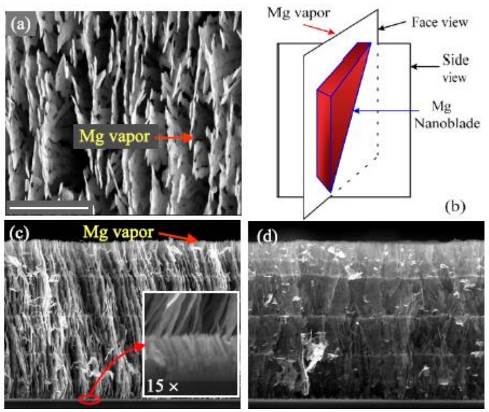

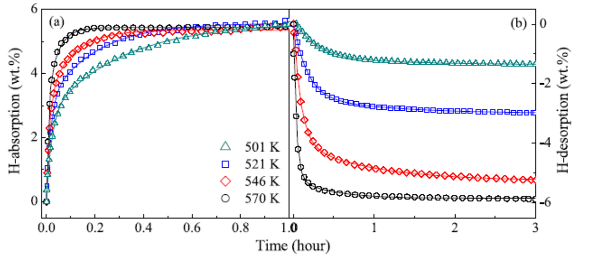

---

*O. Toader and S. John, Science 292(5519) 1133 (2001) **J. Q. Xi et al., Nature Photonics 1(3), 176 (2007)
†J. J. Steele et al., Sens. Actuators B 120(1) 213 (2006); †† Y. Liu et al., Appl. Phys. Lett. 89(17) 173134 (2006)
‡R. Teki et al., Small, 5(20) 2236 (2009); ‡ ‡ N. J. Gerein et al., Sol. Energ. Mater., 94(12) 2343 (2010)
+M. D. Gasda, J. Electro. Soc., 156(5) B614 (2009); #Y. P. He et al., Nanotechnology, 20(20) 204008 (2009)

Synthese nanostrukturierter dünner Schichten
Complex thin film structures

Tuning the optical[1,2], electromagnetic[3,4] and mechanical properties of a material requires simultaneous control over its composition and shape[5]. This is particularly challenging for complex structures at the nanoscale because surface-energy minimization generally causes small structures to be highly symmetric[5]. Here we combine low-temperature shadow deposition with nanoscale patterning to realize nanocolloids with anisotropic three-dimensional shapes, feature sizes down to 20 nm and a wide choice of materials. We demonstrate the versatility of the fabrication scheme by growing three-dimensional hybrid nanostructures that contain several functional materials with the lowest possible symmetry, and by fabricating hundreds of billions of plasmonic nanohelices, which we use as chiral metafluids with record circular dichroism and tunable chiroptical properties.

NATURE MATERIALS DOI: 10.1038/NMAT3685 LETTERS

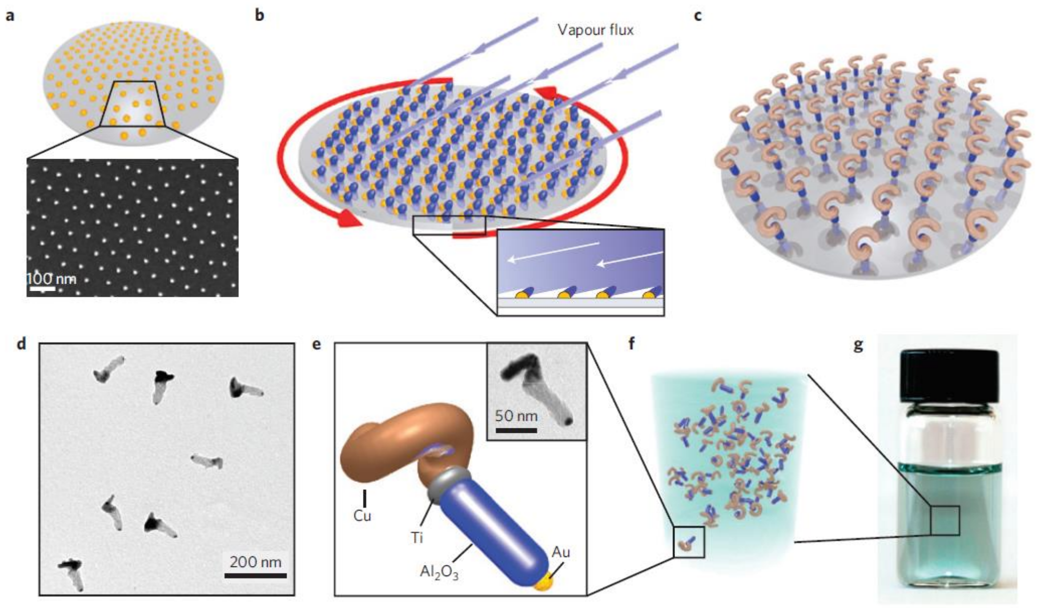

Figure 1 | Fabrication scheme illustrated for nanohooks with C_1 symmetry. a,**b**, The 14 nm gold nanodots patterned by micellar nanolithography (**a**; bottom, SEM image of patterned wafer) act as nucleation sites (**b**) during subsequent shadow growth. **c**, Manipulation of the substrate angle and deposition material creates complex 3D structures. The growth process takes approximately 1 h. **d**, TEM image of hybrid insulator–metal nanohooks. **e**, Model of the designed structure, and TEM image showing the grown structure (inset). **f**,**g**, On sonication the nanoparticles are released into solution

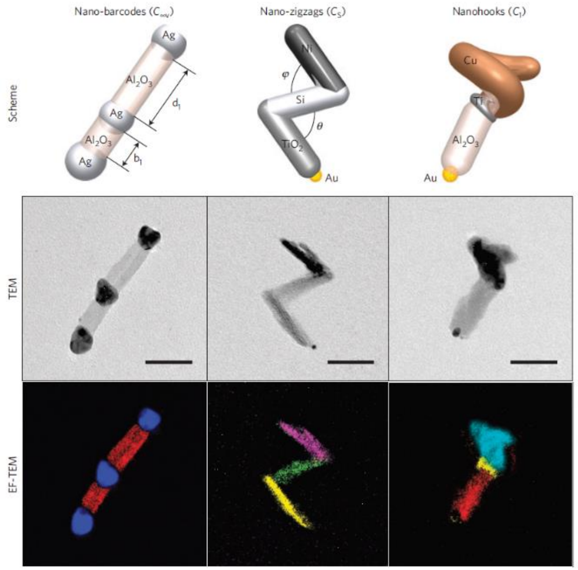

Figure 3 | Hybrid nanoparticles with progressively lower symmetry. Columns from left to right show: $C_{\infty v}$ nano-barcodes, C_S nano-zigzags combining magnetic, semiconducting and insulating materials, and the lowest possible symmetry C_1 nanohooks with defined chirality. First row, structure models. TEM images (second row) and false-colour elemental maps (third row) of the same regions generated by analysing EF-TEM images using the three-window technique (Supplementary Note S9). Colour code (and corresponding core-loss edges): red, aluminium (Al $L_{2,3}$ for nano-barcodes, Al K for nanohooks); blue, silver (Ag $M_{4,5}$); yellow, titanium (Ti $L_{2,3}$); green, silicon (Si $L_{2,3}$); purple, nickel (Ni $L_{2,3}$); cyan, copper (Cu $L_{2,3}$).

Quelle: Mark et al. Nature Materials 2013, S.802

Synthese nanostrukturierter dünner Schichten
Glancing angle deposition (GLAD) @ WdM

Dealloying: fabrication of WO_3 nanostructures for solar water splitting

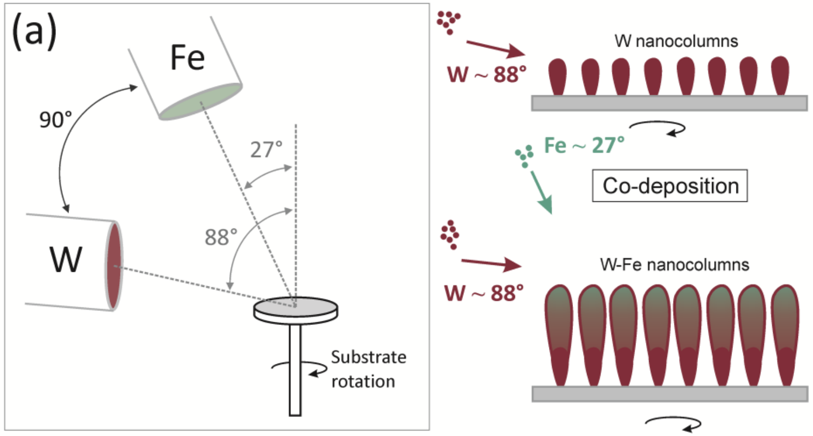

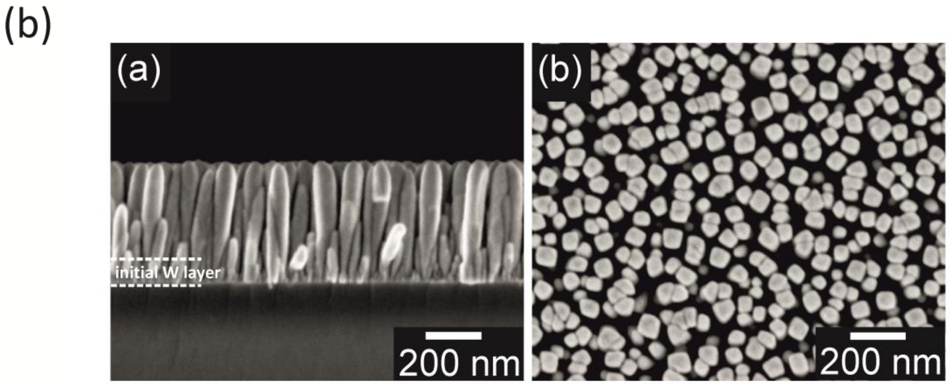

Dealloying in dilute HNO_3

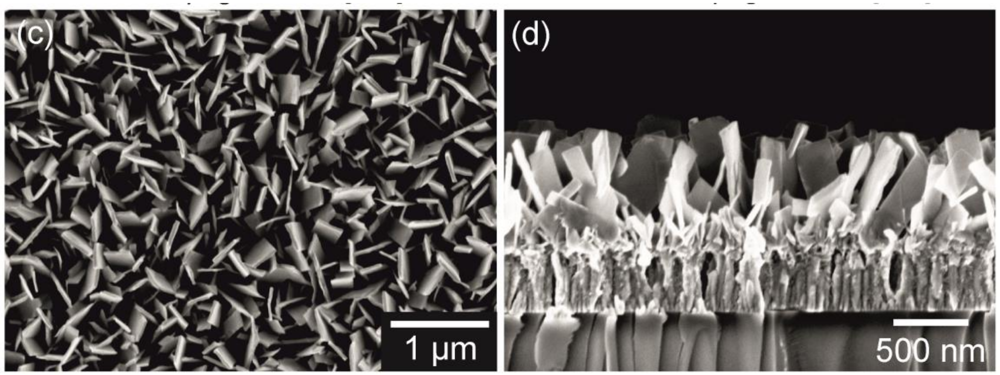

C. Khare et al, Nanotechnology 25, 205606 (2014)

Synthese nanostrukturierter dünner Schichten
Glancing angle deposition (GLAD) @ WdM

Photoelectrochemical solar water splitting

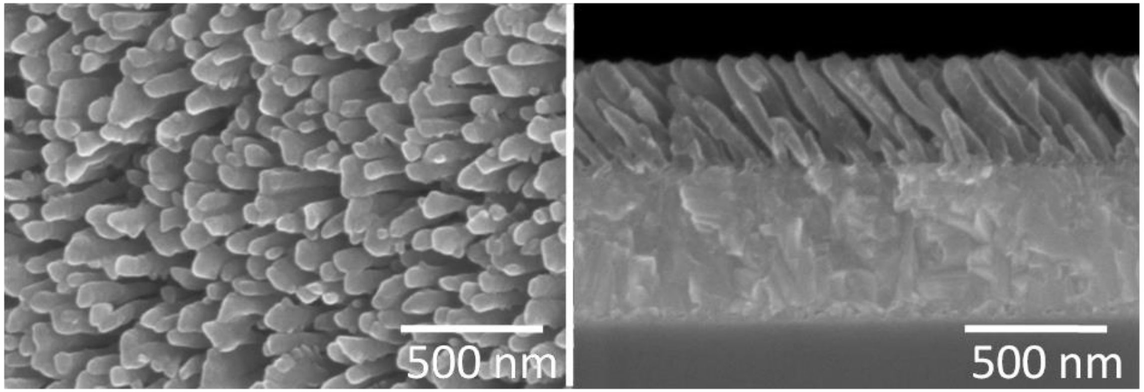

$2hv \rightarrow 2e^- + 2h^*$ (1)
$2h^* + H_2O_{(liquid)} \rightarrow ½\ O_{2(g)} + 2H^+$ (2)
$2H^+ + 2e^- \rightarrow H_2(g)$ (3)
$2hv + H_2O_{(liquid)} \rightarrow ½\ O_{2(g)} + H_{2(g)}$ (4)

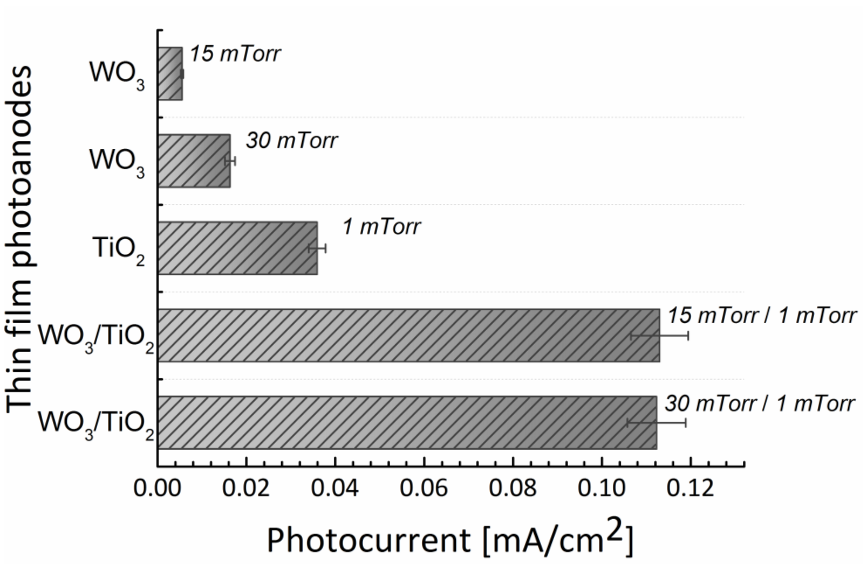

C. Khare et al. Int. J. Hydrogen Energy 38, 15954 (2013)

- Highly porous nanostructures
- Enhanced photocurrent density
- Efficient charge separation

Synthese nanostrukturierter dünner Schichten
Glancing angle deposition (GLAD) @ WdM

Biomaterials:

Adherence of human mesenchymal stem cells

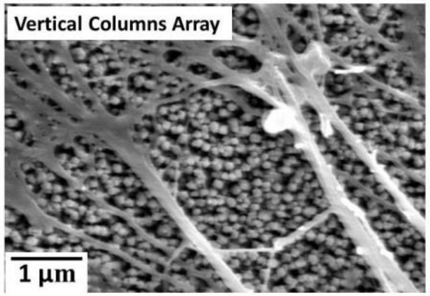

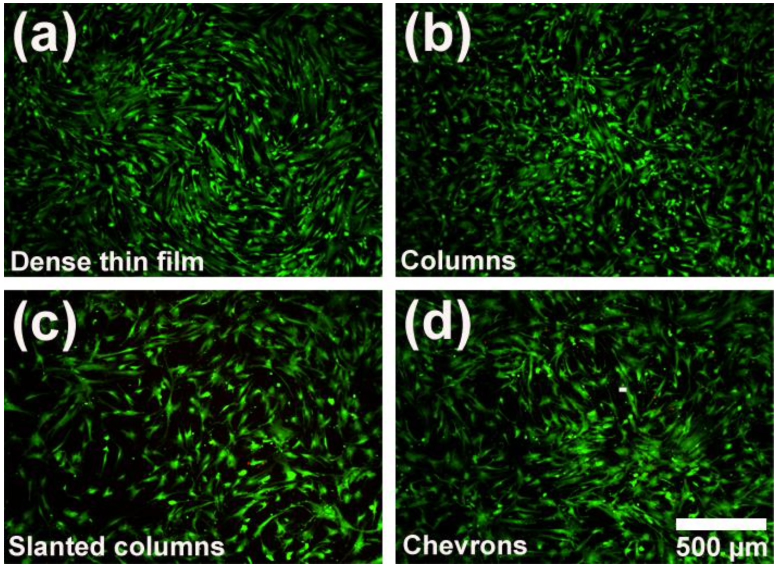

Structure related antibacterial effect

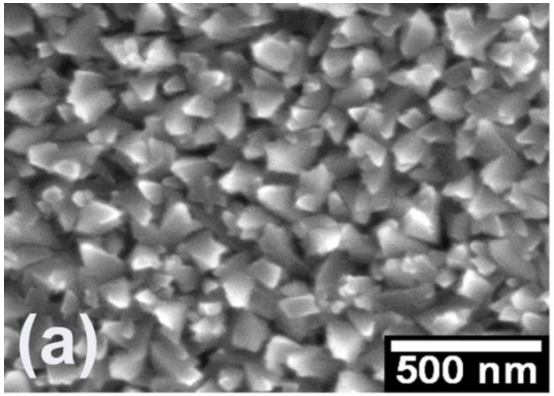

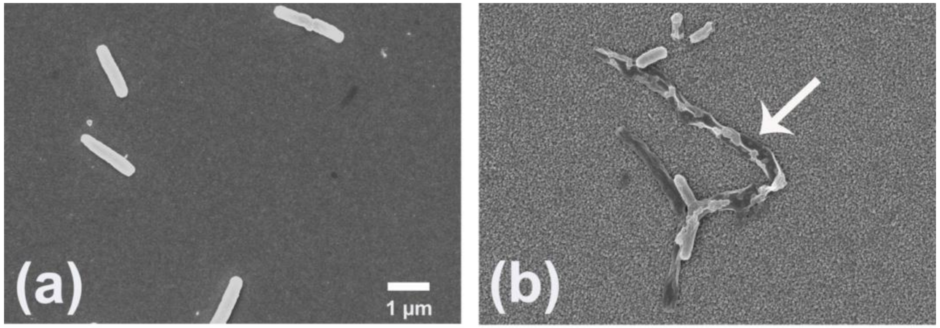

Y. Motemani et al Appl. Surf. Sci. 292, 626 (2014)

C. Sengstock et al Nanotechnology 25, 195101 (2014)

Advanced Materials Processing and Microfabrication

Nanotechnolgie: „2-D Materialien“

Kohlenstoffbasierte Nanomaterialien
Graphen: Prototyp von 2D-Materialien

Graphit

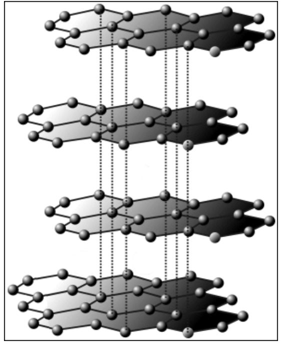

Exfoliation →

Graphen

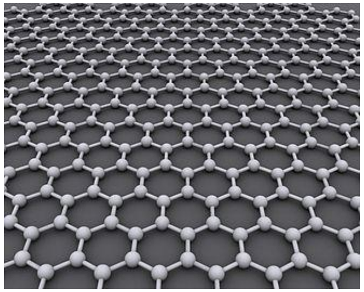

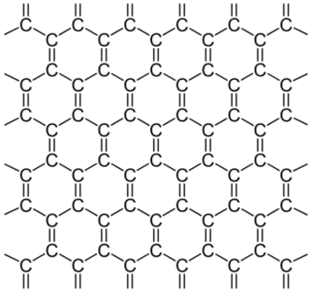

“Our graphene films were prepared by mechanical exfoliation (repeated peeling) of small mesas of highly oriented pyrolytic graphite“

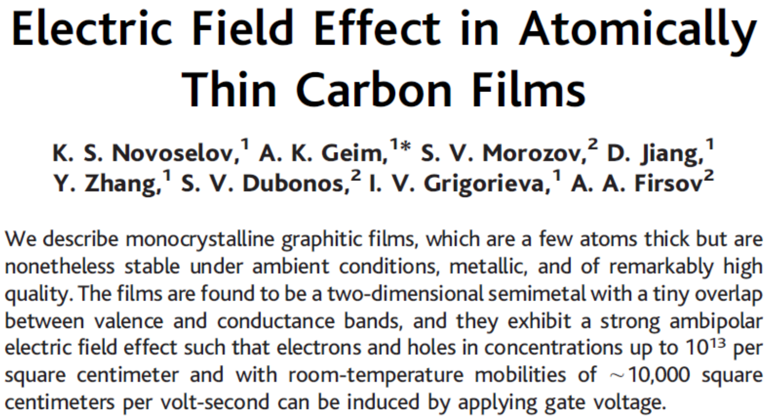

Electric Field Effect in Atomically Thin Carbon Films

K. S. Novoselov,[1] A. K. Geim,[1]* S. V. Morozov,[2] D. Jiang,[1]
Y. Zhang,[1] S. V. Dubonos,[2] I. V. Grigorieva,[1] A. A. Firsov[2]

We describe monocrystalline graphitic films, which are a few atoms thick but are nonetheless stable under ambient conditions, metallic, and of remarkably high quality. The films are found to be a two-dimensional semimetal with a tiny overlap between valence and conductance bands, and they exhibit a strong ambipolar electric field effect such that electrons and holes in concentrations up to 10^{13} per square centimeter and with room-temperature mobilities of $\sim$10,000 square centimeters per volt-second can be induced by applying gate voltage.

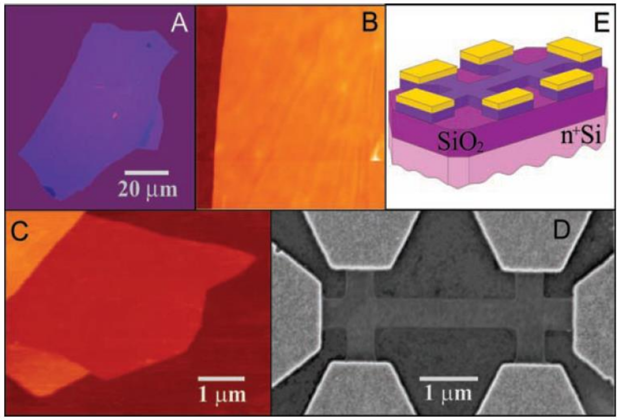

Fig. 1. Graphene films. **(A)** Photograph (in normal white light) of a relatively large multilayer graphene flake with thickness $\sim$3 nm on top of an oxidized Si wafer. **(B)** Atomic force microscope (AFM) image of 2 µm by 2 µm area of this flake near its edge. Colors: dark brown, SiO_2 surface; orange, 3 nm height above the SiO_2 surface. **(C)** AFM image of single-layer graphene. Colors: dark brown, SiO_2 surface; brown-red (central area), 0.8 nm height; yellow-brown (bottom left), 1.2 nm; orange (top left), 2.5 nm. Notice the folded part of the film near the bottom, which exhibits a differential height of $\sim$0.4 nm. For details of AFM imaging of single-layer graphene, see (*15*). **(D)** Scanning electron microscope image of one of our experimental devices prepared from FLG. **(E)** Schematic view of the device in (D).

Science 2004 (< 25000 Zitate)

Figure 1 | Suspended graphene membrane. Bright-field TEM image of a suspended graphene membrane. Its central part (homogeneous and featureless region indicated by arrows) is monolayer graphene. Electron diffraction images from different areas of the flake show that it is a single crystal without domains. We note scrolled top and bottom edges and a strongly folded region on the right. Scale bar, 500 nm.

Nature 2007

Nanotechnologie

Kohlenstoffbasierte Nanomaterialien

Graphen: Prototyp von 2D-Materialien

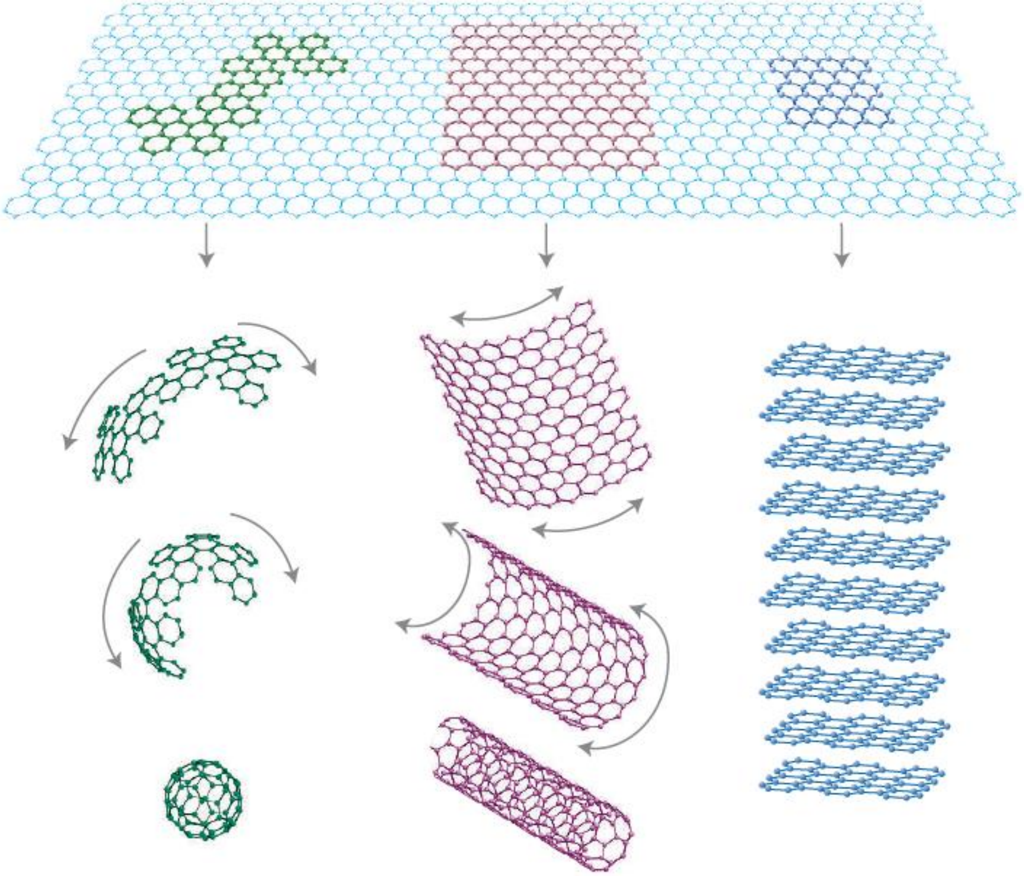

Figure 1 Mother of all graphitic forms. Graphene is a 2D building material for carbon materials of all other dimensionalities. It can be wrapped up into 0D buckyballs, rolled into 1D nanotubes or stacked into 3D graphite.

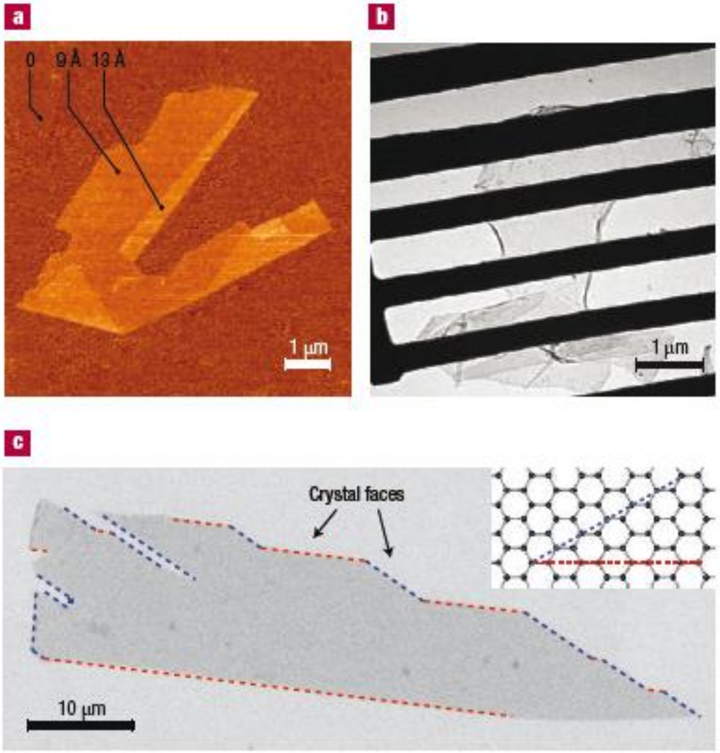

Figure 2 One-atom-thick single crystals: the thinnest material you will ever see. **a**, Graphene visualized by atomic force microscopy (adapted from ref. 8). The folded region exhibiting a relative height of ≈4 Å clearly indicates that it is a single layer. (Copyright National Academy of Sciences, USA.) **b**, A graphene sheet freely suspended on a micrometre-size metallic scaffold. The transmission electron microscopy image is adapted from ref. 18. **c**, Scanning electron micrograph of a relatively large graphene crystal, which shows that most of the crystal's faces are zigzag and armchair edges as indicated by blue and red lines and illustrated in the inset (T.J. Booth, K.S.N, P. Blake and A.K.G. unpublished work). 1D transport along zigzag edges and edge-related magnetism are expected to attract significant attention.

nature materials | VOL 6 | MARCH 2007 | www.nature.com/naturematerials

Nanotechnologie

Kohlenstoffbasierte Nanomaterialien:
Graphen: Prototyp von 2D-Materialien

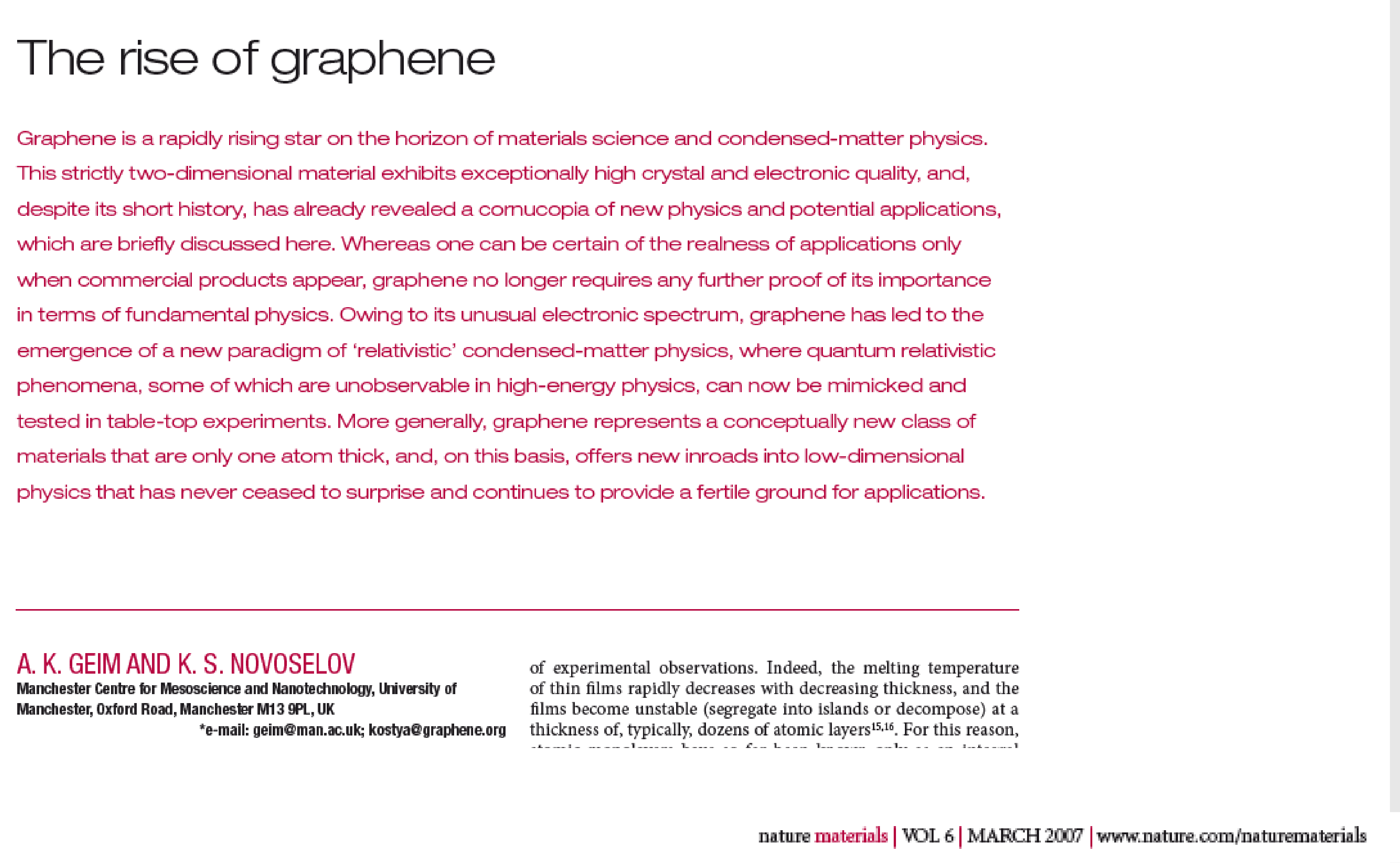

The rise of graphene

Graphene is a rapidly rising star on the horizon of materials science and condensed-matter physics. This strictly two-dimensional material exhibits exceptionally high crystal and electronic quality, and, despite its short history, has already revealed a cornucopia of new physics and potential applications, which are briefly discussed here. Whereas one can be certain of the realness of applications only when commercial products appear, graphene no longer requires any further proof of its importance in terms of fundamental physics. Owing to its unusual electronic spectrum, graphene has led to the emergence of a new paradigm of 'relativistic' condensed-matter physics, where quantum relativistic phenomena, some of which are unobservable in high-energy physics, can now be mimicked and tested in table-top experiments. More generally, graphene represents a conceptually new class of materials that are only one atom thick, and, on this basis, offers new inroads into low-dimensional physics that has never ceased to surprise and continues to provide a fertile ground for applications.

A. K. GEIM AND K. S. NOVOSELOV
Manchester Centre for Mesoscience and Nanotechnology, University of Manchester, Oxford Road, Manchester M13 9PL, UK
***e-mail: geim@man.ac.uk; kostya@graphene.org**

of experimental observations. Indeed, the melting temperature of thin films rapidly decreases with decreasing thickness, and the films become unstable (segregate into islands or decompose) at a thickness of, typically, dozens of atomic layers[15,16]. For this reason,

nature materials | VOL 6 | MARCH 2007 | www.nature.com/naturematerials

Nanotechnologie

2-Dimensionale atomar-skalige Materialien

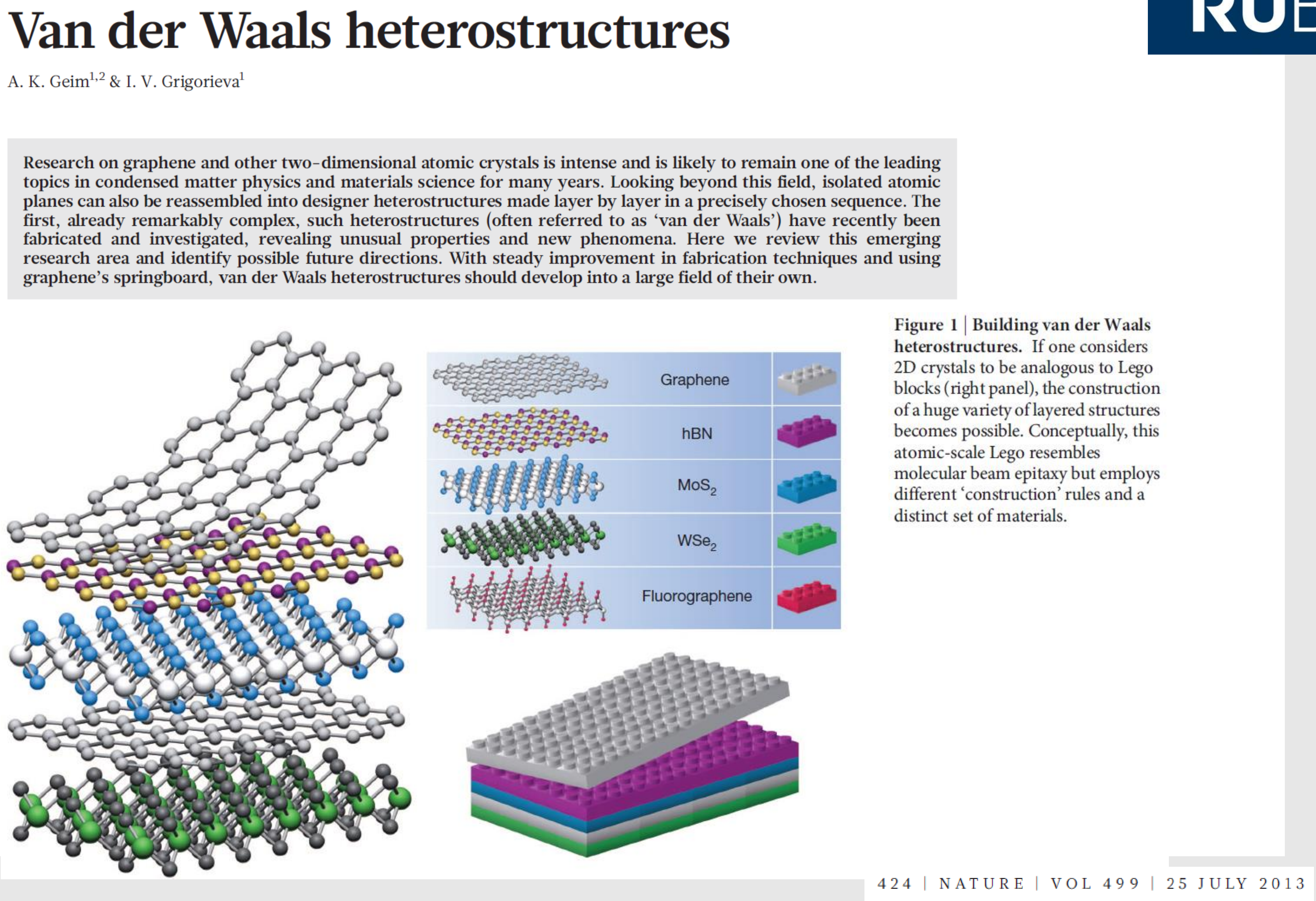

Van der Waals heterostructures

A. K. Geim[1,2] & I. V. Grigorieva[1]

Research on graphene and other two-dimensional atomic crystals is intense and is likely to remain one of the leading topics in condensed matter physics and materials science for many years. Looking beyond this field, isolated atomic planes can also be reassembled into designer heterostructures made layer by layer in a precisely chosen sequence. The first, already remarkably complex, such heterostructures (often referred to as 'van der Waals') have recently been fabricated and investigated, revealing unusual properties and new phenomena. Here we review this emerging research area and identify possible future directions. With steady improvement in fabrication techniques and using graphene's springboard, van der Waals heterostructures should develop into a large field of their own.

Figure 1 | Building van der Waals heterostructures. If one considers 2D crystals to be analogous to Lego blocks (right panel), the construction of a huge variety of layered structures becomes possible. Conceptually, this atomic-scale Lego resembles molecular beam epitaxy but employs different 'construction' rules and a distinct set of materials.

424 | NATURE | VOL 499 | 25 JULY 2013

Nanotechnologie

2-Dimensionale atomar-skalige Materialien

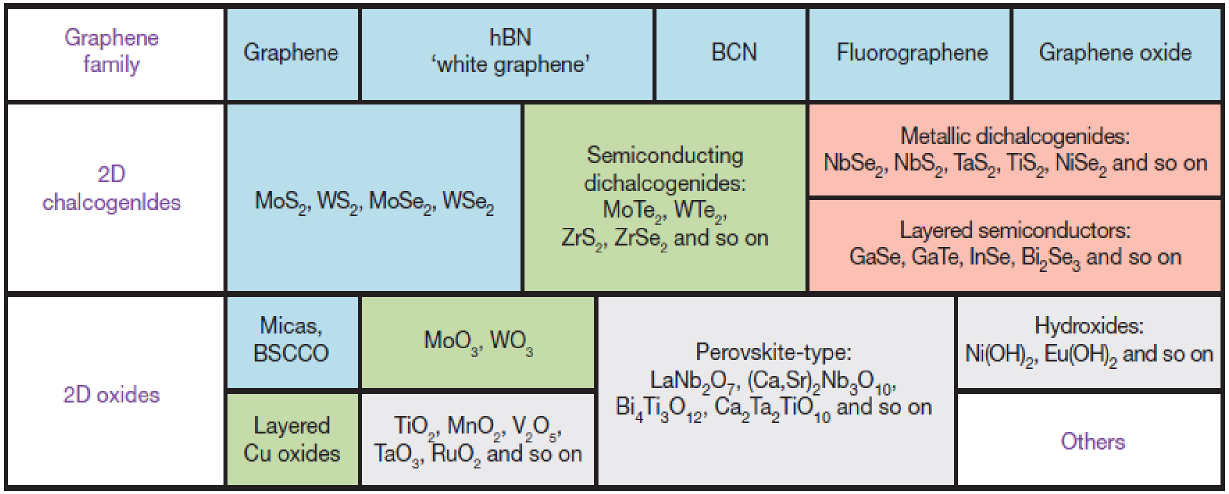

Graphene family	Graphene	hBN 'white graphene'	BCN	Fluorographene	Graphene oxide
2D chalcogenides	MoS_2, WS_2, $MoSe_2$, WSe_2	Semiconducting dichalcogenides: $MoTe_2$, WTe_2, ZrS_2, $ZrSe_2$ and so on	Metallic dichalcogenides: $NbSe_2$, NbS_2, TaS_2, TiS_2, $NiSe_2$ and so on Layered semiconductors: GaSe, GaTe, InSe, Bi_2Se_3 and so on		
2D oxides	Micas, BSCCO Layered Cu oxides	MoO_3, WO_3 TiO_2, MnO_2, V_2O_5, TaO_3, RuO_2 and so on	Perovskite-type: $LaNb_2O_7$, $(Ca,Sr)_2Nb_3O_{10}$, $Bi_4Ti_3O_{12}$, $Ca_2Ta_2TiO_{10}$ and so on	Hydroxides: $Ni(OH)_2$, $Eu(OH)_2$ and so on Others	

Figure 2 | Current 2D library. Monolayers proved to be stable under ambient conditions (room temperature in air) are shaded blue; those probably stable in air are shaded green; and those unstable in air but that may be stable in inert atmosphere are shaded pink. Grey shading indicates 3D compounds that have been successfully exfoliated down to monolayers, as is clear from atomic force microscopy, for example, but for which there is little further information. The data given are summarized from refs 6–11, 42 and 55. We note that, after intercalation and exfoliation, the oxides and hydroxides may exhibit stoichiometry different from their 3D parents (for example, TiO_2 exfoliates into a stoichiometric monolayer of $Ti_{0.87}O_2$; ref. 8). 'Others' indicates that many other 2D crystals—including borides, carbides, nitrides and so on—have probably been[7–11] or can be isolated. BCN, boron carbon nitride.

424 | NATURE | VOL 499 | 25 JULY 2013

Nanotechnologie

2-Dimensionale atomar-skalige Materialien: Übergangsmetall-Chalcogenide

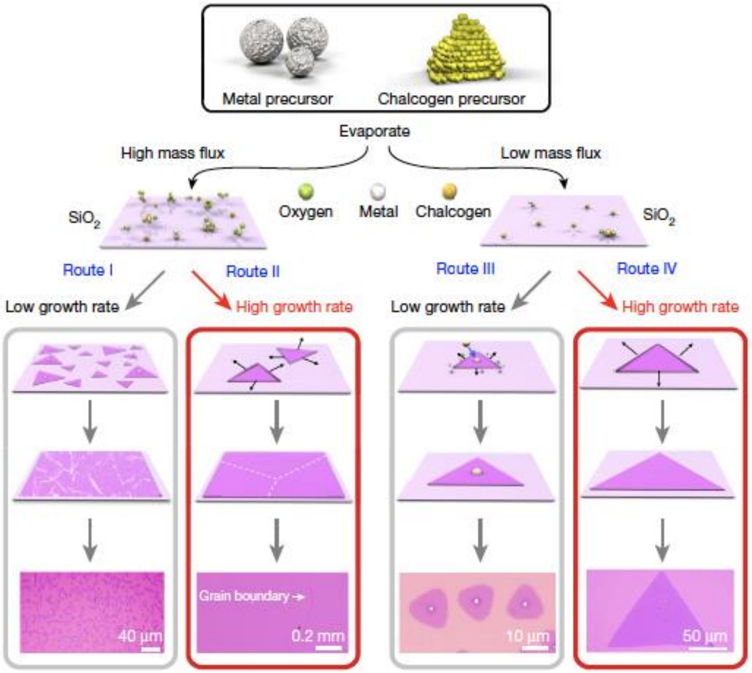

Fig. 1 | Flow chart of the general growth process for the production of TMCs by the chemical vapour deposition method. The growth of 2D TMCs can be classified into four routes based on different mass flux of metal precursor and growth rate. High mass flux of metal precursor offers the opportunity to synthesize large-scale continuous monolayer polycrystalline films with small (route I) or large (route II) domains depending on the growth rate. On the other hand, low mass flux of metal precursor results in discrete single-crystalline monolayers with different sizes. Low growth rate leads to small crystal size with atom clusters decorated in the centre and edge of the monocrystal (route III), while high growth rate gives rise to large monocrystals (route IV).

Fig. 2 | The transition metals and chalcogens used, and optical images of the resulting 47 different atomically thin TMCs and heterostructures. a, Overview of metals (highlighted in purple) and chalcogens (highlighted in yellow and orange) that can form layered sulfides, selenides and tellurides. **b**, Optical images of 47 TMCs synthesized using our method: binary 2D crystals containing Mo (MoS_2, $MoSe_2$, $MoTe_2$), W (WS_2, WSe_2, WTe_2), Re (ReS_2, $ReSe_2$), Ti (TiS_2, $TiSe_2$, $TiTe_2$), Zr (ZrS_2, $ZrSe_2$, $ZrTe_2$), Hf (HfS_2, $HfSe_2$, $HfTe_2$), V (VS_2, VSe_2, VTe_2), Nb (NbS_2, $NbSe_2$, $NbTe_2$), Ta (TaS_2, $TaSe_2$, $TaTe_2$), Pt (PtS_2, $PtSe_2$, $PtTe_2$), Pd (PdS_2, $PdSe_2$) or Fe (FeSe); the ternary alloys MoS_xTe_{2-x}, $MoSe_xTe_{2-x}$, WS_xTe_{2-x}, WSe_xTe_{2-x}, NbS_xSe_{2-x}, $Mo_xNb_{1-x}S_2$, $Mo_xNb_{1-x}Se_2$, $Mo_{1-x}Re_xS_2$, $W_xNb_{1-x}S_2$, $W_xNb_{1-x}Se_2$ and $Mo_xW_{1-x}Te_2$; the quaternary alloy $Mo_xNb_{1-x}S_{2y}Se_{2(1-y)}$; the quinary alloy $V_xW_yMo_{1-x-y}S_{2z}Se_{2(1-z)}$; and the 1 T' $MoTe_2$–2 H $MoTe_2$ in-plane and MoS_2–$NbSe_2$ vertically stacked heterostructures. TMCs that have not been previously synthesized are outlined in blue. Detailed characterizations of the as-grown 2D materials are shown in Supplementary Information.

A library of atomically thin metal chalcogenides

Jiadong Zhou[1,15], Junhao Lin[2,15]*, Xiangwei Huang[3], Yao Zhou[4], Yu Chen[5], Juan Xia[5], Hong Wang[1], Yu Xie[6], Huimei Yu[7], Jincheng Lei[6], Di Wu[8,9], Fucai Liu[1], Qundong Fu[1], Qingsheng Zeng[1], Chuang-Han Hsu[8,9], Changli Yang[3,10], Li Lu[3,10], Ting Yu[5], Zexiang Shen[5], Hsin Lin[8,9,11], Boris I. Yakobson[6], Qian Liu[4], Kazu Suenaga[2], Guangtong Liu[3]* & Zheng Liu[1,12,13,14]*

356 | NATURE | VOL 556 | 19 APRIL 2018

Advanced Materials Processing and Microfabrication

Übungsfragen

1. Erläutern Sie die Begriffe Nanowissenschaft und Nanotechnik
2. Was versteht man unter MEMS und NEMS?
3. In welchen Bereichen der Technik wird Nanotechnologie bereits genutzt?
4. In welchem Größenbereich bewegen sich kritische Abmessungen gegenwärtiger Transistoren?
5. Erläutern Sie „bottom-up“ und „top-down“ Strategien in der Nanotechnologie.
6. Wie können Nanoobjekte klassifiziert werden?
7. Diskutieren Sie das Oberflächen- bzw. Grenzflächen zu Volumenverhältnis für nanostrukturierte Materialien.
8. Nennen Sie Beispiele für 0-, 1, 2 und 3-dimensionale Nanoobjekte.
9. Welche Messmethoden sind besonders wichtig in der Nanotechnik?
10. Wie kann man Nanopartikel herstellen?
11. Warum ist die Lichtemission von Halbleiter-Nanopartikeln größenabhängig?
12. Erläutern Sie Begriffe monodispers und polydispers.
13. Wie können Nanopartikel vor Agglomeration geschützt werden?
14. Beschreiben Sie den GLAD Prozess.
15. Erklären Sie den Abschattungsprozess der zur Bildung von Nanosäulen beim GLAD Verfahren führt.
16. Wie kann man geordnete Nanostrukturen mittels GLAD erzeugen?
17. Beschreiben Sie einige Beispiele für größenabhängige Nanoeffekte.
18. Wie können einzelne Atome auf Oberflächen positioniert werden?
19. Was ist Graphen?
20. Was sind van der Waals Heterostrukturen?

Advanced Materials Processing and Microfabrication

Literatur und Quellen

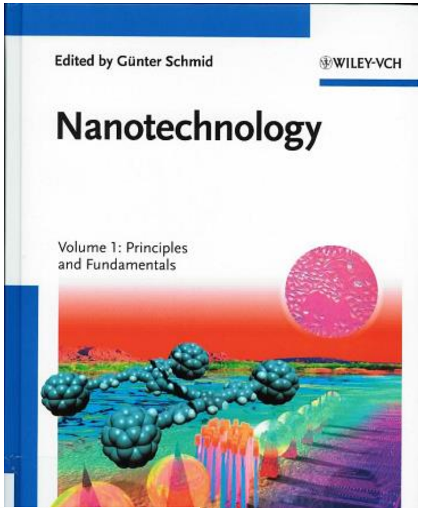

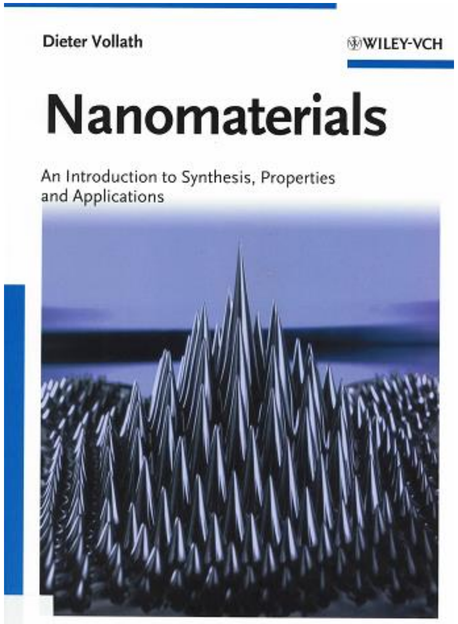

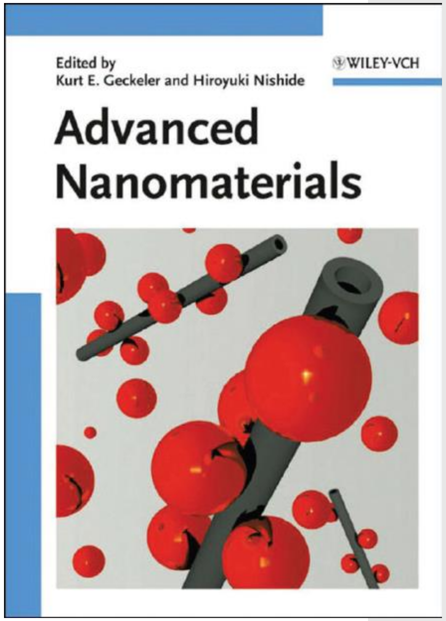

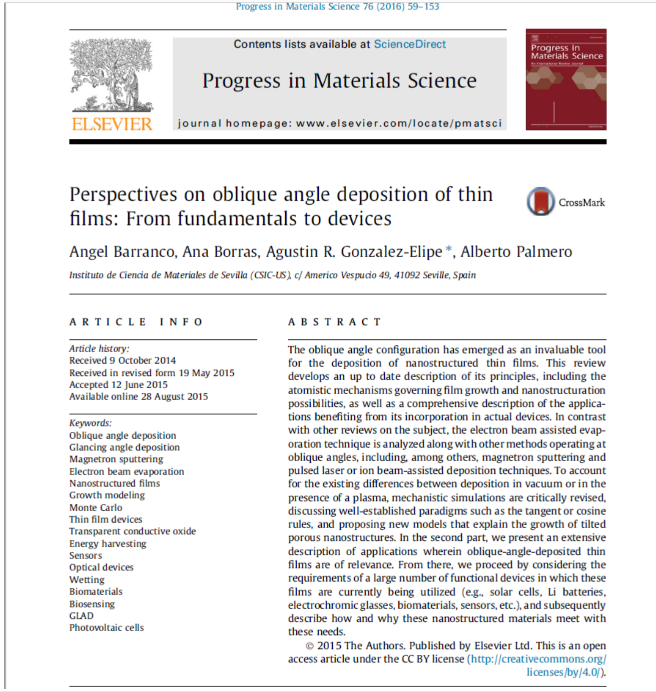

Progress in Materials Science 76 (2016) 59–153

Contents lists available at ScienceDirect

Progress in Materials Science

journal homepage: www.elsevier.com/locate/pmatsci

Perspectives on oblique angle deposition of thin films: From fundamentals to devices

Angel Barranco, Ana Borras, Agustin R. Gonzalez-Elipe *, Alberto Palmero

Instituto de Ciencia de Materiales de Sevilla (CSIC-US), c/ Americo Vespucio 49, 41092 Seville, Spain

ARTICLE INFO

Article history:
Received 9 October 2014
Received in revised form 19 May 2015
Accepted 12 June 2015
Available online 28 August 2015

Keywords:
Oblique angle deposition
Glancing angle deposition
Magnetron sputtering
Electron beam evaporation
Nanostructured films
Growth modeling
Monte Carlo
Thin film devices
Transparent conductive oxide
Energy harvesting
Sensors
Optical devices
Wetting
Biomaterials
Biosensing
GLAD
Photovoltaic cells

ABSTRACT

The oblique angle configuration has emerged as an invaluable tool for the deposition of nanostructured thin films. This review develops an up to date description of its principles, including the atomistic mechanisms governing film growth and nanostructuration possibilities, as well as a comprehensive description of the applications benefiting from its incorporation in actual devices. In contrast with other reviews on the subject, the electron beam assisted evaporation technique is analyzed along with other methods operating at oblique angles, including, among others, magnetron sputtering and pulsed laser or ion beam-assisted deposition techniques. To account for the existing differences between deposition in vacuum or in the presence of a plasma, mechanistic simulations are critically revised, discussing well-established paradigms such as the tangent or cosine rules, and proposing new models that explain the growth of tilted porous nanostructures. In the second part, we present an extensive description of applications wherein oblique-angle-deposited thin films are of relevance. From there, we proceed by considering the requirements of a large number of functional devices in which these films are currently being utilized (e.g., solar cells, Li batteries, electrochromic glasses, biomaterials, sensors, etc.), and subsequently describe how and why these nanostructured materials meet with these needs.